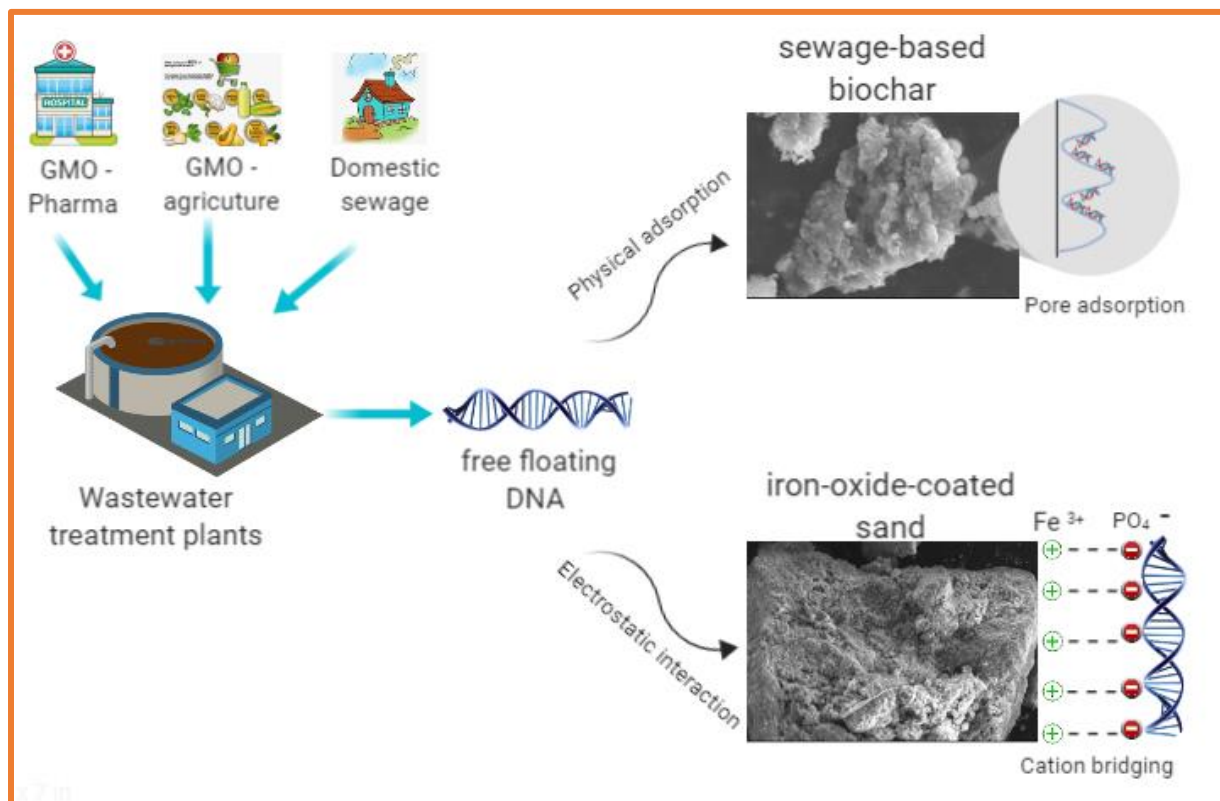


ADSORPTION OF FREE FLOATING DNA AND ANTIMICROBIAL RESISTANCE GENES OUT OF WASTEWATER EFFLUENTS BY SEWAGE-BASED BIOCHAR AND IRON-OXIDE-COATED SANDS

Seeram Apoorva
(MSc Thesis)



Adsorption of free-floating DNA and antimicrobial resistance genes out of wastewater effluents by sewage-based biochar and iron-oxide-coated sands

by

Seeram Apoorva

4703901

in partial fulfillment of the requirements for the degree of

**Master of Science in Civil Engineering
in Environmental Engineering**

at the Delft University of Technology

October 2019

This thesis was performed at the Weissbrodt Group for Environmental Life Science Engineering, Environmental Biotechnology Section, Department of Biotechnology, Faculty of Applied Sciences, van der Maasweg 9, 2629 HZ Delft, Netherlands

Correspondence; D.G.Weissbrodt@tudelft.nl; D.CalderonFranco@tudelft.nl; Seeram94@gmail.com

Thesis direction:

David Weissbrodt, Assistant Professor Thesis Director; Environmental Biotechnology, TU Delft

David Calderon Franco, PhD candidate Co-supervisor; Environmental Biotechnology, TU Delft

Thesis Committee members:

Gertjan Medema, Full professor Chair of committee; Sanitary Engineering, TU Delft

Ralph Lindeboom, Assistant Professor Committee member; Sanitary Engineering, TU Delft

This work is confidential and cannot be made public until new notice from David Weissbrodt, Thesis director.



Acknowledgements

The past 2 years has been a very challenging journey which helped me to develop both personal and academic abilities. This journey of achieving a master's degree would not have been made possible without the support of many people who stood by me all along.

Firstly, I would like to thank my parents for their constant love and sacrifice without whom I would not have made this journey far away from home. I would also like to thank my brother, Seeram Anuraag for his encouragement and support throughout the study.

This thesis as one major part of the master program, I would like to first thank David Weissbrodt for providing me the opportunity to work on this project in Environmental Biotechnology section. I would like to thank my daily supervisor David Calderon Franco whose office doors were always open, patiently hearing me out and giving me feedback during the complete project. I would like to thank my committee Gertjan Medema and Ralph Lindeboom for their valuable inputs and recommendations during the meetings.

I would also like to thank the members of Harnaspolder plant, for water and sludge samples; Olaf van der kolk from Aqua minerals, for iron oxide coated sands. I would like to thank Michel van den Brink and Ruud Hendrix from Department for Material Science and Engineering for pyrolysis and X-ray analysis. I would like to thank John van den Berg from Microlab for nitrogen sorption analysis. I also thank Lulian Dugulun from reactor institute for IOCS characterization and Suellen Espindola for scanning electron microscopy images. I would also like to thank my co master student Yayavaram Sushant in this project for his help during the laboratory work.

Last but not the least having supportive and encouraging friends in any journey provides you to survive the challenges faced. I would like to thank to dear friends KB Sasidhar, Mrinal Roy, Shreya Trikannad, Rubayat Sobhan, Magnolia Garcia Solano and Pooja Halvawaala for their helping hand during the tough moments at TU Delft.

Abstract

The presence of extracellular DNA (eDNA) containing antibiotic resistance genes in the treated wastewater effluents can contribute to the spread of antimicrobial resistance (AMR) among receiving waters. The removal of cell associated antibiotic resistance genes (ARGs) has been widely studied using advance treatments. However, these treatments were not evaluated for cell free or extracellular ARGs resulting from the cell lysis or secretion during metabolic activities. eDNA is known to well adsorb onto clay, suspended particles and other soil components. Thus, in this research the potential and the main mechanisms involved in the removal of eDNA by adsorption onto sewage-based biochar and iron-oxide-coated sands has been studied.

Batch studies and column studies were performed to see the removal of DNA (Salmon sperm DNA as a model eDNA) under various water qualities (ultrapure and effluent wastewater). Results showed that sewage-based biochar has higher adsorption capacity ($\sim 1 \mu\text{g mg}^{-1}$) over iron-oxide-coated sands ($\sim 0.2 \mu\text{g mg}^{-1}$). pH and the presence of cations did not increase the adsorption significantly suggesting that electrostatic interaction as not the main role in the DNA removal. Instead pore size, Vander Waals forces and hydrophobic interactions as the main mechanism for the removal of DNA.

Later, the potential of the adsorbents for the removal of intracellular and extracellular ARGs have been investigated. The removal of 5 antimicrobial resistance genes (ARGs) and 1 mobile genetic element (MGE) and 16S rRNA for all bacteria were evaluated from the effluent wastewater as intracellular and extracellular genes by adsorption. From sewage-based biochar, an average log reduction of 1.19 ± 0.07 and 1.53 ± 0.10 for intracellular and extracellular genes was shown, respectively. On the other hand, iron-oxide-coated sands showed a log reduction of 0.79 ± 0.17 and 0.59 ± 0.09 when test for intracellular and extracellular genes. These results show that adsorption could be a possible solution for treating effluent wastewater for the removal of DNA.

Table of contents

1	INTRODUCTION	1
1.1	Research Background.....	1
1.2	Problem Statement	4
1.3	Research question and objectives.....	6
1.3.1	Research Question	6
1.3.2	Hypothesis.....	6
1.3.3	Objectives	6
2	THEORETICAL BACKGROUND	9
2.1	What is extracellular DNA?.....	9
2.2	Process for the evolution of resistance bacteria	10
2.3	How bacteria resist antibiotics?.....	12
2.4	Spreading of antibiotic resistance from urban to aquatic environment.....	12
2.4.1	Antibiotic resistance bacteria (ARBs)	13
2.4.2	Antibiotic resistance genes (ARGs).....	13
2.4.3	Mobile genetic elements (MGEs).....	13
2.5	Methods for detecting ARGs.....	14
2.5.1	Polymerase chain reaction (PCR).....	14
2.5.2	Real-time polymerase chain reaction.....	15
2.5.3	Metagenomics	15
2.6	Adsorption process in wastewater treatment plants	15
2.7	Mechanisms for DNA adsorption	16
2.8	Possible adsorbents for DNA adsorption	16
3	MATERIAL AND METHODS	19
3.1	Samples used and their collection	19
3.2	Production of sewage-sludge biochar	19
3.3	Characterization of sewage sludge, sewage-based biochar and iron oxide coated sand	20
3.4	DNA and other chemicals	22
3.5	Adsorption of DNA on selected materials	22
3.6	Experiments to find the equilibrium time for adsorption by sewage-based biochar (SBC) and iron oxide coated sand (IOCS).....	22
3.7	Quantification of DNA adsorbed	22
3.8	Adsorption isotherms	23

3.9	Effect of pH, ionic strength and humic acid content on DNA adsorption	23
3.10	Fixed bed column	24
3.11	Extraction of DNA from wastewater effluents.....	28
3.12	Quantification of iDNA and eDNA and their removal efficiency.....	28
3.13	Real-time polymerase chain reaction	29
3.14	Statistical analysis.....	30
3.15	Physical and chemical analysis of wastewater	31
4	RESULTS.....	33
4.1	Selection of a suitable adsorbent.....	33
4.2	Characteristics of the selected adsorbent	34
4.3	Equilibrium time for adsorption.....	37
4.4	Adsorption isotherms parameters.....	38
4.5	Effect of salts, pH, and humic acid on DNA adsorption.....	40
4.6	Column study	43
4.7	Removal efficiencies of All bacteria, ARGs and MGE by adsorption column	52
4.8	Physical and chemical analysis of wastewater.....	55
5	DISCUSSION.....	57
5.1	Sewage-based biochar (SBC) and iron oxide coated (IOCS) as the suitable adsorbents for DNA adsorption in effluent wastewater.....	57
5.2	Proposed removal mechanism of DNA by adsorption.....	58
5.3	Reason for low adsorption with the addition of humic acids.....	58
5.4	Adsorption column behavior.....	59
5.5	Antimicrobial resistance genes removal efficiency	60
5.6	Sewage-based biochar as a potential adsorbent	61
6	CONCLUSIONS.....	65
7	RECOMMENDATIONS	67
	REFERENCES.....	69
	APPENDIX.....	xv

List of figures

Figure 1 Role of wastewater treatment as a key driver in water quality (Water, 2017)	3
Figure 2 Workflow of the experimental approach of the lab experiments and their analysis methods. Created with BioRender	7
Figure 3 Bacterial DNA with a circular bacterial chromosome and plasmid (Science Learning Hub, 2019)	9
Figure 4 The process of conjugation in the evolution of a resistance bacteria (ZJUT - China 2018, 2018)	11
Figure 5 The process of transduction in the evolution of a resistance bacteria (ZJUT - China 2018, 2018)	11
Figure 6 The process of transformation in the evolution of a resistance bacteria (ZJUT - China 2018, 2018)	12
Figure 7 Mineral wool and its properties (Drainblock, 2017)	18
Figure 8 Image showing the sewage-based biochar (left) and iron oxide coated sand (right) used in the research	21
Figure 9 Schematic of the experimental set up of the column used in the study	25
Figure 10 Experimental setup for the column experiments	25
Figure 11 Standards for the qPCR of ARGs and MGE	30
Figure 12 DNA removal in percentage with powdered activated carbon, sewage-based biochar, iron oxide coated sands, granular activated carbon and mineral wool in (a) ultrapure water (b) tap water (c) effluent wastewater	34
Figure 13 Scanning electron microscopy (SEM) image of sewage-based biochar	37

Figure 14 Scanning electron microscope image (SEM) of iron oxide coated sand.....	37
Figure 15 Equilibrium time for sewage-based biochar with an initial DNA concentration of 100 mg L ⁻¹ with the adsorbent ranging from 0 to 100 g L ⁻¹ (a) sewage-based biochar (b) iron-oxide-coated sands	38
Figure 16 The influence of solution pH (4,7 and 9) on adsorption of DNA by sewage-based biochar and iron-oxide-coated sands with an initial concentration of (a)20 µg mL ⁻¹ and (b)100 µg mL ⁻¹ . No significant difference was found in the DNA adsorption due to change in the pH (p > 0.05).....	40
Figure 17 The influence of Na ⁺ , Ca ²⁺ and Mg ²⁺ ranging from 1 mM to 60 mM on DNA adsorption with an initial concentration of 100 µg mL ⁻¹ by (a) sewage-based biochar (b) iron oxide coated sands. (*) p > 0.05, ns: no significant changes.....	42
Figure 18 The influence of humic acids on adsorption of DNA by iron oxide coated sand and sewage-based biochar with an initial concentration of 20 µg mL ⁻¹	42
Figure 19 Comparison of experimental breakthrough curves for adsorption of DNA onto sewage-based biochar at different initial DNA concentrations 0.1 mg mL ⁻¹ , 0.3 mg mL ⁻¹ , and 0.5 mg L ⁻¹ (a) Ultrapure water (b) Effluent wastewater The arrow represents the effect of interruption of the column overnight	44
Figure 20 Comparison of experimental breakthrough curves for adsorption of DNA onto iron oxide coated sand at different initial DNA concentrations 0.1 mg mL ⁻¹ , 0.3 mg mL ⁻¹ , and 0.5 mg L ⁻¹ (a) ultrapure water (b) effluent wastewater	45
Figure 21 Experimental breakthrough curves for adsorption of DNA onto sewage-based biochar at different flow rates 0.1 mL min ⁻¹ , 0.3 mL min ⁻¹ and 0.5 mL min ⁻¹ (a) Ultrapure water (b) Effluent wastewater. The arrow represents the effect of interruption of the column overnight	46
Figure 22 Experimental breakthrough curves for adsorption of DNA onto iron-oxide-coated sands at different flow rates 0.1 mL min ⁻¹ , 0.3 mL min ⁻¹ and 0.5 mL min ⁻¹ (a) Ultrapure water (b) Effluent wastewater	47

Figure 23 iDNA and eDNA removal percentage by sewage-based biochar and iron-oxide-coated sand by adsorption	53
Figure 24 Absolute concentration of intracellular 16S rRNA gene, ARGs and MGE in raw influent, sewage-based biochar treated effluent and iron-oxide-coated sands treated effluent. Different types of (16S, ARGs, and MGE) are separated by straight lines. ns refers to concentrations below detection limit by qPCR. Significant differences observed after adsorption by sewage-based biochar and iron-oxide-coated sands are expressed as (*): $p < 0.05$; (**): $p < 0.005$	54
Figure 25 Absolute concentration of extracellular 16S rRNA gene, ARGs and MGE in raw influent, sewage-based biochar treated effluent and iron-oxide-coated sands treated effluent. Different types of (16S, ARGs, and MGE) are separated by straight lines. ns refers to concentrations below detection limit by qPCR. Significant differences observed after adsorption by sewage-based biochar and iron-oxide-coated sands are expressed (*) $p < 0.05$; (***) $p < 0.0005$; (****) $p < 0.00005$	54
Figure 26 Chemical oxygen demand in the effluent wastewater before and after treatment with sewage-based biochar and iron oxide coated sand	55
Figure 27 True color reduction percentage after treatment with sewage-based biochar and iron oxide coated sand	56
Figure 28 Visual representation of the samples obtained after passing through the columns. Right image: iron-oxide-coated sands effluent, Left image: sewage-based biochar effluent.....	56

List of tables

Table 1 Physical properties of sewage sludge	35
Table 2 Physical and chemical properties of sewage-based biochar	35
Table 3 Properties of iron oxide coated sands	36
Table 4 Freundlich and Langmuir parameters for DNA adsorption on adsorbents in ultrapure water, tap water and effluent wastewater.....	39
Table 5 Parameters of Thomas model using nonlinear regression analysis and the equilibrium DNA uptake ($q_{e (exp)}$) for sewage-based biochar under various conditions in (a) ultrapure water (b) effluent wastewater. SS as the deviation from empirical data	48
Table 6 Parameters of Thomas model using nonlinear regression analysis and the equilibrium DNA uptake ($q_{e (exp)}$) for iron-oxide-coated sands under various conditions in (a)ultrapure water (b) effluent wastewater. SS as the deviation from empirical data	49
Table 7 Parameters of Yoon-Nelson model using nonlinear regression analysis and the equilibrium DNA uptake ($q_{e (exp)}$) for sewage-based biochar under various conditions in (a)ultrapure water (b) effluent wastewater. SS as the deviation from empirical data.....	50
Table 8 Parameters of Yoon-Nelson model using nonlinear regression analysis and the equilibrium DNA uptake ($q_{e (exp)}$) for iron-oxide-coated sands under various conditions in (a)ultrapure water (b) wastewater effluent. SS as the deviation from empirical data.....	51
Table 9 Comparison of sludge treatment by incineration and pyrolysis (Tsybina & Wuensch, 2018)	62

Symbols and abbreviations

WWTP	Wastewater treatment plant
ARB	Antibiotic resistance bacteria
ARG	Antibiotic resistance gene
MGE	Mobile genetic elements
iDNA	Intracellular DNA
eDNA	Extracellular DNA
GMO	Genetically modified organisms
HGT	Horizontal gene transfer
ICE	Integrative conjugative elements
PCR	Polymerase chain reaction
qPCR	Quantitative polymerase chain reaction
SBC	Sewage-based biochar
IOCS	Iron oxide coated sand
AC	Activated carbon
GAC	Granular activated carbon
PAC	Powdered activated carbon
Co	Initial adsorbate concentration
Ce	Equilibrium adsorbate concentration
Ct	Concentration at time t minutes
K_F	Freundlich constant related to adsorption capacity
K_L	Langmuir constant related to heat of adsorption
K_{Th}	Thomas rate constant
q_e	Adsorption capacity
K_{YN}	Yoon Nelson rate constant
τ	Time required for 50% breakthrough

Chapter

1 INTRODUCTION

1.1 Research Background

Population growth and population shift from rural to urban areas are trends that create a great deal of resource deficit problems. Water essential for the development of life, human activities and fundamental for sustainable ecosystem is an example of such resource. In the present century, water scarcity and access to potable water has been the major concern of the society. In addition to rising population, climate change scenarios, spatial and temporal variations of water cycle dynamics also increase the differences between water supply and demand (Voulvoulis, 2018). According to the World Wildlife Fund, about 1.1 billion people in the world are inaccessible to potable water and 2.4 billion people are vulnerable to poor sanitation (World Wildlife Fund, 2019). As per the World Bank report cities like Mexico, Bangkok, Beijing, Shanghai, Madras, and Manila have experienced water aquifers to drop between 10 to 50 meters (Foster et al., 1998). If this trend follows, it is then anticipated that by 2050, about 2.3 billion people will suffer from water shortage, mainly, in North and South Africa and South and Central Asia (Guppy & Anderson, 2017).

The rise in economic development limits the freshwater supplies in many countries. The availability of water resources is questioned by its quality due to the release of pollutants with the potential to harm humans and the ecosystem. There is no single definition of water quality as it depends widely on the origin, location, and its use. According to the Environmental Performance Index report, approximately 80 percent of the wastewater in the world is not treated effectively before its release to the environment (Wendling Z.A et al., 2018). This discharge untreated wastewater negatively impacts the sustainable economic development, human health, the quality of ambient freshwater resources and ecosystems (Water, 2017). Thus, it has been reflected by the policymakers that wastewater treatment is a main factor in water quality as it plays a major role in water cycle (Figure 1) (Hsu A et al., 2016).

The development of any country in the world, is governed by accessibility of safe drinking water in terms of quality and quantity. More than 80 percent of the earth's available water is used in field of agriculture, for cattle and energy. Over the coming years, drastic increase in population and high standards of living, will create a scarcity on the availability of water resources (Shannon et al., 2010). Therefore, new and alternate solutions to provide clean water need to be addressed to tackle the growing demand for water. To this end wastewater reclamation or reuse or recycling of wastewater is seen as one of the viable options worldwide (Asano & Levine, 1996). However, the main problem with the reuse of wastewater is the final effluent quality; different levels of treatment is necessary based on the end use of this reclaimed water. The main aims of the Sustainable Development Goals (SDG 6.3) is to provide high water quality by reducing the use of hazardous materials, to increase the proportion of treated water thus increasing recycling and safe reuse.

Conventional treatment plants are (WWTPs) are generally designed to remove solids, organic matter and nutrients (such as nitrogen, phosphorus) from wastewater. However, are not really designed to treat a number of compounds that still persist in the effluents of WWTP in an altered form known as Emerging Pollutants or contaminants (Justo Llopis, 2015). In a broader sense, an emerging pollutant can be defined “as any synthetic or naturally occurring chemical or microorganism that is not monitored in the environment with potentially known adverse ecological or human health effects” (UNESCO, 2019).

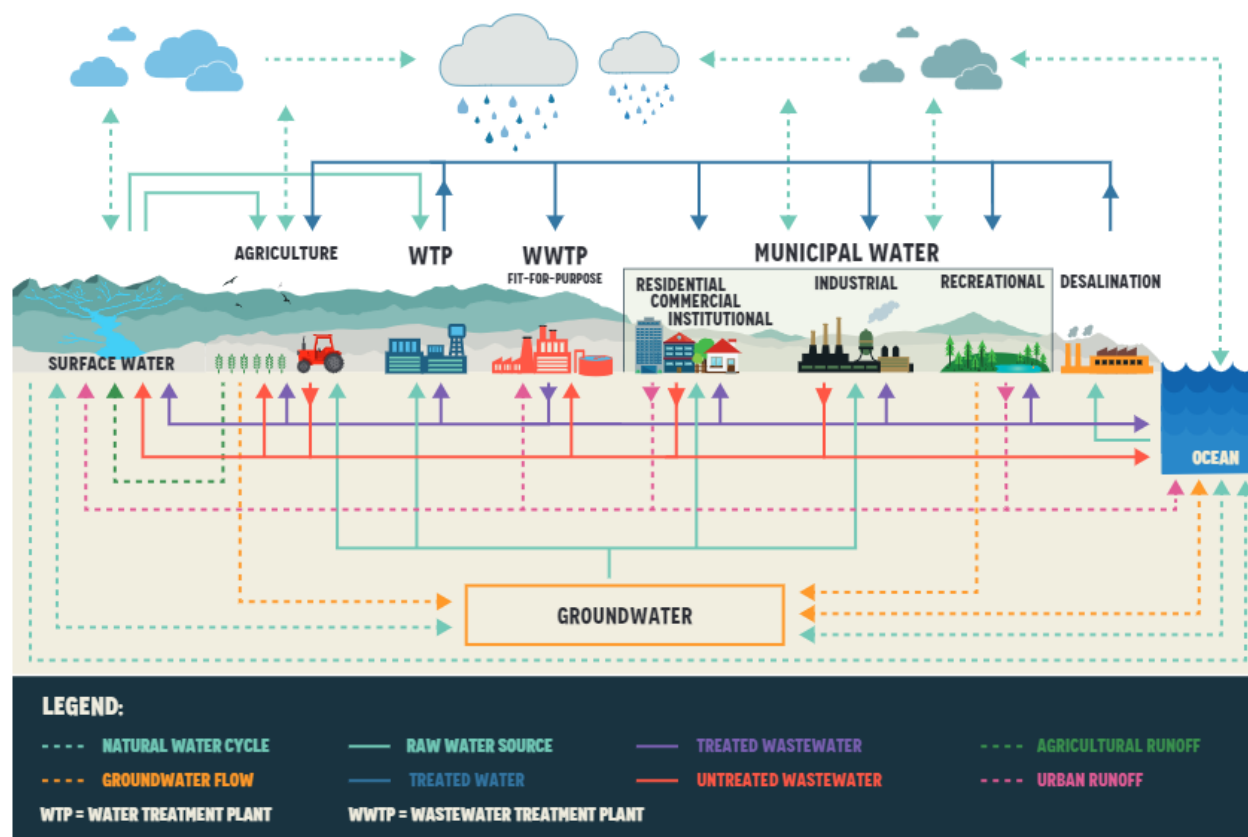


Figure 1 Role of wastewater treatment as a key driver in water quality (Water, 2017)

WWTPs receive sewage from different sources: domestic; institutions including hospitals; industrial effluent; stormwater and other urban runoff; agricultural, horticultural and aquaculture runoff (Water, 2017) (Figure 1). In the past few years, overuse and misuse of antibiotics has reached to a level that these do not have the same impact on the disease-causing bacteria (N. Li et al., 2017). According to a study, it is said that in the year of 2013, about 162 000 top of antibiotics were taken up and 58 percent of which were excreted back into the environment (Dong et al., 2019). Continuous release of antibiotics in WWTP may create a selective pressure leading to the development Superbugs or Antibiotic Resistance Bacteria (ARB) and in turn release of Antibiotic Resistance Genes (ARG). These resistance may confer resistance to more than one antibiotic (Fayad et al., 2018). The resistance in these organisms is developed by mutation or taking in the exogenous genetic material (eDNA or free DNA) (Morris et al., 1998). If this is not controlled, these superbugs may spread around the environment and a sanitary emergency could occur.

The required level of wastewater treatment depends on the capacity of the receiving water, focusing on the influence on human health and ecosystem. Tertiary treatment or advanced

treatment step is designed for meeting the specific requirements to meet the public health safety regulations set by the law. The suitability of a tertiary treatment step is evaluated on the basis of reliability, cost of operation, ability to reach the regulations set, environmental impacts etc., UV disinfection, membrane filtration, ozonation, advanced oxidation process are the most common tertiary treatment systems applied worldwide. Although these technologies have effectively removed the ARBs and ARGs, these are very expensive, and no studies have yet been done for the removal extracellular genetic material.

The need for effective and economical technologies has led to the increase of physiochemical processes for treating pollutants in wastewater. Adsorption is a process which is widely used and most efficient method for removing organic contaminants in wastewater treatment systems. Adsorption is an efficient technique as it does not provide any harmful disinfection by products. The removal capacity by adsorption for soluble and insoluble organic pollutants is known to reach almost 99.9 % (Ali et al., 2012). It can be described as surface or interface phenomenon between the pollutant and the adsorbent. Some reviews have been done to observe the adsorption of DNA onto clays, humic acids, silicas, but, no one is yet focusing on the removal of free DNA (with respect to antimicrobial resistance) in the effluent wastewater (Pietramellara et al., 2001; Solberg & Landry, 2006; Yu et al., 2013).

Transmission of Antibiotic Resistance Genes and Engineered DNA from Transgenic Biosystems in Nature (TARGETBIO) is a joint project launched by Leiden University and the Delft University of Technology, funded by the Biotechnology and Biosafety Program of Applied and Engineering Sciences Division of the Netherlands Organization for Scientific Research (NWO). This project researches the spread of foreign DNA used in the genetically modified organisms into the microbial communities present in nature.

1.2 Problem Statement

According to World Health Organization (WHO), resistance to antibiotics are one of the major threat for the global health, food security and development (World Health Organisation, 2018). In this regard, WWTPs are among the major origins of ARG and ARB dissemination in the environment (Karkman et al., 2018). WWTPs are suitable environment for a plethora of microorganisms forming complex microbial communities being the major source for the distribution of emerging pathogens, antibiotic resistance bacteria/genes (ARBs and ARGs), transgenes and mobile genetic elements (MGEs) (von Wintersdorff et al., 2016).

Conventional treatment systems can reduce ARGs by 3 orders of magnitude, 10^5 - 10^9 genomic copies L^{-1} are still in the discharged effluents (Zhang et al., 2017). Concentrations of 3.4×10^4 to 6.4×10^3 of tetracycline resistance genes were found in the effluent of WWTPs having activated sludge and chlorination as disinfection treatment (Al-Jassim et al., 2015; Pei et al., 2006). In addition, it was also found that the concentration of microbial resistance genes in the natural river (Cache La Poudre River) were in the range of 10^{-7} to 10^{-3} ARGs, normalized to 16S rRNA (Barancheshme & Munir, 2018). Therefore, concentration in the effluents of WWTPs is high and ineffective treatment before its release could lead to the spreading of antimicrobial resistance genes in the environment.

Tertiary treatments such as effluent disinfection using UV, chlorination, etc., have succeeded in ARB inactivation (Destiani & Templeton, 2019; Wu & Xu, 2019; Q.-B. Yuan et al., 2015). These studies neglected the cell-free or extracellular DNA (eDNA) which is released during cell lysis or secreted during growth. Zhang et al (2017) found that even though disinfection reduces cell-associated DNA, the cell free DNA is increased.

The advancements in the use of genetically modified organisms (GMO) raises the issue that DNA released from GMOs may increase the spread of pathogenicity, emergence of new disease by horizontal gene transfer etc., (Wang et al., 2014). The increased use of transgenic and non-transgenic crops also release high amounts of DNA into the environment (Bravo et al., 2010).

Studies have shown that eDNA in nature and in marine culture, can persist for several months or even years. These can get attached to suspended particles, sand, clay humic acids and can retain their ability to transform into bacteria (Y. Zhang et al., 2018). The concentrations of eDNA in surface water is around 0.03 to $30 \mu g L^{-1}$ and freshwater 1 to $17 \mu g L^{-1}$ (Bravo et al., 2010; Nielsen et al., 2007).

eDNA or free floating DNA has shown to well adsorb onto humic acids, clays, suspended particles due to the presence of hydrophobic interactions between the siloxane surface of the clays and proteins of the DNA. In addition to hydrophobic interactions, van der Waals forces are also said to play a role in the DNA adsorption onto minerals (Yu et al., 2013).

Bacteria can take up DNA for genetic diversity, repair and as a source for food (carbon, nitrogen, and phosphorus) (I. Chen & Dubnau, 2004). *Escherichia* and *Klebsiella* both are considered natural competent genus, being able to take free eDNA although neither of them has shown any transformation capacity in lab scale (Lerminiaux & Cameron, 2018). This would imply that if eDNA is not removed completely from the treated wastewater these could be reintroduced into nonrelated microorganisms generating new bacteria (MacGowan & Macnaughton, 2017).

Thus, focus of this research is to assess the capability of sustainable materials to adsorb DNA from the effluents of wastewater. Also, to study the mechanism of electrostatic interaction involved in the process of adsorption by changing solution chemistry. Additionally, the removal of antibiotic resistance genes/mobile genetic element and bacteria by quantifying the number of 16S rRNA, is studied in the effluent wastewater as their removal is essential before discharging into the environment.

1.3 Research question and objectives

1.3.1 Research Question

What sustainable material can be used for the removal of free floating DNA and antimicrobial resistance genes from the effluent wastewater?

1.3.2 Hypothesis

Free floating DNA can be efficiently adsorbed by porous adsorbents in the presence of effluent wastewater quality parameters by electrostatic interactions. Mobile genetic elements, antibiotic resistance genes and bacteria can also be removed by the adsorption column.

1.3.3 Objectives

The main objective of this research is to assess if adsorption could be a suitable method for the removal of free floating DNA (eDNA) from effluent wastewater at lab scale in combination with sustainable porous materials as adsorbent. The usage of porous materials is hypothesized to provide a larger surface area for the adsorption of DNA. As a case study, could adsorption be also used to remove ARGs and MGEs from the effluents of wastewater. A total of 5 ARGs – *ermB*, *sul1*, *sul2*, and *bla_{CTXM}*; 1 MGE – *int11*; All bacteria – *16S rRNA*.

The research approach to achieve the objectives can be summarized as follows (Figure 2): -

- i. Literature review to understand the what is eDNA, fate of eDNA in the process of antimicrobial spreading in the water bodies, methods to detect these DNA, mechanisms involved in the DNA adsorption.
- ii. Selection of suitable porous adsorbents for the adsorption of DNA.
- iii. Investigating the ability and mechanism involved in the DNA removal by the adsorbents in batch experiments.
- iv. The performance of the selected adsorbents was evaluated in a column by changing initial DNA concentrations and flow rate of the column.
- v. Case study - Application of the column adsorption to remove extracellular and intracellular genes from wastewater effluents separately.

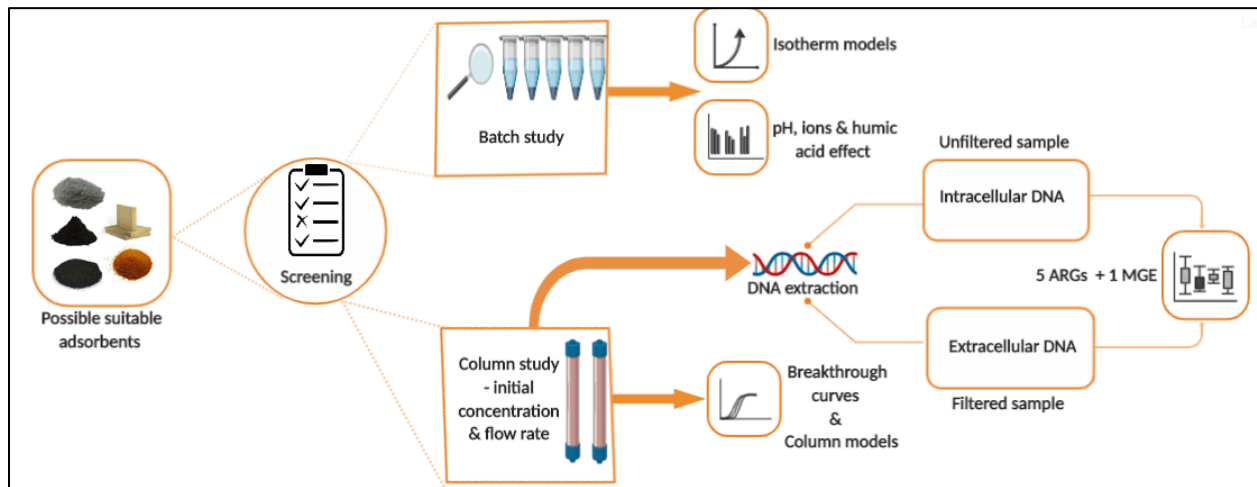


Figure 2 Workflow of the experimental approach of the lab experiments and their analysis methods. Created with BioRender

Chapter

2 THEORETICAL BACKGROUND

2.1 What is extracellular DNA?

Deoxyribonucleic acid, generally known as DNA is a molecule that contains all the necessary information necessary to build a life form. Typically, DNA is found inside the cell, around the cytoplasm (prokaryotes) or inside a differentiated nucleus (eukaryotes) which can be termed as intracellular DNA (iDNA). Like any other organism, bacteria also use DNA to store their genetic material. DNA of a bacteria is generally organized as a complex single circular or linear molecule known as bacterial chromosome (Figure 3). In addition to chromosome, bacterial cells also contain plasmids which are extra circular DNA fragments that confer to a specific property which are beneficial for the survival of a cell. Although plasmids contain useful genes such as antibiotic resistance genes, these are not necessary for growth of the bacteria as long as there is no selective pressure. Plasmids can replicate on their own of the bacterial genome and can be transferred from cell to cell (David P. Clark & Nanette J. Pazdernik, 2013; Science Learning Hub, 2019).

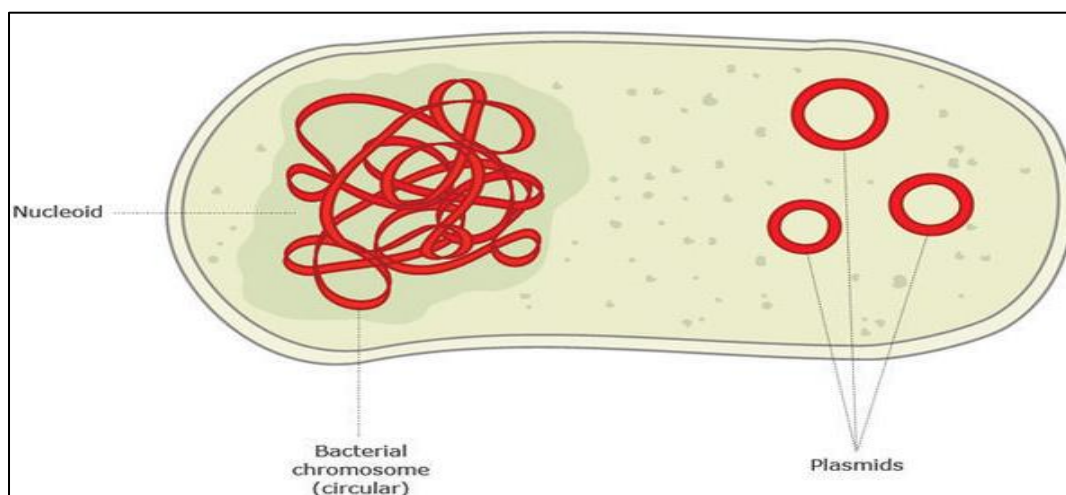


Figure 3 Bacterial DNA with a circular bacterial chromosome and plasmid (Science Learning Hub, 2019)

Like iDNA, DNA which is outside the cell membrane can be termed as extracellular DNA or eDNA. The existence of eDNA in the environment was first studied in the early 1950s and their

ability to form new microorganism through bacterial transformation (Nagler et al., 2018). The terms eDNA, naked DNA or free DNA can be defined as “the molecules present, in or released from, cells in which energy production has permanently ceased, viral DNA, and DNA secreted from metabolically active cells ” (Torti et al., 2015). eDNA may be released from single celled or multicellular organisms and can be adsorbing onto suspended particles, sand, clay, humic acids. The adsorption DNA thus, is protected from nuclease degradation. (Cai et al., 2006)

2.2 Process for the evolution of resistance bacteria

Bacterial resistance is a natural evolutionary process due to their continuous exposure to the drugs. It can be defined as the “ability of the bacterial cell to grow and survive in the presence of a drug” (Luby et al., 2016). The mechanism of acquiring genetic information by the transfer of genes between bacterium is known as Horizontal Gene Transfer (HGT). As HGT is common among bacteria, it forms the main basis for causing the rapid spread of microbial resistance. This process of gene transferring could occur between the same species or different species which can result in pathogenic bacteria producing drug resistance (Davies & Davies, 2010; Francino, 2012; Khachatourians, 1998). The transfer of genetic information having resistance could occur anywhere in the environment. HGT involves mainly 3 mechanisms namely: -

- **Conjugation** is the transfer of genetic material that takes place through a multi-step process by physical contact with donor cell and recipient cell. Conjugative systems are encoded by plasmids or by chromosome borne MGEs known as integrative conjugative elements (ICEs) (Wozniak & Waldor, 2010). ARGs are mainly associated with conjugative elements such as plasmids or transposons. The donor bacterium contains a conjugative plasmid (F plasmid) or conjugative transposon which is self-transmissible and contains all the necessary genes that can be transmitted by itself to the recipient bacteria. The genetic information in these plasmids is different from that which is already present in the chromosomes of the bacterial chromosome. Donor cell which contains a copy of the conjugative pilus or F-plasmid is called an F positive, F plus or F⁺, and the recipient cell which does not contain an F-plasmid is known as F negative, F minus or F⁻ (Biology dictionary, 2019). Transposons (transposable elements or jumping genes) are pieces of DNA encoding specific enzymes that can cut themselves from the bacterial nucleoid and reintroduce into another nucleoid of another bacterium (Kaiser, 2019). These plasmids and

transposons containing genes which could be advantageous to the neighboring species can get transferred to distantly related species of organism (Rogers, 2008).

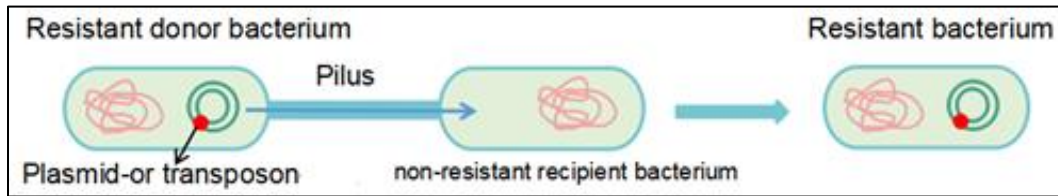


Figure 4 The process of conjugation in the evolution of a resistance bacteria (ZJUT - China 2018, 2018)

- **Transduction** is the process of DNA transfer from one bacterium to another by a virus that infect the cell (bacteriophage) and does not require any physical contact. The bacteriophage along with the pieces of DNA gets transferred to the new genome inducing the virus.

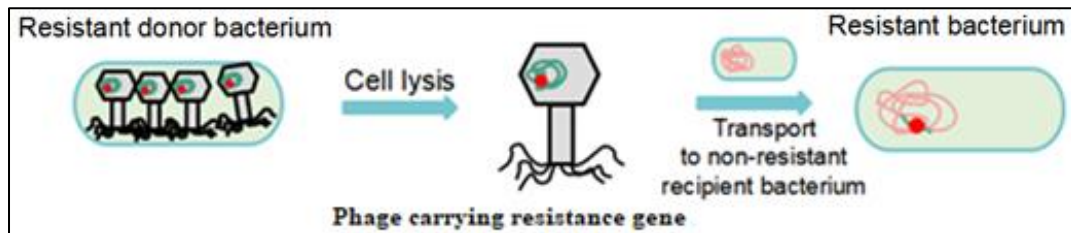


Figure 5 The process of transduction in the evolution of a resistance bacteria (ZJUT - China 2018, 2018)

- **Transformation** is the process of gene transfer which takes place by the uptake of DNA of dead bacteria or active DNA release during growth, from the environment. It is the first example that has been discovered for the exchange of genetic DNA in *Streptococcus pneumoniae* in 1972 (Israel, 2001). For the transformation to occur, the bacteria must be competent, meaning the ability of the cell to alter its genetics by taking extracellular DNA. Several bacteria such as *Acinetobacter*, *Hemophilus*, *Neisseria*, *Pseudomonas*, *Staphylococcus* and *Streptococcus* are capable of taking the free DNA and become resistant if the DNA contains resistant traits. (Lerminiaux & Cameron, 2018).

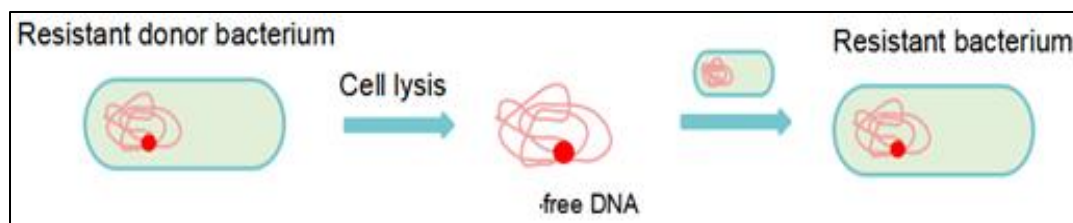


Figure 6 The process of transformation in the evolution of a resistance bacteria (ZJUT - China 2018, 2018)

2.3 How bacteria resist antibiotics?

Antibiotics are the often used group of pharmaceuticals for controlling bacterial diseases/infections in humans and animals and for livestock breeding (Barancheshme & Munir, 2019). The fast-growing resistant bacteria have made it challenging in identifying new antibiotics (Sabri et al., 2018). As given by Chroma and Kolar (2010), the resistance is achieved by

- (i) Alteration of target DNA sequences of antibiotics – mutational changes at the target gene by reducing the susceptibility to inhibition and retaining the cellular function.
- (ii) Permeability changes in the cell wall of a bacteria by restricting the antimicrobial access.
- (iii) Antibiotic efflux – pumping out the antibiotic out of the cell
- (iv) Enzymatic degradation – enzymes selectively target and destroy the function of antibiotic

2.4 Spreading of antibiotic resistance from urban to aquatic environment

The resistance can be naturally occurring or can be acquired extrinsically. Naturally occurring resistance is the characteristic of all the bacterial species or genus. Organisms which undergo a genetic change resulting in a mutant gene carrying antibiotic resistance is known as acquired resistance. Clinically, the resistance acquired extrinsically is more important due to the possibility of spreading the resistant genes in a microbial population (Chroma & Kolar, 2010). Antibiotic resistance in the environment can be spread through various modes through bacteriophages, integrons, plasmids, etc., of which genes, bacteria, and mobile genetic elements are the three main modes. (Uzuegbu, 2018).

2.4.1 Antibiotic resistance bacteria (ARBs)

Microorganisms are used to develop antibiotics. As a natural tendency these organisms also contain resistant genes to survive against their antibiotics (Munita & Arias, 2016). Thus, the presence of antibiotics in the nature is well known before the interference of humans. Resistant elements have been observed in the bacterial DNA of 30,000-year-old permafrost samples (D'Costa et al., 2011). Significant use of antibiotics in anthropogenic activities have increased the risk of bacterial resistance. The presence of residual antibiotics and metals in WWTP creates pressure on certain bacteria to acquire the resistant genes horizontally leading to the increase of ARBs (Uzuegbu, 2018). *Enterococci* and *Escherichia coli* can be used as indicator organisms for studying the presence of antibiotic resistance in wastewater as they show a history of acquired resistance (Łuczkiwicz et al., 2010; Manaia, 2014; Rizzo et al., 2013). ARBs such as *Acinetobacter* spp, *Pseudomonas*, *Enterobacteriaceae*, etc., are shown to exist in wastewater samples (Bouki et al., 2013).

2.4.2 Antibiotic resistance genes (ARGs)

The extensive of antibiotics and their partially metabolized residual discharge into the environment. Around 30-90% of the antibiotics consumed end up in WWTPs, through urine and feces where a widespread of microorganisms are present (Massé et al., 2014; Sabri et al., 2018). The occurrence of resistant bacteria is genetically controlled by ARGs (Uzuegbu, 2018). ARGs have the ability for the bacterial cells to grow in the presence of antibiotics.

ARGs have been detected in most WWTPs that receive wastewater from the community, hospital, and industry. Due to the continuous contact with bacteria in the WWTP, antibiotic residues create a driving force for the spread of ARGs. Antibiotics present in the low concentration can selection for ARG. Thus making WWTPs a potential hotspot for dissemination of ARGs (Karkman et al., 2018).

2.4.3 Mobile genetic elements (MGEs)

MGEs are fragments of DNA encoding proteins than can jump between and within the genome (Frost et al., 2005). These play an important role in the process of HGT. MGEs take the

form of plasmids, insertion sequences, transposons, and phages or combinations thereof and carry genes that are advantageous for the host bacteria in certain environmental conditions (Jansen & Aktipis, 2014).

Integrans are genetic elements that are found mostly in gram-negative bacteria having a capacity of capture and mobilize genes (Van Hoek et al., 2011). Integrans consist of gene encoding integrase enzyme (*intI*), the attachment site (*attI*) and promoter for recombination of target sites (Carattoli, 2001). Mobile integrans are widely distributed and carry gene cassettes which generally encodes antibiotic resistance and known as resistant integrans. There are four types of mobile integrans class 1 (*intI1*), class 2 (*intI2*), class 3 (*intI3*) and class 4 (*intI4*) based on the integrase enzyme. The most commonly found integrans in the effluents of WWTPs are class 1 type with concentrations ranging from 10^{10} – 10^{12} copies per liter. Class 2 and Class 3 are found in much lower concentrations (Uzuegbu, 2018).

2.5 Methods for detecting ARGs

Direct monitoring of ARGs provides valuable information on the spread of antibiotic resistance in the environment due to their rapid growth in marine systems (Luby et al., 2016). Two main approaches are applied for the identification of ARGs – classical (by culturing) and molecular (by culture-independent). Culturing the wide range of organisms is not feasible due to very costly and labor-intensive procedures. Molecular methods are such as polymerase chain reaction (PCR), real time PCR and recently Metagenomics are being extensively used for the identifying antimicrobial resistance genes. Also, only about 1% of the total known bacteria can be cultivated. In this study, the traditional method qPCR has been used for the identification of the various genes.

2.5.1 Polymerase chain reaction (PCR)

PCR is the most commonly method for detecting ARGs in both pure and mixed environmental samples which was developed in the 1980s by Kary Mullis (Anjum et al., 2017). This method is popular due to its high sensitivity, for its rapid results and direct information of the target gene sequence (Luby et al., 2016). The process of amplification of the interested gene is done in 3 steps (i) separation of the double-stranded DNA at 95°C (ii) the attachment of PCR primers to the separated single-stranded DNA (iii) elongation of the primers to produce two copies

of original DNA strand. The PCR amplified gene is then visualized by agarose gel and DNA stain by fluorescent dyes. (Anjum et al., 2017). Simultaneously false negatives are likely to be observed as several reactions occurs under the same conditions, amplification of wrong target can be observed (X.-X. Zhang et al., 2009). Another drawback of the conventional PCR is that, it's not quantitative and provides information only is the gene is present or not (Luby et al., 2016).

2.5.2 Real-time polymerase chain reaction

Real-time PCR, also known as quantitative PCR (qPCR) is developed with some improvements on traditional PCR, which along with qualitative (presence or absence) provides quantitative (copy numbers) information about the abundance of the target ARG (Luby et al., 2016). qPCR combines real-time amplification and detection target gene in a single step in the presence of fluorescent dyes in the reaction (Anjum et al., 2017). The principle of qPCR is that the initial concentration can be estimated by the threshold cycle (Ct), i.e., fluorescence reported which is greater than the minimum detection level (Arya et al., 2005). The major drawback of the design of the primers is that the sequence of gene of interest must be known prior. However, several studies for screening ARGs using PCR have been done and extensive number of primers are available in the literature (Gorecki et al., 2019).

2.5.3 Metagenomics

Metagenomics is being used for the identification of ARG in environmental samples in recent years though it was known for 20 years. Metagenome is defined as “the genomes of the total microbiota found in nature” (Y. Yang & Zhang, 2017). The advantage of this method over traditional methods is that it is culture-independent and collective genomes in a sample can be sequenced in a single step using Next Generation Sequencing (NGS) unlike PCR or qPCR (Borthong et al., 2018; Luby et al., 2016). The sequenced genomes are then can be compared with online databases for ARGs and MGEs (Y. Yang & Zhang, 2017).

2.6 Adsorption process in wastewater treatment plants

The process of adsorption in the water treatments is widely used and the most efficient method for reducing the concentrations of organic pollutants in wastewater treatment. The

advantages of using adsorption in the treatment system include low cost, flexibility, versatile design and low energy requirements (Bonilla-Petriciolet et al., 2017). The rate of adsorption, maximum amount of adsorption for the adsorbent can be found by simple batch studies. Column adsorption studies help us to determine the saturation capacity, breakthrough times, bed adsorption capacity that can be used to design the scale-up columns for treating large volumes (Bonilla-Petriciolet et al., 2017). The most widely used adsorbent in the adsorption process are is activated carbon. However, many other adsorbents such as clay, clay minerals, chitosan, nano adsorbents, zeolites, etc., are proposed for the treating wastewater. The adsorption efficiency depends on properties of the adsorbent such as grain size, surface area, pore volume; properties of the solute such as solubility, charge, aromaticity; water quality parameters such as pH, ionic strength, temperature, natural organic matter.

2.7 Mechanisms for DNA adsorption

DNA from organisms is adsorbed on clays, humic acids, and soil which protect them against degradation and retain their ability to form competent bacterial cells (Pietramellara et al., 2001). According to Wang et al. (2014) the adsorption of DNA onto mineral and organic substances can be due to

- Electrostatic Interactions
- Ligand exchange between OH^- groups on the mineral surface and OH^- groups on DNA molecules
- Hydrophobic interactions - DNA is broken down at low pH and adsorbed by soil organic matter

2.8 Possible adsorbents for DNA adsorption

Various sustainable and low-cost porous materials are available as an adsorbent. Five porous materials namely Porous Activated Carbon – Powdered and Granular, Sewage-based Biochar, Iron-oxide-coated sands and Mineral wool have been tested to choose suitable material for the study. These materials have been chosen based on their characteristics such as pore diameter, specific surface area and that could have the potential to adsorb DNA from the wastewater.

Activated carbon (AC)

Due to the high adsorption capacity of activated carbon (AC) they are used in water treatments. It is the combined name given for porous carbon that can be produced by almost any carbon-containing materials such as mainly wood, sawdust, nutshells, etc. The use of AC process in the treatment of wastewater is done is generally applied after biological treatment so that any residual organic matter and micropollutants are adsorbed. J. Chen *et al.* (2016) ARGs in constructed wetlands are removed by physical adsorption. The potential of AC in remove antibiotics has been proven but fewer studies have been done in the removal of ARG and ARB (Ahmed et al., 2015; Choi et al., 2008; Ma et al., 2017).

Biochar (BC)

Biochar or BC is a charcoal that is produced in the same manner as that of AC. The raw material used in the production of BC is a sustainably sourced biomass (Hagemann et al., 2018). BC is highly porous material with a high surface area and it is generally intended for use in soil amendment (Lehmann & Joseph, 2015). Biochar can be made with various materials such as wood biomass, sewage sludge, agricultural remains, etc., Biochar has shown as a suitable sorbent for removing micropollutants from aqueous solutions. Specifically, previous work shown by batch experiments that Biochar from wood remains was effective in adsorbing DNA from aqueous solution (Wang et al., 2014).

Iron oxide coated sand (IOCS)

The use of the coagulation process as a tertiary treatment has been extensively used in water treatment systems for treating residual particles, organic matter, and phosphorus. ARGs have been removed from the wastewater effluent using iron coagulants by the process of coagulation (N. Li et al., 2017). Silica is extensively used in the process of DNA isolations, purifications from concentrated samples in both clinical and in research because of their large specific surface area and pore size. Lorenz and Wackernagel (1987) has studied the adsorption and desorption of DNA on sand filled columns showed that the adsorption increased with the increase in salt concentration, salt valency, and pH. Combining the properties of iron and silica, iron-oxide-coated sands could be a suitable adsorbent for the DNA.

Mineral wool

Mineral wool is chemically and biologically inert substrate which is made from natural ingredients basalt rock and chalk (volcanic rock). It is made by melting stones at a temperature over 1500C and pulling it to form a fibrous material (Jørgensen, 1975). The physical properties of the mineral wool can be altered by adding additives such as calcium carbonate and can be made hydrophilic or hydrophobic (De Rijck & Schrevens, 1998). It was mainly used as thermal and acoustic insulation and later used as a growing medium in the 1960s in Denmark (De Rijck & Schrevens, 1998). Mineral wool is slightly alkaline with a pH a little higher than 7; the fibers are kept at a permanent distance with a phenol resin ensuring that the material does not lose its shape for a long time (Jørgensen, 1975). With a high porosity and good capillary qualities, the interior and the surface of the mineral wool will have a close contact with the water and hence could help trap the DNA into them. A study in India has shown that due to the large surface area of mineral wool the adsorption of ARBs has increased in wetlands (Trikannad, 2018). The material has almost no ions with an electrical conductivity of 50-100 μ S cm⁻¹ and will supply adequate water and air inside the material (De Rijck & Schrevens, 1998). Mineral wool is known to have a slow degradation rate due its composition (Wanko et al., 2016). Figure 7 shows the image of mineral wool and its characteristics.

	Characteristics Of Mineral Wool	
	Water Retention	95%
	Porosity	98%
	Density	80kg/m ³

Figure 7 Mineral wool and its properties (Drainblock, 2017)

The persistence of free DNA in the environment could create a selective pressure for the evolution of resistant bacteria by transformation. The strong evidence of free DNA adsorbing on clays, humic acids, suspended particle due to electrostatic interaction, ligand exchange and hydrophobic interaction can help us to use this phenomenon for their removal from effluent wastewater by the process of adsorption. Conducting batch and column studies on possible potential adsorbents can give us a deeper insight in understanding the mechanism to provide a solution for reducing the antimicrobial resistance from the wastewater effluent.

Chapter 3

3 MATERIAL AND METHODS

3.1 Samples used and their collection

Dewatered sewage sludge for the preparation of biochar was obtained from Harnaspolder, Dutch activated sludge municipal wastewater treatment plant without disinfection. 3 L of dewatered sludge was collected and stored at 4° C until for analysis.

Effluent wastewater was also collected from municipal wastewater plant for the study. For reducing the sample storage time and to avoid the degradation of DNA, fresh samples were used for each experiment. 1-2 L for batch studies and 4 L for the case study were collected and brought back to the lab in about 1 hour and was stored at 4° C until further experiments.

2 kg of reclaimed IOCS (1-4 mm) were obtained from AquaMinerals®, company giving a second life to the resources from (waste) water treatment. The obtained IOCS were sieved under 600 µm and stored in airtight containers.

3.2 Production of sewage-sludge biochar

The preparation of SBC was followed as per Agrafioti *et al.*, (2013). Dewatered sludge was dried in an oven at $100 \pm 1^\circ \text{C}$ for 24 h to completely remove moisture present. It was then stored in airtight bags until pyrolysis. A thick paste with a mixture of 30 g of stored sludge with 100 mL of distilled water was made by heating at 250° C. The paste was pyrolyzed in a muffle furnace at 600° C. The temperature increase rate was kept at $17^\circ \text{C min}^{-1}$. Oxygen free conditions were maintained by supplying nitrogen at a rate of 200 mL min^{-1} . After reaching the target temperature of 600° C the sample was kept for 30 min in the muffle furnace. The crucibles were then cooled to room temperature using a desiccator. The samples were then crushed and sieved at 150 µm. The sieved biochar was then stored air-tight plastic containers until further experiments.

3.3 Characterization of sewage sludge, sewage-based biochar and iron oxide coated sand

Moisture Content for Sewage sludge

The moisture content of the sewage sludge was determined by oven drying at $100 \pm 1^\circ\text{C}$ until constant weight. The equation for calculating moisture content is shown in equation 1

$$\text{Moisture content (\%)} = \frac{(W_2 - W_3)}{(W_2 - W_1)} \times 100$$

equation 1

Where W_1 is the empty mass of aluminum dish; W_2 is the mass of aluminum dish and sample; W_3 is the mass of the aluminum dish and sample at constant weight.

Ash content for sewage sludge

The ash content in the sewage sludge was calculated by oven drying at $500 \pm 50^\circ\text{C}$ for 1 hour. The heating was performed for 30 min each time, until constant weight. The ash content was determined by equation 2

$$\text{Ash content (\%)} = \frac{A - C}{A - B} \times 100$$

equation 2

Where A is the mass of aluminum dish; B is the mass of aluminum dish and sample; C is the mass of the residue and aluminum dish after heating.

Biochar yield

The yield of biochar was determined as the ratio of the produced mass to the dry mass before subjecting to pyrolysis. The equation for the biochar yield is shown in equation 3

$$\text{Biochar yield (\%)} = \left(\frac{W_2}{W_1} \right) \times 100$$

equation 3

Where W_1 is the dry mass of the sample before to pyrolysis; W_2 is the mass of the biochar after pyrolysis.

Composition of sewage-based biochar and iron oxide coated sand

Elemental analyzer (Mikrolab Kolbe, Germany) was used for determining the elemental carbon, hydrogen, nitrogen and sulfur contents of SBC and IOCS.

X-ray fluorescence diffraction technique with a Panalytical Axios Max WD-XRF spectrophotometer and the data was evaluated with SuperQ5.0i/Omnian software. The sample was sieved under 75 μm before analysis for the determination of inorganic compounds.

Surface area and pore size of sewage-based biochar and iron oxide coated sands

Nitrogen gas adsorption analyzer was used to find the surface area and pore size of SBC and IOCS, Gemini VII 2390 Surface area analyzer, Micromeritics. The adsorption equilibrium time was set to 3 s. Brunauer – Emmett – Teller (BET) method was used to calculate the surface area which incorporates a multilayer coverage. Barret, Joyner, and Halenda (BJH) method was used to calculate the pore size using the Kelvin model of pore filling. Figure 8 shows the image of SBC and IOCS.



Figure 8 Image showing the sewage-based biochar (left) and iron oxide coated sand (right) used in the research

Scanning electron microscopy

Scanning electron microscopy (SEM) using JOEL model JSM – 6010LA, was used to see the morphology. The analysis of the uncoated samples was performed in a high vacuum mode with an accelerating voltage 5 – 15 kV.

Valence state of IOCS

Mössbauer Spectroscopy technique was used to determine the valence state of iron in IOCS at Reactor Institute Delft. With a conventional constant – acceleration spectrometer the absorption

spectra for 300 K and at 4.2 K with a sinusoidal velocity spectrometer, using a ^{57}Co (Rh) source were measured. and 4.2 K. A velocity calibration curve using an $\alpha\text{-Fe}$ foil at room temperature was done. The Mössbauer spectra and the parameters can be found in the Figure A1 and Table A1, respectively (appendix).

3.4 DNA and other chemicals

UltraPure™ Salmon sperm DNA solution (Thermo Fischer Scientific, USA) for batch and column studies was used as a representative model for eDNA. The chemical and other reagents were obtained from Sigma Aldrich. Stock solutions of 1 M of salts (NaCl, $\text{CaCl}_2 \cdot 2\text{H}_2\text{O}$, $\text{MgCl}_2 \cdot 6\text{H}_2\text{O}$) and 800 mg L^{-1} humic acids were prepared by adding in ultrapure water.

3.5 Adsorption of DNA on selected materials

Batch adsorption studies were done in 2 mL sterile eppendorfs with a working solution of 1 mL. These experiments were done in triplicates and with three quality of water: Ultrapure, Tap water, and Effluent wastewater. Initial salmon sperm DNA concentration of 0, 20, 40, 60, 80, 100, 120 and 140 $\mu\text{g mL}^{-1}$ and 40 mg of tested material. The eppendorfs were mixed continuously at a constant speed of 180 rpm at 25° C until equilibrium. The mixture was then centrifuged at 13000 x g for 20 min. The DNA concentration in the supernatant was measured.

3.6 Equilibrium time for adsorption by sewage-based biochar (SBC) and iron-oxide-coated sand (IOCS)

To find the equilibrium time required for the adsorption by SBC and IOCS, batch experiments were done in 6 apothecary glass bottles of 100 mL, with a working solution of 5 mL. Initial salmon sperm DNA concentration of 100 $\mu\text{g mL}^{-1}$ was added. The mass of the adsorbent (SBC or IOCS) was added increased from 0 to 100 mg mL^{-1} in separate bottles. The bottles were kept for mixing at room temperature continuously for 24 hours. 0.5 mL of the sample was taken after every 1 h and centrifuged at 13000 x g for 20 min. The DNA concentration in the supernatant was measured.

3.7 Quantification of DNA adsorbed

The DNA concentration in the supernatant was measured by spectrophotometry at 260 nm (Biotek, Gen 5 plate reader, USA). 96-well UV flat-bottom plates (Greiner UV Star 96, Germany)

were used for the absorbance. The amount of DNA adsorbed onto the adsorbent at equilibrium was calculated using the equation 4

$$\begin{aligned} \text{Amount of DNA adsorbed } \left(\frac{\mu\text{g}}{\text{mg}}\right) \\ = \frac{\text{Initial DNA concentration } \left(\frac{\mu\text{g}}{\text{mL}}\right) - \text{Final DNA concentration } \left(\frac{\mu\text{g}}{\text{mL}}\right) * \text{Volume of sample (mL)}}{\text{Weight of adsorbent (mg)}} \end{aligned} \quad \text{equation 4}$$

3.8 Adsorption isotherms

Both Freundlich and Langmuir isotherms were used to describe DNA adsorption from the solution onto the adsorbent. The Freundlich isotherm is expressed by equation 5

$$q_e = K_F C_e^{1/n} \quad \text{equation 5}$$

Where q_e is the amount of solute adsorbed; C_e is the equilibrium adsorbate concentration; K_F is the Freundlich constant related to the adsorption capacity; $1/n$ is the heterogeneity factor and favorability of adsorption.

The Langmuir isotherm is expressed as equation 6

$$q_e = \frac{q_{max} K_L C_e}{1 + K_L C_e} \quad \text{equation 6}$$

Where q_e is the amount of adsorbate adsorbed; C_e is the equilibrium adsorbate concentration; q_{max} is the maximum monolayer adsorption capacity; K_L is the Langmuir empirical constant related to the heat of adsorption. K_L represents the adsorption affinity of the adsorbate onto the adsorbent.

3.9 Effect of pH, ionic strength and humic acid content on DNA adsorption

To evaluate the influence of pH on adsorption, experiments were done in 10mM Tris-HCl buffer with initial DNA concentration of 20 and 100 $\mu\text{g mL}^{-1}$ at pH 5, 7 and 9. The cation species effect on adsorption was also studied at initial DNA concentration of 100 $\mu\text{g mL}^{-1}$ in the presence of 0 – 60 mM Na^+ (as NaCl), Mg^{2+} (as MgCl_2), and Ca^{2+} (as CaCl_2) at pH 7, respectively. Competition with organic matter on DNA adsorption was investigated using humic acid to represent natural organic matter. The experiments were done in the presence of 0-100 mg L^{-1} humic

acids at pH 7. In order to maintain constant pH, the effect of cation species and competition with humic acids were done in Tris-HCl buffer.

3.10 Fixed bed column

Chromatography columns of dimensions 1 (inner diameter) X 15 (length) cm glass (Omnifit) with polytetrafluoroethylene fittings were used. Experiments were done with two adsorbents (IOCS and SBC) with two qualities of water: Ultrapure and effluent wastewater. 0.5 g of glass beads (250 – 300 μm) were placed at the bottom of the column for the distribution of the flow evenly through the bed. The columns were packed with adsorbents with a bed height of 5 cm (SBC – 3g, IOCS – 4g) separately. The column was fed with the aqueous solution of salmon sperm DNA using an HPLC liquid chromatography pump (Shimadzu LC-8A) employing an upward flow. To study the effect of initial DNA concentration, the experiment was conducted under three concentrations of 0.1 mg mL^{-1} , 0.3 mg mL^{-1} , and 0.5 mg L^{-1} . The inlet flow rate was kept at 0.1 mL min^{-1} . To study the effect of flow rate, experiments were conducted at 0.1 mL min^{-1} , 0.3 mL min^{-1} and 0.5 mL min^{-1} and the initial concentration was fixed at 0.3 mg L^{-1} . Schematic and the experimental setup used are shown in Figure 9 and Figure 10, respectively. 200 μL of the effluent was collected after every 15 min and were analyzed for DNA concentration spectrophotometrically. The column was kept running until the ratio of C_o/C_t reached a constant value.

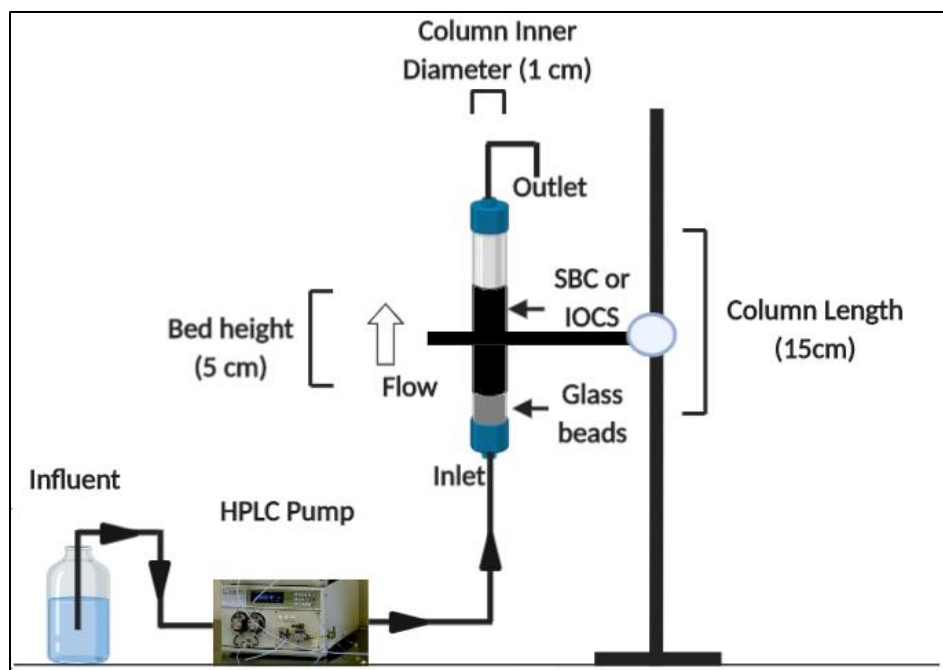


Figure 9 Schematic of the experimental set up of the column used in the study



Figure 10 Experimental setup for the column experiments

Residence time in the column

For any particle flowing through a volume, residence time can be described as the amount of time the particle spends in the volume. Residence time distribution for SBC and IOCS in the column has been performed by using NaCl salt tracer. The columns were filled with SBC or IOCS with a bed height of 10 cm and a flow rate of 1 ml min^{-1} was used. A concentration of 60 mM

NaCl salt was pulse dosed into the column. The concentration changes in the effluent was measured by electrical conductivity using PRIMO 5 Microprocessor Conductivity Meter (Hanna instruments, USA), as a function of time.

Column data analysis

Performance of a fixed bed column can be explained by the breakthrough curves. The amount of time needed for breakthrough and the shape of the curve gives the dynamic behavior of the column. The point when the effluent concentration (C_t) coming out of the column reaches 0.1% of the influent concentration (C_o) is known as the breakthrough point. Breakthrough curves are expressed as C_t/C_o versus time.

The total capacity of the column (q_{total} in mg) gives the maximum amount of DNA that can be adsorbed and is calculated by the area under the breakthrough curve given by equation 7 (S. Chen et al., 2012; Han, Wang, et al., 2009; Rouf & Nagapadma, 2015)

$$q_{total} = \frac{Q}{1000} \int_{t=0}^{t=total} C_{ad} dt$$

equation 7

Where Q is the flow rate (mL min^{-1}); t_{total} is the total flow time (min); C_{ad} is the adsorbed DNA concentration ($C_o - C_t$) (mg L^{-1}).

Equilibrium DNA uptake or maximum adsorption capacity of the column $q_{eq(exp)}$ (mg g^{-1}) of the column is given by equation 8

$$q_{eq(exp)} = \frac{q_{total}}{x}$$

equation 8

Where x is the mass of the adsorbent (SBC or IOCS) in the column (g).

Modeling of fixed-bed column

The prediction of breakthrough curve and adsorbent capacity for the adsorbate under controlled conditions can be used to design an adsorption column, prediction. Data obtained from the experiments helps in designing a full-scale column operation. Many column are available for

evaluating the efficiency of column adsorption on a full scale. In this research, data from column studies have been analyzed using the Thomas model, and Yoon-Nelson model.

Thomas model is used to estimate the absorptive capacity of the adsorbent. It uses the Langmuir isotherm and assumes no axial dispersion (Chatterjee et al., 2018). The expression for the Thomas model is given as equation 9

$$\frac{C_t}{C_o} = \frac{1}{1 + \exp\left[\left(\frac{k_{Th} q_e x}{Q}\right) - k_{Th} C_o t\right]}$$

equation 9

Where k_{Th} (mL min⁻¹ mg⁻¹) is the Thomas model constant; q_e (mg g⁻¹) is the predicted adsorption capacity; x is the mass of adsorbent (g); Q is the flow rate (mL min⁻¹); C_o is initial DNA concentration (mg L⁻¹); C_t is the effluent concentration at time t (mg L⁻¹).

Yoon-Nelson model can be used to predict the time of run before regeneration or replacement of the column becomes necessary. This model does not require any data about the characteristics of the system and the physical properties of the adsorbent (Rouf & Nagapadma, 2015). equation 10 represents Yoon-Nelson's model

$$\frac{C_t}{C_o - C_t} = \exp(K_{YN}t - \tau k_{YN})$$

equation 10

Where K_{YN} (min⁻¹) is the rate constant; τ (min) is the time required for 50% adsorbate breakthrough.

Error analysis

Nonlinear regression analysis according to the least square of errors was used to find the constants of the model. MS Excel with solver add-in function was used for estimating the values. Along with the determined coefficient (R^2), error analysis was also performed to confirm the suitability of the model. The formula for SS is shown by equation 11

$$SS = \frac{\sum[(C_t/C_0)_c - (C_t/C_0)_e]^2}{N}$$

equation 11

$(C_t/C_0)_c$ is the calculated value; $(C_t/C_0)_e$ the experimental value; N is the number of experimental points.

3.11 Extraction of DNA from wastewater effluents

In this research, two types of DNA were extracted: extracellular DNA (eDNA) and intracellular (iDNA). For assessing the eDNA the raw effluent samples were filtered with 0.22 μm filters to intercept iDNA and cell/particle-associated DNA before feeding to the column. For the extraction of eDNA, diethylaminoethyl cellulose anion exchange column (BIA separations, Slovenia) was used according to the manufacturer's instructions. The composition of the buffers used are given in the Table A2 (appendix).

35 mL were eluted from the column for the extraction. DNA from the eluted sample was precipitated by ethanol method (H. Chen et al., 2010). 60 μL of acrylamide were added to the sample and incubated the sample at -2°C for 5 min; to precipitate the DNA, 70 mL of cold pure ethanol were added and was again incubated at -20°C for 20 min and centrifuged at $4000 \times g$ for 1 hour. The supernatant from the centrifuged sample was discarded. 10 mL of 70% ethanol was used to remove the salts from viscous pellet and centrifuged at $4000 \times g$ for 10 min. The washed pellet was air-dried by removing the centrifuged supernatant. The pellet was dissolved by 100 μL of molecular grade water and stored at -20°C until further analyses. Intracellular DNA was extracted from the raw water sample without filtering using DNeasy kit Power Water (Qiagen, NL) as per the instructions given by the manufacture. The experiments were performed in duplicates

3.12 Quantification of iDNA and eDNA and their removal efficiency

The extracted DNA from filtered and unfiltered samples were quantified by fluorometry using Qubit® (Thermo Fisher Scientific, USA). The removal efficiency of iDNA and eDNA by SBC and IOCS has been calculated according to Equation 12

$$DNA\ removal\ (\%) = \frac{DNA\ in\ the\ infleunt\ (ng) - DNA\ in\ the\ effleunt\ (ng)}{DNA\ in\ the\ infleunt\ (ng)} * 100$$

Equation 12

qPCR analysis was done on the extracted genes of Table 2.

Table 2 Details of the genes used for the study (Pallares-Vega et al., 2019)

Group	Gene	Function
All Bacteria	<i>16S rRNA</i>	Normalization to the concentration of bacteria
	<i>ermB</i>	Resistance to macrolides
	<i>sul1</i>	Resistance to sulfonamides
ARGs	<i>sul2</i>	Resistance to sulfonamides
	<i>qnr S</i>	Resistance to quinolones
	<i>bla_{CTXM}</i>	Resistance to extended spectrum β-lactams
MGE	<i>int11</i>	Integrase of type 1 integrons

3.13 Real-time polymerase chain reaction

The details about oligonucleotides, probes, reaction mix and conditions for qPCR were followed as per another study (Pallares-Vega et al., 2019).

Primers and g-blocks design

gBlocks Gene Fragment (IDT, US) were used as synthetic templates for qPCR. The sequences have been taken from ResFinder for the design of primers. Four standards were used for the genes used in this study as shown in Figure 11. The sequences of the standards are given in Table A3 (appendix).

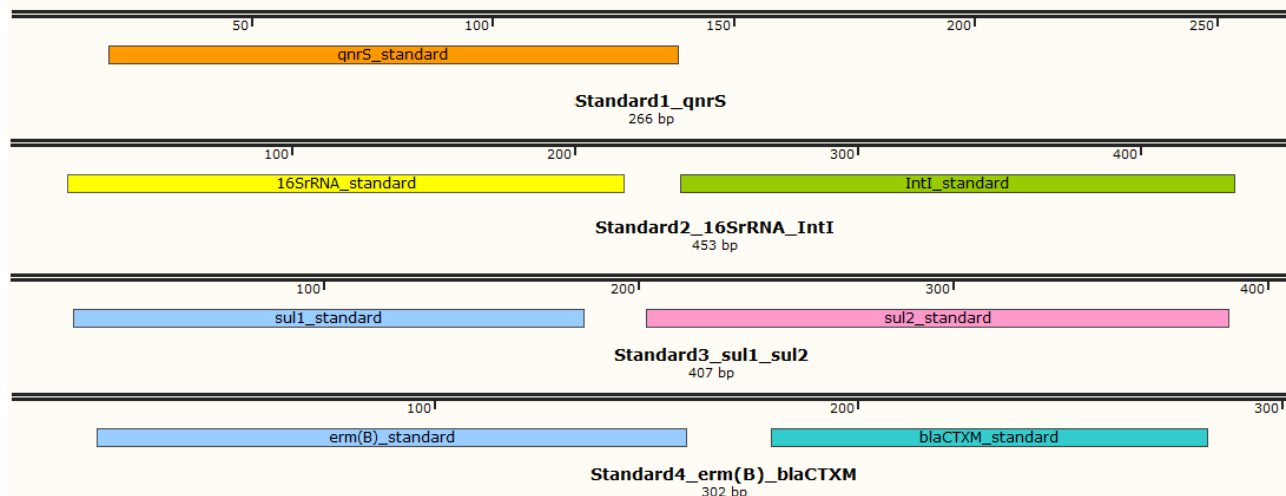


Figure 11 Standards for the qPCR of ARGs and MGE

Reaction condition and protocol for qPCR

20 μ l, consisting of 10 μ L reaction mixture (IQTM SYBR Green supermix BioRad), 7.6 μ L of molecular grade water, 0.2 μ L of forward and reverse primer, and 2 μ L of DNA were used for the qPCR analysis. These reactions were done in qTOWER3 Real-Time PCR machine, Westburg. The qPCR condition was as follows: pre-denaturation for 5 min at 95 °C, 40 cycles for separating the strands at 95 °C for 30 s, annealing at 60 °C for all genes except *sul1* (65 °C) and *sul2* (61 °C) for 30 s, expanding at 72 °C for 30 s, followed by final elongation at 80 °C for 2 min.

A melting curve was performed from 65°C to 95°C at a temperature gradient of + 0.5 °C s⁻¹. Synthetic DNA fragments containing each of the target genes were used to create a standard curve. Serial dilutions were prepared using sheared salmon sperm DNA 5 μ g mL⁻¹ (m/v) diluted in molecular grade water. Every sample was analyzed in technical triplicates. Standard curves were included in each PCR run made with at least 7 serial dilutions point and in triplicates. The average standard curve based on a standard curve from every run for each gene was created. Gene concentration values were then calculated from the curve.

3.14 Statistical analysis

Statistical analyses for the significant changes in the adsorption were done by one ANOVA and Post hoc test using MS excel for batch studies. The significant changes in *16S rRNA*, ARGs, and MGE removal by SBC and IOCS were performed with R 3.5.1 (R Foundation for Statistical

Computing., 2018) and RStudio (<https://www.rstudio.com/>). For the analysis and determination of normality of the data Shapiro-Wilk test was performed. Standard t-test for the data within normality and Wilcoxon test for non-parametric data were performed.

3.15 Physical and chemical analysis of wastewater

The wastewater pH was measured using Consort C931 pH meter. Analysis of the ions – NO_2^- , NO_3^{2-} , NO_4^+ , and PO_4^{3-} in the samples were carried out by Metrohm 881 basic IC plus and 883 compact IC pro Ion chromatography. Chemical oxygen demand (COD) was done using HACH test kits (LCK 1414 – 5-60 mg L^{-1}) in a HACH direct reading DR 3900 Spectrophotometer. Color was analyzed in the samples before and after treatment using UV-VIS spectrophotometer at a wavelength of 410 nm.

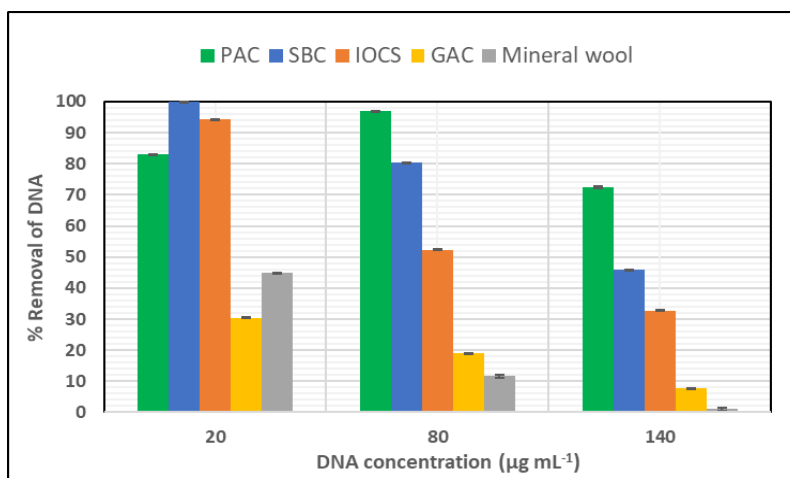
Chapter

4 RESULTS

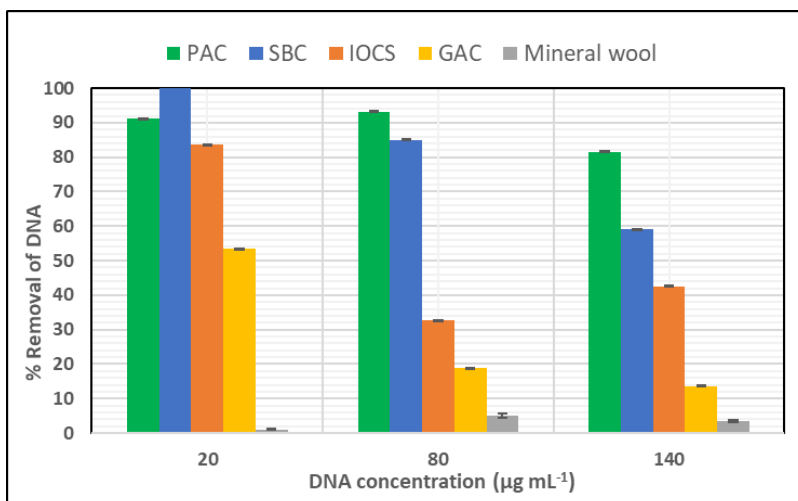
The results of the various experiments conducted in the study are presented in this chapter. The results are presented in the order of the experiments conducted.

4.1 Selection of a suitable adsorbent

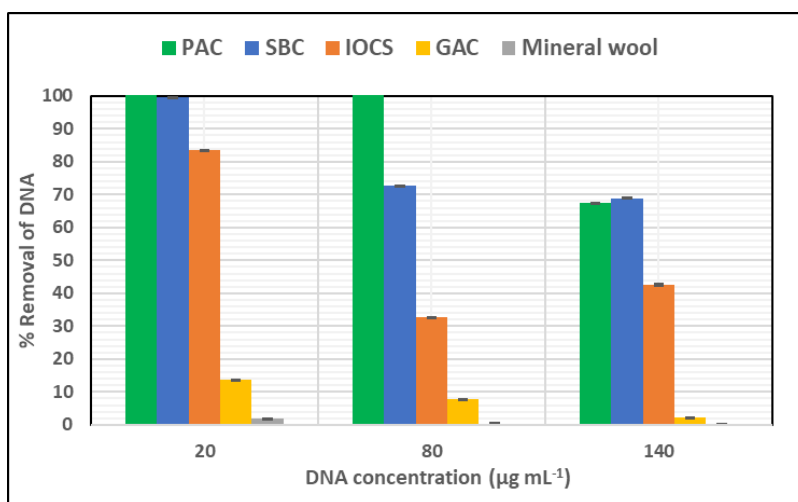
Figure 12 (a), (b) and (c) show the percentage of salmon sperm DNA removed by adsorption on to the various adsorbents chosen in ultrapure water, tap water, and effluent wastewater respectively. Highest removal (80 – 100%) was seen in powdered activated carbon at 20, 80 and 140 $\mu\text{g mL}^{-1}$ of DNA concentrations in ultrapure water, tap water, and effluent wastewater. Sewage-based biochar (SBC) and Iron-oxide-coated sands (IOCS) showed similar results (80 – 100%) as that of PAC at all DNA concentration. Granular activated carbon and mineral wool showed the least removal (<50%) at all concentrations.



(a) ultrapure water



(b) tap water



(c) effluent wastewater

Figure 12 DNA removal in percentage with powdered activated carbon, sewage-based biochar, iron oxide coated sands, granular activated carbon and mineral wool in (a) ultrapure water (b) tap water (c) effluent wastewater

4.2 Characteristics of the selected adsorbent

Table 1 shows the physical properties of sewage sludge. These are calculated on raw sludge as obtained from the treatment plant. The physical and chemical properties of SBC are shown in Table 2. High oxygen content (37 %) was seen. This could be due to the absorption of oxygen from the surrounding as they were not dried before the analysis. The slight difference in the percentage from the previous works could be due to the difference composition of the sewage sludge. Carbon, hydrogen, and nitrogen are in the range from the sewage-based biochar produced

in other works (Agrafioti et al., 2013; Xu et al., 2018). Other minor compounds such as copper, potassium, zinc, chloride, manganese was below 1%.

Table 1 Physical properties of sewage sludge

Parameter	Unit	Value
Moisture	%	78.9 ± 0.7
Volatile	%	68.1 ± 1.0

Table 2 Physical and chemical properties of sewage-based biochar

Parameter	Sewage-based biochar
Biochar yield (%)	38.6
BET surface area (m² g⁻¹)	32.4
Pore size (nm)	10.1
Carbon (%)	14.1
Hydrogen (%)	1.7
Oxygen (%)	37.4
Nitrogen (%)	1.9
Sulphur (%)	19.5
Phosphorus (%)	7.7
Calcium (%)	4.26

Magnesium (%)	5.6
Iron (%)	3.9
Silica (%)	3.2
Aluminum (%)	1.3

Table 3 shows the properties of IOCS. The pore size of SBC is greater than the IOCS although the surface area of IOCS is almost 5 times higher than SBC. The high surface area (in $164 \text{ m}^2 \text{ g}^{-1}$) in IOCS could be due to the presence of more pores (porosity) of smaller size.

Table 3 Properties of iron oxide coated sands

Parameter	Iron-oxide-coated sand
Particle size	< 13 nm
BET surface area ($\text{m}^2 \text{ g}^{-1}$)	164.95
Pore size (nm)	6.2
Valence of iron	Ferrihydrite (Fe^{3+})
Iron (%)	27.30
Silica (%)	23.61
Carbon (%)	2.07
Hydrogen (%)	3.28
Nitrogen (%)	0.01

Figure 13 and Figure 14 show the SEM micrograph of SBC and IOCS, respectively. A lot of lumps and holes are seen in IOCS and the size of the holes are large. Whereas SBC shows fine pores with uneven cavities.

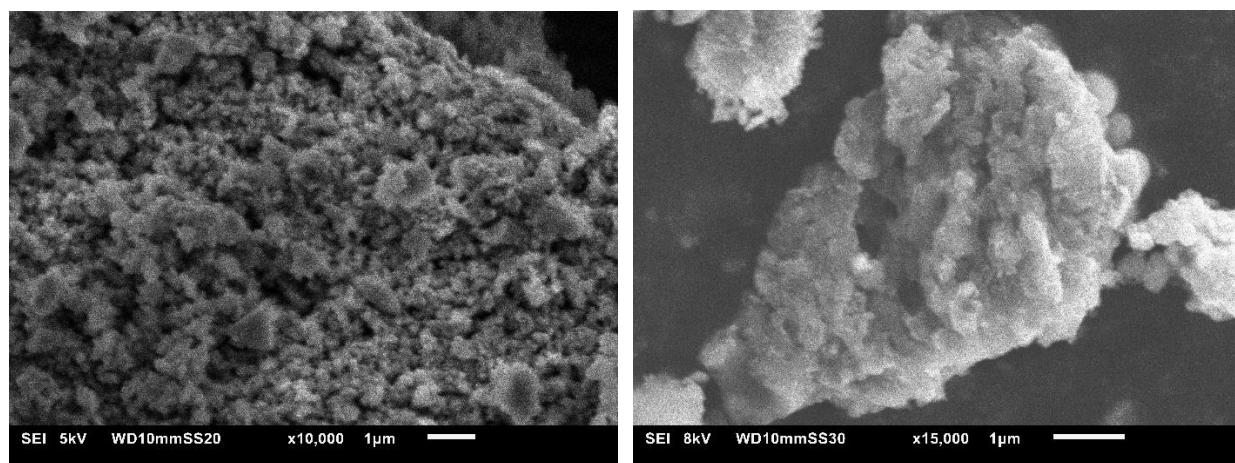


Figure 13 Scanning electron microscopy (SEM) image of sewage-based biochar

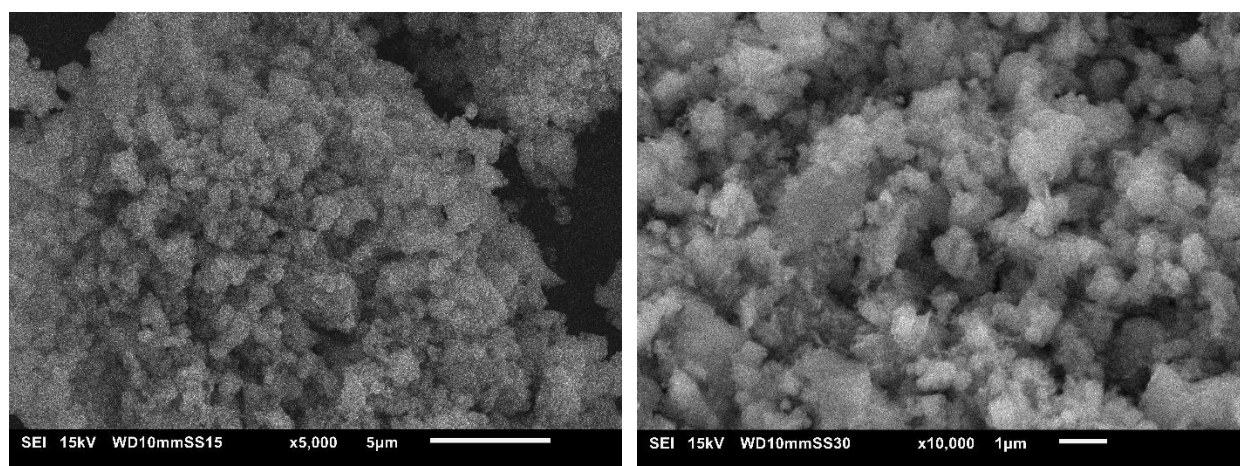
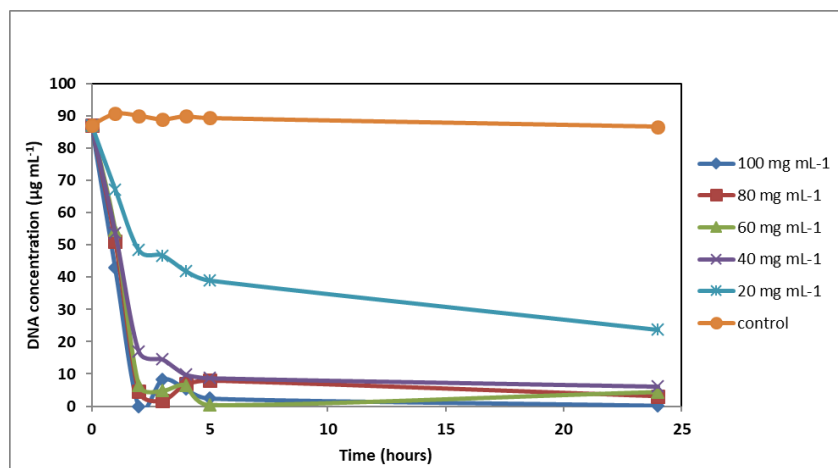


Figure 14 Scanning electron microscope image (SEM) of iron oxide coated sand

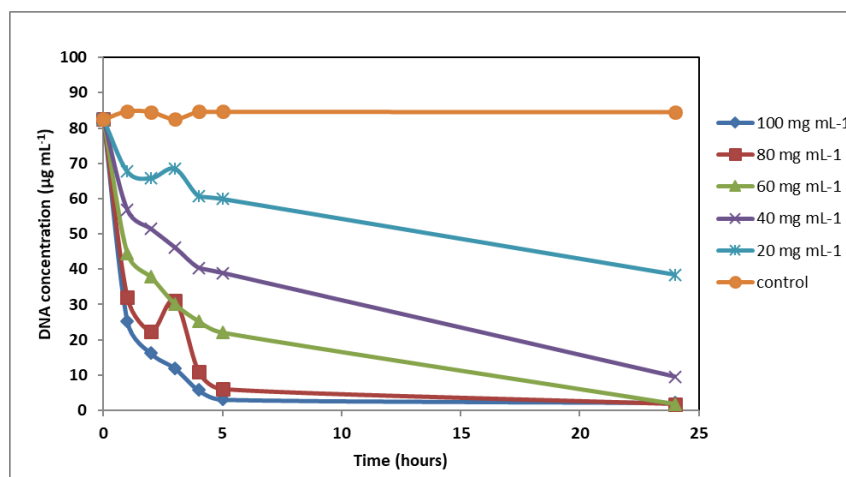
4.3 Equilibrium time for adsorption

Figure 15 (a), (b) and (c) show the adsorption capacity of SBC and IOCS with reaction time from 0 to 24 h respectively. The initial DNA concentrations in these experiments was $100 \mu\text{g mL}^{-1}$. Rapid adsorption process was seen, with a significant increase in DNA adsorption from 0 to 2 h in both SBC and IOCS and slowed down over the next 2 - 24 h. The equilibrium adsorption

for SBC was 2 h and 5 h for IOCS, after which amount of DNA was observed with time was not significant. This phenomenon of IOCS needed a longer equilibrium time is also seen in the column study as will be discussed further. Also, it can be observed that 40 – 60 mg mL⁻¹ of SBC was sufficient to adsorb 100 µg L⁻¹ of DNA. Almost double the amount of SBC (80 – 100 mg mL⁻¹) is needed for IOCS to completely adsorb 100 µg L⁻¹ of DNA.



(a) Sewage-based biochar



(b) Iron oxide coated sands

Figure 15 Equilibrium time for sewage-based biochar with an initial DNA concentration of 100 mg L⁻¹ with the adsorbent ranging from 0 to 100 g L⁻¹ (a) sewage-based biochar (b) iron-oxide-coated sands

4.4 Adsorption isotherms parameters

Both Langmuir and Freundlich isotherms were used to fit the data. Table 4 shows the Langmuir and Freundlich parameters for SBC and IOCS in different qualities of water. Figure A2 (appendix), Figure A3 (appendix) and Figure A4 (appendix) show the adsorption isotherms of

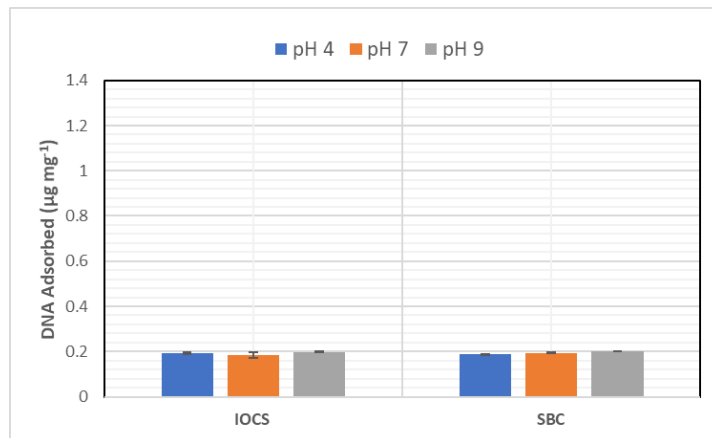
DNA in ultrapure water, tap water and effluent water, respectively for SBC and IOCS. Comparing the R^2 value, the adsorption data can be better described by the Freundlich isotherm model suggesting multilayer adsorption with heterogeneous distribution of active adsorption sites. R^2 of 0.99 and 0.91 for the effluent water for SBC and IOCS, respectively could also suggest that the water matrix in effluent water could increase the adsorbent-adsorbate interaction (Reed & Matsumoto, 1993). From the Freundlich parameters:- the smaller the $1/n$ is, the greater the heterogeneity (Dada et al., 2012). For the adsorption to be favorable the value of n should lie between one to ten (Desta, 2013). From the parameters in Table 4, the value of n lies within the range indicating that adsorption of DNA onto the SBC and IOCS is favorable and the adsorption is driven by physical process.

Table 4 Freundlich and Langmuir parameters for DNA adsorption on adsorbents in ultrapure water, tap water and effluent wastewater

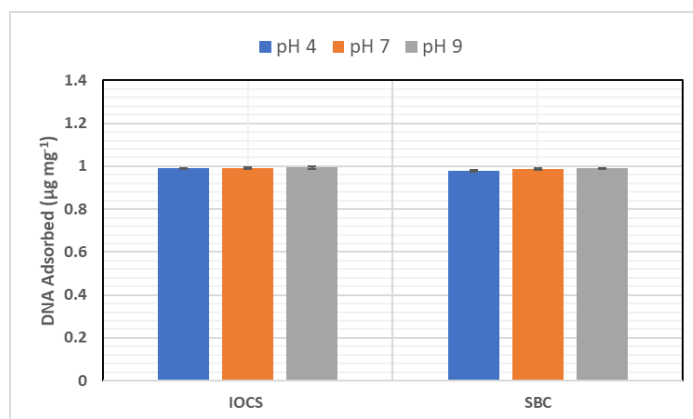
Adsorbent	Type of water	Freundlich			Langmuir		Correlation coefficient R^2	
		K_F (mg g ⁻¹)	$1/n$	n	q_{max} (mg g ⁻¹)	K_L (L mg ⁻¹)	Freundlich	Langmuir
Sewage-based biochar	Ultrapure water	1.395	0.127	7.874	2.211	1.808	0.95	0.89
	Tap water	1.071	0.171	5.848	2.099	0.433	0.86	0.85
	Effluent water	0.976	0.194	5.155	1.998	0.612	0.99	0.92
Iron oxide coated sand	Ultrapure water	0.336	0.313	3.195	1.607	0.056	0.81	0.78
	Tap water	3.224	0.244	4.098	2.944	41.190	0.89	0.84
	Effluent water	0.205	0.614	1.629	5.762	0.013	0.93	0.89

4.5 Effect of salts, pH, and humic acid on DNA adsorption

The effect of pH on DNA adsorption by SBC and IOCS has been shown in Figure 16 (a) and (b) with initial concentration of DNA were $20 \mu\text{g mL}^{-1}$ and $100 \mu\text{g mL}^{-1}$ respectively. DNA has shown to be adsorbed efficiently by clays or humic acid at low pH due to the decrease in repulsion between clays and DNA as both are considered to be negatively charged (Saeki et al., 2011). One way ANOVA was conducted to compare the effect of pH on the DNA adsorption by SBC and IOCS. There were no significant differences ($p > 0.05$) in the DNA adsorption values as a result of different pH conditions tested. The statistical values are given in Table A8 - Table A11 (appendix). The pH effect on DNA adsorption by SBC observed in this study contradicts the previous work done on DNA adsorption with willow wood biochar. (Wang et al., 2014).



(a) $20 \mu\text{g mL}^{-1}$



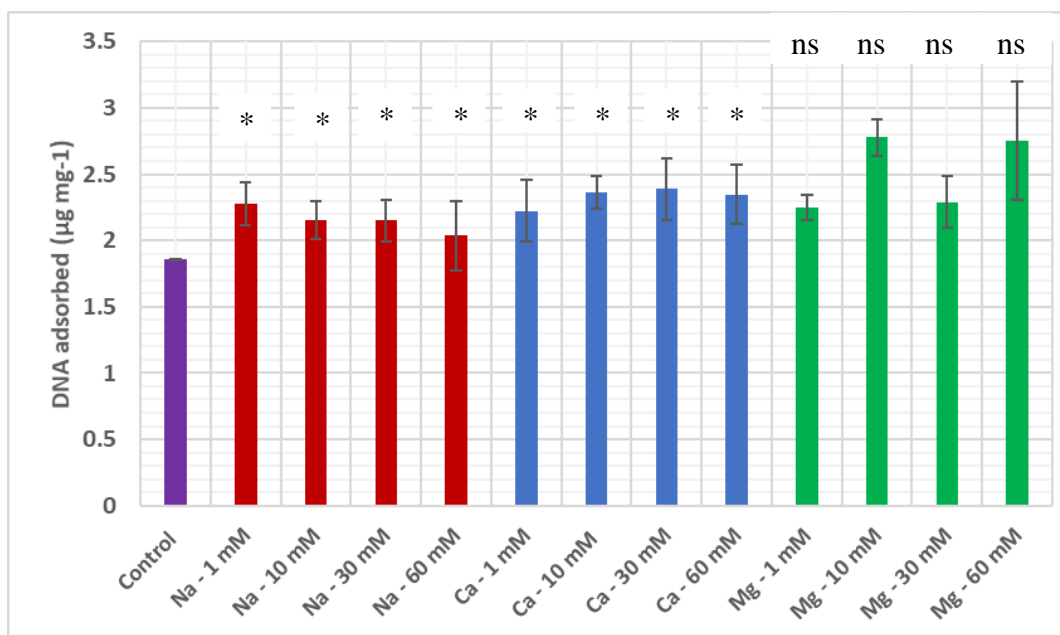
(b) $100 \mu\text{g mL}^{-1}$

Figure 16 The influence of solution pH (4,7 and 9) on adsorption of DNA by sewage-based biochar and iron-oxide-coated sands with an initial concentration of (a) $20 \mu\text{g mL}^{-1}$ and (b) $100 \mu\text{g mL}^{-1}$. No significant difference was found in the DNA adsorption due to change in the pH ($p > 0.05$)

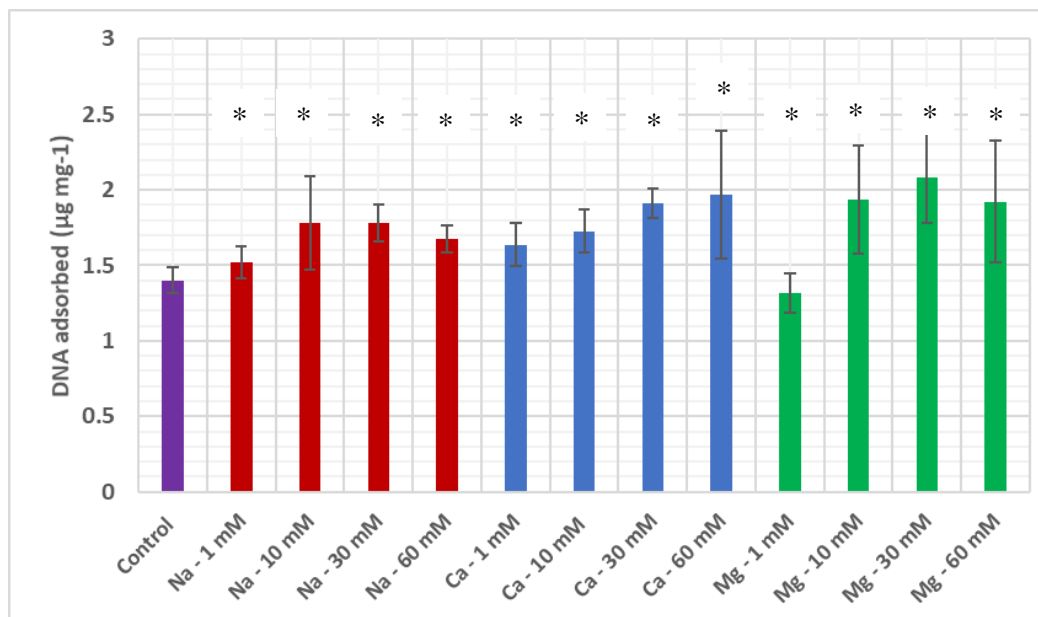
Figure 17 (a) and (b) show the influence of ions on the adsorption of DNA by SBC and IOCS at pH 7 with DNA concentration of $100 \mu\text{g mL}^{-1}$. Significant differences in the DNA adsorption were seen by one way ANOVA and Post hoc test.

The addition of Na^+ ions from 1 – 30 mM shows a significant decrease from $2.3 \mu\text{g mg}^{-1}$ to $2.0 \mu\text{g mg}^{-1}$ ($p > 0.05$) in DNA adsorption in SBC relative to control (without any addition of ions). A significant amount of increase in the DNA adsorption was seen with the addition of Ca^{2+} ($p > 0.05$). The addition of Ca^{2+} ions from 1 – 30 mM increased the adsorption from 1.4 to $2 \mu\text{g mg}^{-1}$. On the other hand, no significant differences ($p < 0.05$) were seen in DNA adsorption with the addition of Mg^{2+} ions.

A significant increase ($P < 0.05$) of adsorption was seen in with the addition of Mg^{2+} and Ca^{2+} was also seen in IOCS. The addition of Ca^{2+} also increased the adsorption from 16.9 – 40.5 %. The addition of 1 – 60 mM of Mg^{2+} increased the adsorption from 37.3 – 48.8 % relative to the control (without any ions).



(a) sewage-based biochar



(b) iron oxide coated sands

Figure 17 The influence of Na^+ , Ca^{2+} and Mg^{2+} ranging from 1 mM to 60 mM on DNA adsorption with an initial concentration of $100 \mu\text{g mL}^{-1}$ by (a) sewage-based biochar (b) iron oxide coated sands. (*) $p > 0.05$, ns: no significant changes

Figure 18 shows the effect of humic acids on DNA adsorption with DNA concentration of $20 \mu\text{g mL}^{-1}$ at a pH 7. The increase in the humic acid concentration showed a clear reduction in DNA adsorption with SBC whereas no clear effect was seen with IOCS.

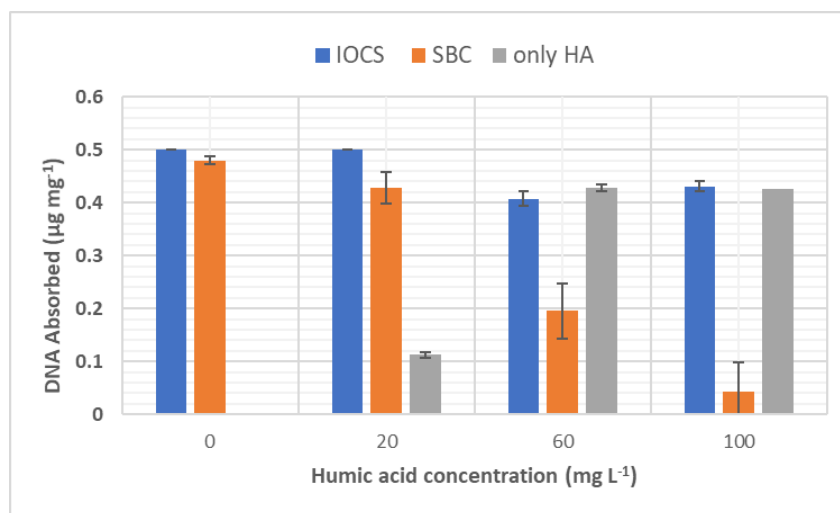
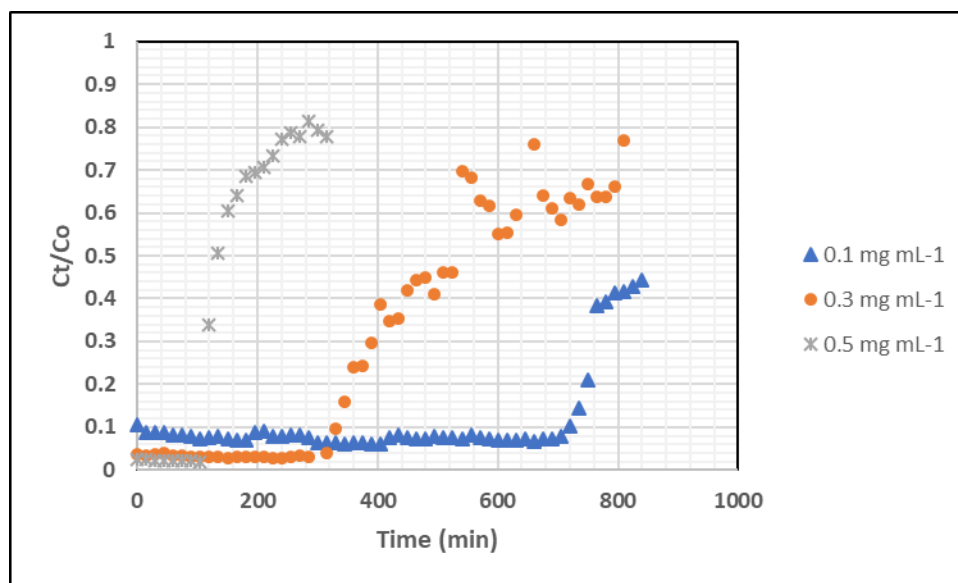


Figure 18 The influence of humic acids on adsorption of DNA by iron oxide coated sand and sewage-based biochar with an initial concentration of $20 \mu\text{g mL}^{-1}$

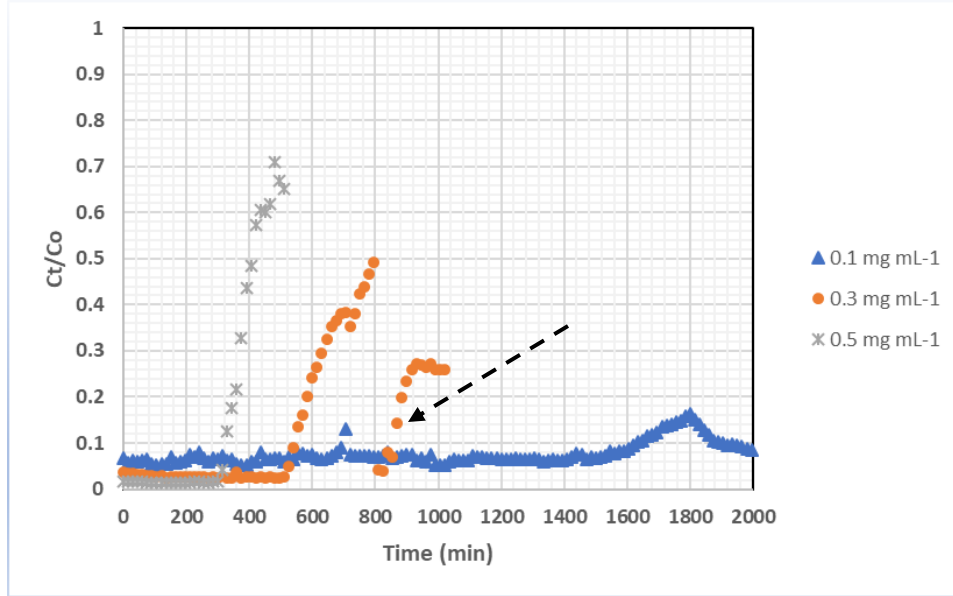
4.6 Column study

Effect of initial concentration

The performance of the column with SBC and IOCS was done at various initial DNA concentrations keeping other conditions constant in ultrapure and effluent water. Figure 19 and Figure 20 represent the breakthrough curves for SBC and IOCS respectively. The breakthrough time appears to increase when the initial concentration from 0.1 to 0.5 mg mL⁻¹ in effluent water than in ultrapure water. This trend is seen in both SBC and IOCS which might be due to the interaction of ions in the effluent water with DNA that could enhance the DNA adsorption. A drop in the breakthrough curve of SBC of effluent water is observed with an initial concentration of 0.3 mg mL⁻¹ as seen in Figure 19 (b) effluent water and with a flow rate of 0.1 mL min⁻¹ Figure 21(b). The column was stopped overnight (~ 12 h) as samples could not be collected, thus creating an interruption in the flow of the column. After restarting the flow, a new breakthrough curve was observed.

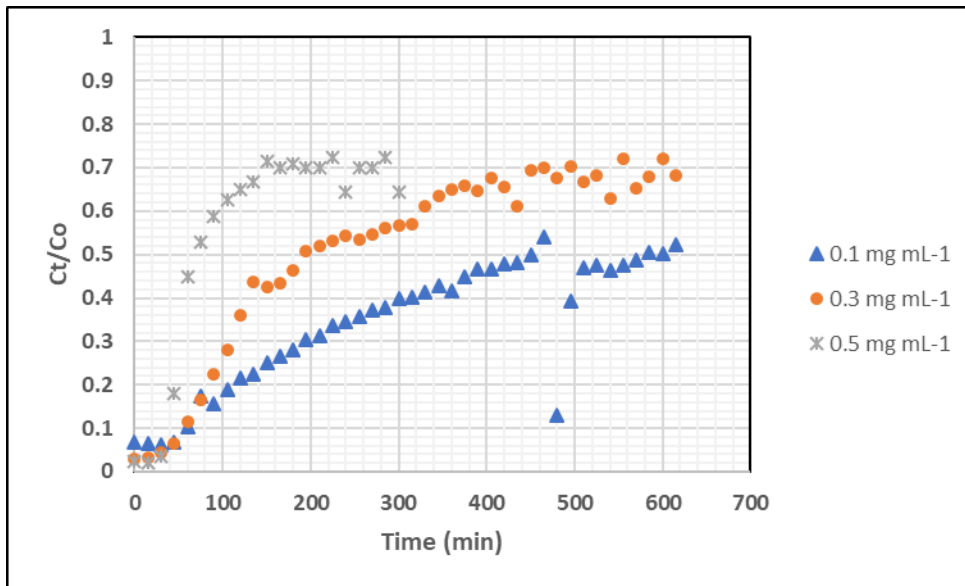


(a) Ultrapure water

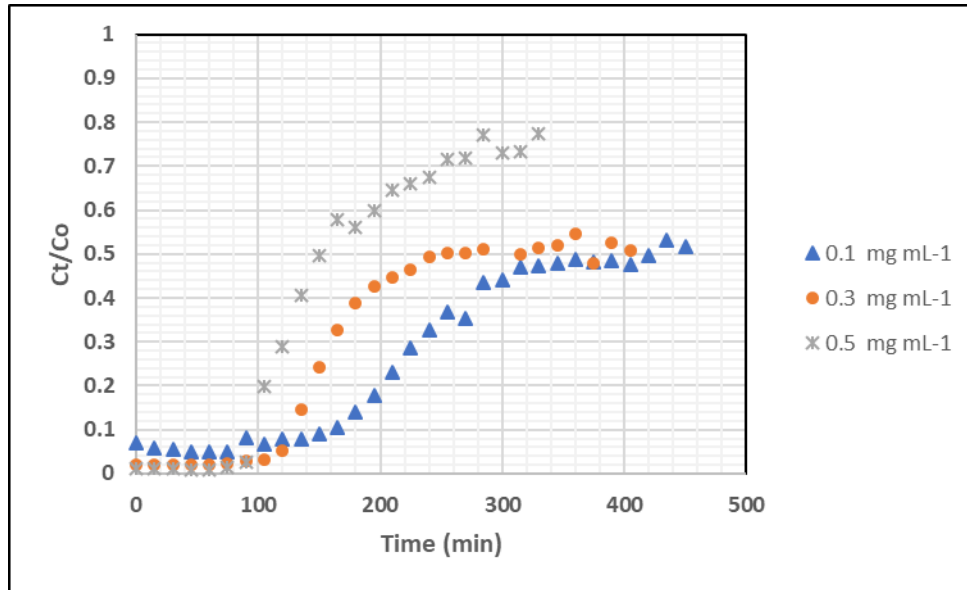


(b) Effluent wastewater

Figure 19 Comparison of experimental breakthrough curves for adsorption of DNA onto sewage-based biochar at different initial DNA concentrations 0.1 mg mL^{-1} , 0.3 mg mL^{-1} , and 0.5 mg L^{-1} (a) Ultrapure water (b) Effluent wastewater The arrow represents the effect of interruption of the column overnight



(a) ultrapure water

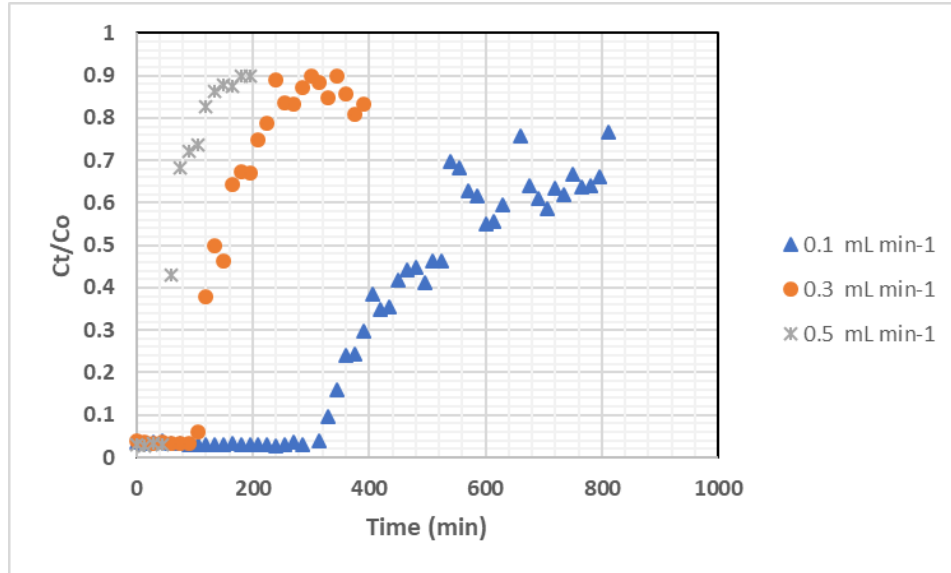


(b) effluent wastewater

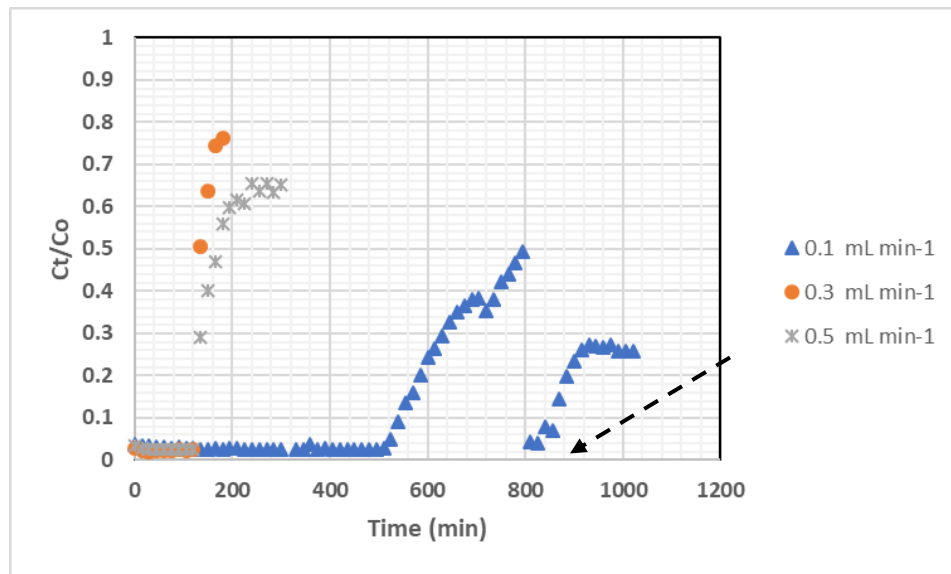
Figure 20 Comparison of experimental breakthrough curves for adsorption of DNA onto iron oxide coated sand at different initial DNA concentrations 0.1 mg mL^{-1} , 0.3 mg mL^{-1} , and 0.5 mg L^{-1} (a) ultrapure water (b) effluent wastewater

Effect of change of flow rate

The effect of the feed flow rate was conducted by changing the flow rate from $0.1 - 0.5 \text{ mL min}^{-1}$ keeping other conditions constant in ultrapure and effluent water. Figure 21 and Figure 22 show the breakthrough curves for different flow rates in SBC and IOCS respectively. The breakthrough occurred in less time (within 60 min) with the increase in the flow rate from 0.1 to 0.5 min mL^{-1} in ultrapure and effluent water. The curve becomes steeper as the flow rate increases indicating that mass transfer zone to be reduced. The residence time distribution of SBC and IOCS has been shown in Figure A12 (appendix).

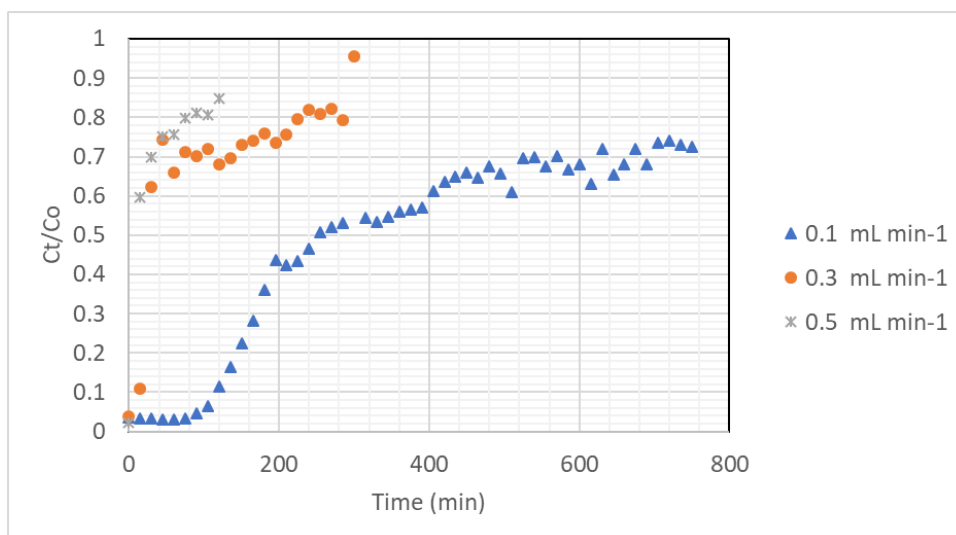


(a) Ultrapure water

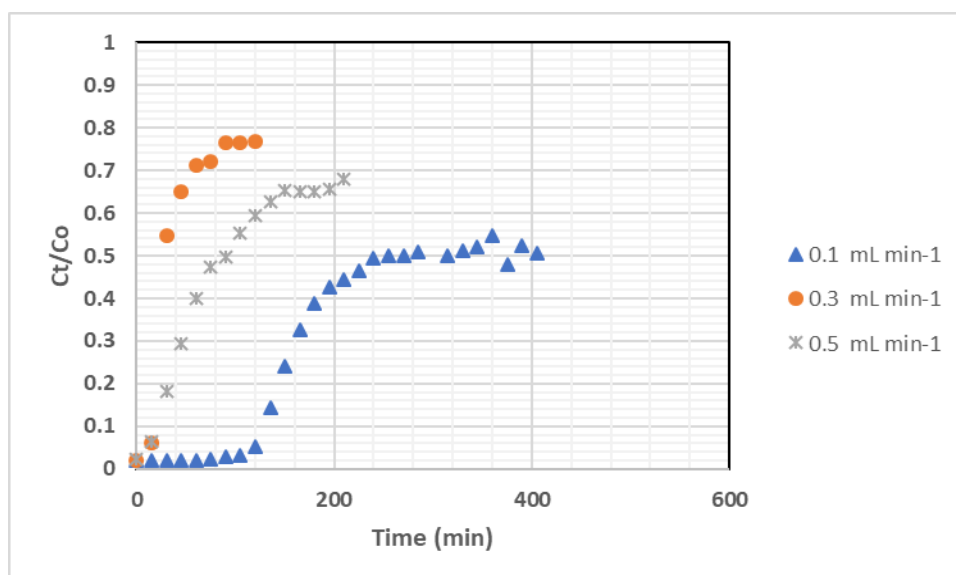


(b) Effluent wastewater

Figure 21 Experimental breakthrough curves for adsorption of DNA onto sewage-based biochar at different flow rates 0.1 mL min^{-1} , 0.3 mL min^{-1} and 0.5 mL min^{-1} (a) Ultrapure water (b) Effluent wastewater. The arrow represents the effect of interruption of the column overnight



(a) Ultrapure water



(b) Effluent wastewater

Figure 22 Experimental breakthrough curves for adsorption of DNA onto iron-oxide-coated sands at different flow rates 0.1 mL min^{-1} , 0.3 mL min^{-1} and 0.5 mL min^{-1} (a) Ultrapure water (b) Effluent wastewater

Thomas model

The data from the column study experiments was fitted with Thomas model to investigate the behavior of DNA adsorption onto SBC and IOCS in ultrapure and wastewater effluent. The Thomas rate constant (k_{th}) ($\text{mL min}^{-1} \text{ mg}^{-1}$) and maximum DNA adsorption per gram of SBC or ICOS (mg g^{-1}) were calculated by nonlinear regression. The determined coefficient (R^2) and SS values and the calculated and experimental values of adsorption capacity are listed in Table 5 (a)

and (b) and Table 6 (a) and (b) for SBC and IOCS respectively. A comparison of the R^2 (> 0.80 for ultrapure water, > 0.90 for effluent wastewater), SS values (less than 0.05) suggesting a good fit of the model. Also, comparing the adsorption capacity values obtained from calculation (q_e) and experiment ($q_{e (exp)}$) were close for the given operating conditions suggesting that Thomas model could be used to describe the column data for DNA adsorption. The plots of the Thomas model are shown in Figure A8 and Figure A9 for IOCS and SBC respectively.

Table 5 Parameters of Thomas model using nonlinear regression analysis and the equilibrium DNA uptake ($q_{e (exp)}$) for sewage-based biochar under various conditions in (a) ultrapure water (b) effluent wastewater. SS as the deviation from empirical data

C_0 (mg L^{-1})	Q (mL min^{-1})	$k_{th} (10^{-3})$ ($\text{mL min}^{-1} \text{mg}^{-1}$)	q_e (mg g^{-1})	R^2	SS (10^{-3})	$q_{e (exp)}$ (mg g^{-1})
100	0.1	90.3	2.33	0.83	4	2.91
300	0.1	27.2	3.38	0.92	4.3	3.24
500	0.1	44.9	2.13	0.89	10.9	2.87
300	0.3	39.3	6.44	0.88	9.1	7.16
300	0.5	133.5	3.33	0.93	13.4	3.85
<i>(a) ultrapure water</i>						
C_0 (mg L^{-1})	Q (mL min^{-1})	$k_{th} (10^{-3})$ ($\text{mL min}^{-1} \text{mg}^{-1}$)	q_e (mg g^{-1})	R^2	SS (10^{-3})	$q_{e (exp)}$ (mg g^{-1})
100	0.1	-	-	-	-	-
300	0.1	39.7	4.34	0.95	0.8	3.30
500	0.1	32.7	6.08	0.96	3.1	7.20
300	0.3	199.5	4.34	0.94	5.8	4.27
300	0.5	80.1	7.43	0.90	6.7	7.06
<i>(b) effluent wastewater</i>						

Table 6 Parameters of Thomas model using nonlinear regression analysis and the equilibrium DNA uptake ($q_{e (exp)}$) for iron-oxide-coated sands under various conditions in (a) ultrapure water (b) effluent wastewater. SS as the deviation from empirical data

C_0 (mg L ⁻¹)	Q (mL min ⁻¹)	$k_{th} (10^{-3})$ (mL min ⁻¹ mg ⁻¹)	q_e (mg g ⁻¹)	R^2	SS (10 ⁻³)	$q_{e (exp)}$ (mg g ⁻¹)
100	0.1	34.6	1.26	0.93	1.2	1.31
300	0.1	19.4	2.06	0.85	6.8	1.65
500	0.1	11.2	2.72	0.78	16.2	1.63
300	0.3	18	2.81	0.64	12.4	3.66
300	0.5	91.2	1.61	0.78	18	1.81

(a) ultrapure water

C_0 (mg L ⁻¹)	Q (mL min ⁻¹)	$k_{th} (10^{-3})$ (mL min ⁻¹ mg ⁻¹)	q_e (mg g ⁻¹)	R^2	SS (10 ⁻³)	$q_{e (exp)}$ (mg g ⁻¹)
100	0.1	35.5	1.46	0.74	10.1	1.24
300	0.1	48.8	1.52	0.89	4.9	1.64
500	0.1	26.3	1.93	0.88	9.6	2.61
300	0.3	68.6	1.60	0.77	15.4	1.71
300	0.5	31.7	3.69	0.84	5.1	2.54

(b) effluent wastewater

Yoon- Nelson model

The breakthrough behavior of DNA adsorption on SBC and IOCS was also studied by applying a model developed by Yoon -Nelson to obtain the values of K_{YN} rate constant ($L \text{ min}^{-1}$) and τ the time required for the 50% DNA breakthrough. The determined coefficient (R^2), SS values (deviations from actual empirical data) and constants are listed in the Table 7 (a) and (b) and Table 8 (a) and (b) for SBC and IOCS respectively. As seen from the table the values of K_{YN} increased and τ decreased with increasing initial concentration and with increasing flow rate until 0.3 mL min^{-1} . The experimental τ were not similar to the computed values of τ , so the correlation between the experimental and Yoon-Nelson model deviated significantly. The plots of the Yoon- Nelson model is shown in Figure A10 and Figure A11 for IOCS and SBC respectively.

Table 7 Parameters of Yoon-Nelson model using nonlinear regression analysis and the equilibrium DNA uptake ($q_e \text{ (exp)}$) for sewage-based biochar under various conditions in (a)ultrapure water (b) effluent wastewater. SS as the deviation from empirical data

C_0 (mg L^{-1})	Q (mL min^{-1})	K_{YN} (10^{-3}) (L min^{-1})	τ (min)	R^2	SS (10^{-3})	τ_{exp} (min)
100	0.1	10.57	849	0.87	7.22	855
300	0.1	5.97	521	0.79	81.84	530
500	0.1	7.98	119	0.87	34.11	135
300	0.3	12.24	106	0.88	953.25	150
300	0.5	20.71	36	0.95	230.52	50

(a) *ultrapure water*

C_0 (mg L ⁻¹)	Q (mL min ⁻¹)	K_{YN} (10 ⁻³) (L min ⁻¹)	τ (min)	R^2	SS (10 ⁻³)	τ_{exp} (min)
100	0.1	-	-	-	-	-
300	0.1	6.81	793.	0.95	3.37	795
500	0.1	14.58	420	0.96	14.4	405
300	0.3	29.95	137	0.93	89.24	135
300	0.5	14.2	156	0.89	50.55	145

(b) *effluent wastewater*

Table 8 Parameters of Yoon-Nelson model using nonlinear regression analysis and the equilibrium DNA uptake ($q_{e(exp)}$) for iron-oxide-coated sands under various conditions in (a)ultrapure water (b) wastewater effluent. SS as the deviation from empirical data

C_0 (mg L ⁻¹)	Q (mL min ⁻¹)	K_{YN} (10 ⁻³) (L min ⁻¹)	τ (min)	R^2	SS (10 ⁻³)	τ_{exp} (min)
100	0.1	2.39	525	0.72	30.2	450
300	0.1	2.45	223	0.84	114.59	195
500	0.1	4.2	48	0.61	216.42	75
300	0.3	7.52	118	0.79	557.44	195
300	0.5	16.45	25	0.81	645.24	30

(a) *ultrapure water*

C_0 (mg L ⁻¹)	Q (mL min ⁻¹)	K_{YN} (10 ⁻³) (L min ⁻¹)	τ (min)	R^2	SS (10 ⁻³)	τ_{exp} (min)
100	0.1	3.02	505	0.71	58.58	420
300	0.1	4.05	260	0.87	344.88	255
500	0.1	7.96	163	0.91	138.75	150
300	0.3	51.74	95	0.86	936.7	45
300	0.5	6.47	36	0.86	40.82	60

(b) *effluent wastewater*

4.7 Removal efficiencies of All bacteria, ARGs and MGE by adsorption column

Figure 23 shows the iDNA and eDNA removal percentage after adsorption treatment with SBC and IOCS. Adsorption experiments reflecting the real situations resulted in the eDNA to below detection level confirming that all the eDNA has been adsorbed in SBC. 90% of the iDNA was removed by SBC treatment. Whereas IOCS could only remove 40% of eDNA from the effluent. Absolute values of iDNA and eDNA in ng μl^{-1} is given in Table A 4 and Table A 5 (appendix)

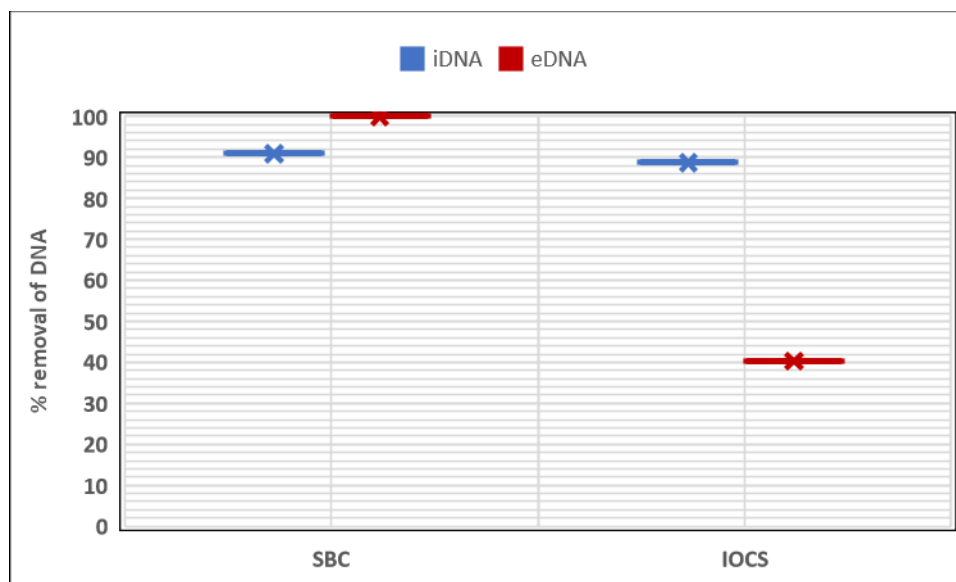


Figure 23 iDNA and eDNA removal percentage by sewage-based biochar and iron-oxide-coated sand by adsorption

To see the performance of ARG and MGE removal, the genes were assessed in two ways – intracellular ARG/MGE and extracellular ARG/MGE. For intracellular ARGs unfiltered effluent water was used and for eARGs, filtered effluent water was used. Figure 24 and Figure 25 show the intracellular ARGs and eARGs removal respectively. The removal is expressed in log removal (adsorption) values. These experiments were done with fresh samples collected on separate days. Significant changes in the presence of gene after column treatment were assessed by t-test and Wilcoxon tests are indicated above each gene (*) $p < 0.05$, (**) $p < 0.005$, (***) $p < 0.0005$, and (****) $p < 0.00005$; ns refers to concentrations below detection level by qPCR analysis.

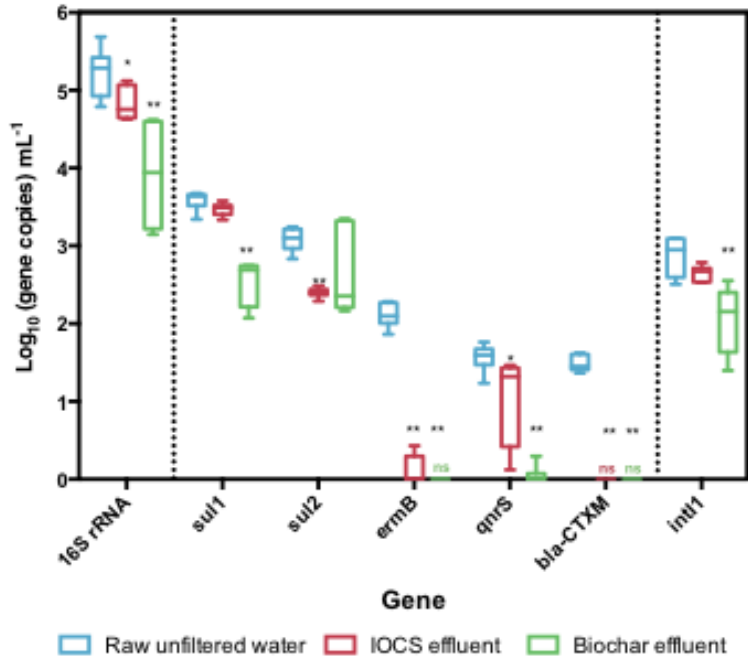


Figure 24 Absolute concentration of intracellular 16S rRNA gene, ARGs and MGE in raw influent, sewage-based biochar treated effluent and iron-oxide-coated sands treated effluent. Different types of (16S, ARGs, and MGE) are separated by straight lines. ns refers to concentrations below detection limit by qPCR. Significant differences observed after adsorption by sewage-based biochar and iron-oxide-coated sands are expressed as (*): $p < 0.05$; (**): $p < 0.005$

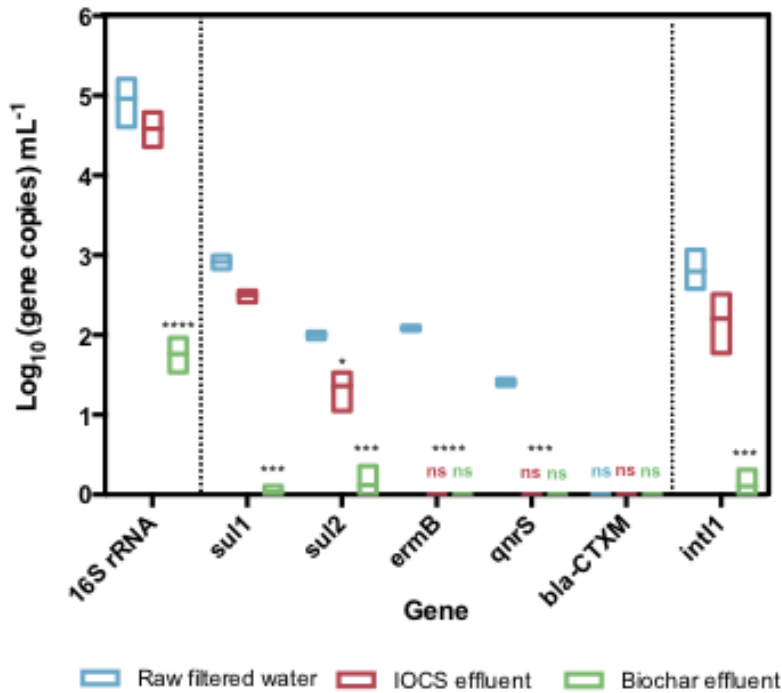


Figure 25 Absolute concentration of extracellular 16S rRNA gene, ARGs and MGE in raw influent, sewage-based biochar treated effluent and iron-oxide-coated sands treated effluent. Different types of (16S, ARGs, and MGE) are separated by straight lines. ns refers to concentrations below detection limit by qPCR. Significant differences observed after adsorption by sewage-based biochar and iron-oxide-coated sands are expressed as (*) $p < 0.05$; (***) $p < 0.0005$; (****) $p < 0.00005$

From sewage-based biochar, an average log reduction of 1.19 ± 0.07 and 1.53 ± 0.10 for intracellular and extracellular genes was shown, respectively. On the other hand, iron-oxide-coated sands showed a log reduction of 0.79 ± 0.17 and 0.59 ± 0.09 when test for intracellular and extracellular genes. These results are comparable to those obtained with advanced treatment systems for the removal of ARGs (H. Chen & Zhang, 2013; Hiller et al., 2019; Slipko et al., 2019)

4.8 Physical and chemical analysis of wastewater

The removal of chemical oxygen demand (COD) and true color of the effluent wastewater was also analyzed during the treatment. Figure 26 shows the COD concentration in the effluent wastewater before and after treating with SBC and IOCS. The final concentration in both unfiltered and filtered water was similar for SBC and IOCS individually indicating that a maximum reduction could be achieved irrespective of the filtration. The results of the ions NO_2^- , NO_3^{2-} , NO_4^+ , and PO_4^{3-} in the samples measured by ion chromatography are given in Figure A5, Figure A 6 and Figure A7 (appendix).

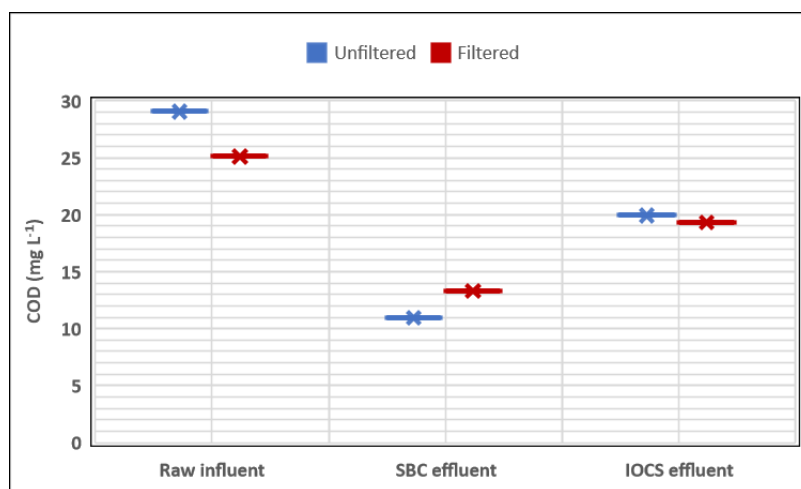


Figure 26 Chemical oxygen demand in the effluent wastewater before and after treatment with sewage-based biochar and iron oxide coated sand

Figure 27 shows the reduction of true color with SBC and IOCS after the treatment. The sample obtained from SBC was observed to be very clear in appearance as compared to the IOCS (Figure 28). This could be due to the mild release of iron during the treatment. The overall efficiency was higher for SBC (80%) than in IOCS (40%).

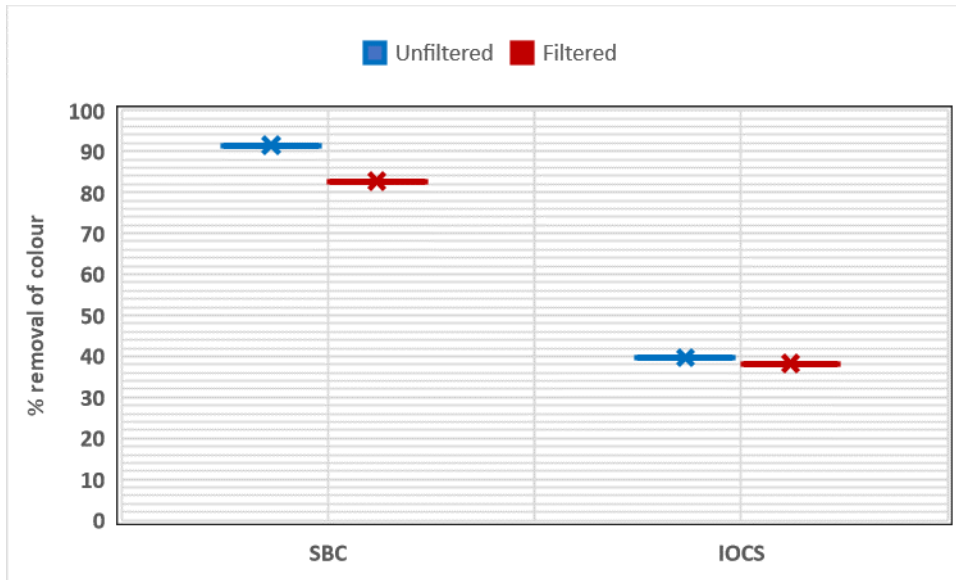


Figure 27 True color reduction percentage after treatment with sewage-based biochar and iron oxide coated sand



Figure 28 Visual representation of the samples obtained after passing through the columns. Right image: iron-oxide-coated sands effluent, Left image: sewage-based biochar effluent

Chapter

5 DISCUSSION

Here, we delivered thorough insights crossing the gap between DNA adsorption, fate and removal of intracellular ARGs/MGE and extracellular ARGs/MGE in real effluent wastewater. Our rational approach to this neglected pollutant eDNA in the treated wastewater, which can add risks to the effluent receiving water takes source within the project of TARGETBIO, the spread of foreign DNA used in the genetically modified organisms into the microbial communities in nature. We highlighted the effect of solutions chemistry (pH, cation species, humic acid); effect of initial DNA concentration and flow rate in a fixed bed column adsorption; removal efficiency of all bacteria 16S rRNA, intracellular and extracellular ARGs/MGE in a fixed bed column. This with the integrated aim of minimizing the eDNA concentrations from the effluent wastewater.

5.1 Sewage-based biochar (SBC) and iron oxide coated (IOCS) as the suitable adsorbents for DNA adsorption in effluent wastewater

DNA is known to be well adsorbed onto mesoporous particles with large surface areas, and narrow pore size (Fujiwara et al., 2005; Solberg & Landry, 2006). Highest DNA removal (80 – 100 %) was achieved by adsorption onto powdered activated carbon (PAC) and sewage-based biochar (SBC) followed by iron-oxide-coated sands (IOCS) and less than 50 % removal in granular activated carbon (GAC). This can be explained due to the lower particle size of GAC. The particle size of PAC is generally 10 to 100 times lower than GAC which enhances the spreading of DNA to interior parts of the adsorbent (Greenbank & Knepper, 2002). The aim of this study was to use sustainable materials for adsorption of DNA from effluent wastewater. Hence, SBC and IOCS was selected over PAC for further experiments.

From the adsorption isotherms it was seen that the removal efficiency of SBC ($\sim 1 \mu\text{g mg}^{-1}$) was higher than IOCS ($\sim 0.3 \mu\text{g mg}^{-1}$) in the presence and absence of wastewater quality parameters. The adsorption capacity of SBC was highest in ultrapure water, which is void of any wastewater quality parameters, followed by tap water and wastewater effluent. Whereas for IOCS the adsorption capacity is similar for both ultrapure and wastewater effluent. Although the

adsorption capacity was higher in ultrapure water, the high R^2 value (0.99) from the isotherms in effluent water suggests a high interaction between DNA and adsorbent in the presence of wastewater quality parameters.

5.2 Proposed removal mechanism of DNA by adsorption

The increase in the DNA adsorption by cations can be explained by Ion bridges and charge neutralization (Cai et al., 2006; Saeki et al., 2010; Sheng et al., 2019). Cations like Na^+ , Mg^{2+} , and Ca^{2+} are likely to form links between the biochar and DNA molecules. As the pH increases above 3, biochar is more negatively charged (J.-H. Yuan et al., 2011) and DNA fragments are also negatively charged because of the phosphate groups (Cai et al., 2006).

The negative charge on biochar on the biochar get neutralized by cations such as Na^+ , Mg^{2+} , Ca^{2+} , and Fe^{3+} . The increased DNA adsorption by SBC in the presence of Mg^{2+} , Ca^{2+} can be speculated to the formation of cation links, between oxygen atoms of the negatively charged phosphate group of DNAs and the cations added.

It has also been observed that the amount of DNA adsorbed onto montmorillonite was the highest in the presence of Fe^{3+} following Na^+ and Ca^{2+} (Sheng et al., 2019). Similar results have been found that by increasing the valence and concentration of cations, DNA adsorption can be enhanced (Kan et al., 2015; Lorenz & Wackernagel, 1987; Paget et al., 1992). Physical attraction forces (van der Waals forces) takes place in the presence of monovalent ions, whereas cation bridges are formed with polyvalent ions. Thus, explaining the interaction between the anions of DNA and the cations added, playing a major role for the adsorption of DNA onto IOCS.

In this study the addition of divalent cations, Mg^{2+} , and Ca^{2+} increased the adsorption of DNA from 1 to 1.5 times in both SBC and IOCS which is much lower than previous study. Another study has shown that by adding cations, DNA adsorption could be increased up to 5 times (Sheng et al., 2019). Though the effect of ions on DNA adsorption was not similar, leading to the interpretation that electrostatic interaction between the phosphate groups of DNAs and the cations added, was probably one of the mechanisms involved.

5.3 Reason for low adsorption with the addition of humic acids

Natural organic matter (NOM) is one of the key contaminants that disrupt the adsorption by competing for adsorption sites. NOM particles of size similar to the target compound to be removed, creates a competition for the available adsorption sites on the adsorbent (L. Ding et al.,

2006). Besides competing for the sites of adsorption, the negatively charged NOM when adsorbed increases the negative charge on the biochar surface resulting in an increased electrostatic repulsion (Newcombe & Drikas, 1997; Summers et al., 1989). With the increasing humic acids, the repulsive forces also increase which reduces the adsorption of negatively charged DNA onto SBC.

As seen in previous studies, DNA is adsorbed onto humic acids and organic matter by cation bridging (Cai et al., 2009; Levy-Booth et al., 2007; Saeki et al., 2011). Also, IOCS is considered to be a promising solution for adsorption of organic matter from water (C. Ding et al., 2008; C. Ding et al., 2010). No significant change in the DNA adsorption was seen in IOCS, it can be hypothesized that DNA could have possibly first adsorbed onto the humic acids and these humic acids, in turn, were adsorbed onto IOCS.

5.4 Adsorption column behavior

Column experiments help in the design of scale up data, by predicting the amount of water that can be treated before the column needs to be regenerated or replaced as the data obtained from the adsorption isotherm is not enough. (Maiti et al., 2008).

At lower values of initial DNA concentration, the shape of the curve is not very distinct which tells that the rate of adsorption is low. The steepness of the curve increases with increasing DNA concentration making the adsorbent to saturate in less time. At lower DNA concentrations, the breakthrough curves were more dispersed suggesting a decrease in the diffusion coefficient. At low influent concentration, DNA is moved slowly from the aqueous solution to the layer of the adsorbent, lower concentration gradient is developed at the interface of the particle (Singh & Pant, 2006). Also, at low initial concentrations, the surface area and the availability of adsorption sites is relatively higher, and DNA could have been easily adsorbed. With an increase in DNA concentration, the driving force for mass transfer increases resulting in a low adsorption zone (Futalan et al., 2011; Han, Zou, et al., 2009). Similar results were found in column adsorption studies of dyes using activated carbon, ions using charcoal (Biswas & Mishra, 2015; Charola et al., 2018; W. Li et al., 2011; Lim & Aris, 2014)

Studies have reported that if the flow rate is increased beyond a certain limit causes the rate of adsorption to decrease, as the adsorbate gets transported out of the system with increase in flow, due to less contact time for the interaction of adsorbate and adsorbent in the column (McKay & Bino, 1990). It is seen very clearly from the curves that increasing the flow rate above 0.3 mL min^{-1} would not improve the performance of column as the breakthrough of the bed reached within 60 min. Also, not much difference was seen in the breakthrough curves for 0.3 and 0.5 mL min^{-1} owing to the decrease of service time of the adsorbent bed. Due to higher contact time at low flow rates, DNA can better penetrate the pores of adsorbent (Hanen & Abdelmottaleb, 2013; Jahangiri-Rad et al., 2014). It can also be said that increasing the flow rate, the DNA particles would not have enough contact time with the adsorbent before equilibrium is reached.

Effect of interruption of operation

In order to know the concentration of DNA in the effluent from the column, samples were collected every 15 min at the outlet. For some operational conditions, the columns were subjected to an interruption (~12 h overnight) due to unfeasibility of collecting samples which can be seen in Figure 19 (b) and Figure 21 (b). It has been observed that after restarting the column, about 100 – 150 min is needed for C_t/C_o to get to a constant value, this could be explained by intraparticle diffusion. The concentration gradient at the surface of the adsorbent is the driving force for intraparticle diffusion governing the overall rate. The interruption in the column could have possibly allowed the adsorbed DNA to spread out evenly within the adsorbent thus forming a new concentration gradient at the interface. A faster uptake rate was observed after interruption suggesting intraparticle diffusion could be a rate-limiting step for SBC column. Other studies have confirmed intraparticle diffusion governs the kinetics in an adsorption process (DeMarco et al., 2003; P. Li & SenGupta, 2000).

5.5 Antimicrobial resistance genes removal efficiency

In this study, the average removal of extracellular ARGs was higher than the intracellular ARGs with both SBC and IOCS treatment. This could be due to the interaction of free floating DNA with the molecules or ions in wastewater matrix and on the adsorbent, which could be seen with the column experiments. In the intracellular ARGs/MGE removal, *sul2* and *int 1* have showed a less removal (51.99 % and 84.74 % respectively) as they can also be found in a large number of

pathogenic and non-pathogenic bacteria and thus being able to change its host cell by moving between bacteria by horizontal gene transfer (Gillings et al., 2015).

5.6 Sewage-based biochar as a potential adsorbent

The production of sewage sludge has been rising gradually increasing during wastewater treatment process due to rising world population and many households connected to sewers. It is estimated that at the European level sludge production would reach 12.9 million tons by the year 2020 (Capodaglio & Callegari, 2018). The treatment and discarding of sewage sludge (landfilling, agriculture and incinerations) is an expensive and ecologically burden as the sludge production continues to increase as new WWTPs are being built. Sewage sludge directive 86/278/EEC have set more stringent regulations on the use of sewage sludge as landfilling due to the presence of high concentrations heavy metals and pathogens. Incineration is carried out in most of the EU-15 countries with Netherlands being the highest increasing trends (Agrafioti et al., 2013; Callegari & Capodaglio, 2018). Table 9 shows the comparison of sludge treatment by incineration and pyrolysis.

Large scale incineration requires high investment and operating costs as extensive cleaning, or gas purification is required for safe emission into the environment. Another solution to incineration is pyrolysis which can reduce the sludge volume, completely remove pathogens and convert the organic matter into biofuel, bio-oil or biochar. Pyrolysis is done under less or no oxygen conditions which reduces the amount of flue gases cleaning, generation of acidic gases (Hwang et al., 2007). Biochar from sewage have high cation exchange capacity and surface adsorption sites due to high porosity are useful in removing pollutants from wastewater (Fathi Dokht et al., 2017).

Table 9 Comparison of sludge treatment by incineration and pyrolysis (Tsybina & Wuensch, 2018)

	Incineration	Pyrolysis
Cost of treatment	€157 - €510 per ton of dry substance (depending on the capacity of the plant)	€400 – €650 per ton of dry substance
Energy efficiency	80 % of the energy of flue gases can be recovered in bigger plants In smaller plants only heat can be recovered	Energy balance is negative as the overall production from drying to dewatering needs more energy than what is required for the production
Nutrient recovery	Most of the nutrients, organic pollutants, pathogens are destroyed Phosphorus can be converted into low solubility mineral	Nutrients can be saved by converting into biochar which can be used as soil amendment, as an energy source (biofuel), water treatments, air cleaning etc.,
Market value of the by products	The energy recovered as heat and electricity during combustion can be reused in the plant The ash can be used as a constructional material	Operated to maximize the bio-yield, which can be used for drying or creating temperature for the process
Feasibility	Major disadvantage in terms of downscaling due to high costs needed for smaller plants.	Compact and an easily incorporated at smaller treatment plants with low sludge load

Sewage-based biochar has less surface area (maximum of $400 \text{ m}^2 \text{ g}^{-1}$) than commercially activated carbon ($500 - 1200 \text{ m}^2 \text{ g}^{-1}$), yet they have shown to effectively remove some of the contaminants from water (Arvanitoyannis et al., 2008). Apart from applying biochar for soil amendment, biochar derived from sewage sludge has shown to reduce dyes, heavy metals, phenol, organic pollutants from the wastewater (Jindarom et al., 2007; Otero et al., 2003; Rozada et al., 2008; L. Yang et al., 2019). According to our knowledge this is the first time the potential of using sewage-based biochar for the removal of antimicrobial resistance genes being tested.

Transforming sewage sludge into biochar, not only reduces the need to construct a conventional treatment system (incineration plant) for sludge disposal, but their use in various applications as mentioned can give a second life.

Chapter

6 CONCLUSIONS

From the analysis of the experiments conducted to study the mechanism of DNA adsorption in batch and column, and the removal of ARGs in effluent wastewater, it can be concluded that:

- The adsorption of salmon sperm DNA as the representation of free DNA, onto sewage-based biochar was higher ($\sim 1 \mu\text{g mg}^{-1}$) than iron-oxide-coated sands ($\sim 0.2 \mu\text{g mg}^{-1}$) due to the high pore size. Furthermore, iron-oxide-coated sands needed longer contact time (5 hours) than sewage-based biochar (2 hours) to reach equilibrium stage. Changing the pH (from 3 to 9) did not provide any significant changes in adsorption thus maintaining the pH during the treatment is not necessary. Increasing ionic conditions on DNA adsorption had minor effect as compared to the previous studies. The humic acids present in the solution can compete with DNA for adsorption sites in SBC.
- From the physical perspective of initial experiments, it can be proposed that the DNA adsorption may be related to the specific surface area and pore size. As DNA was removed by almost 100 % by powdered activated carbon, sewage-based biochar and iron coated sand whose pore size is lower as compared to granular activated carbon and mineral wool.
- Column adsorption capacity was 2 - 3 fold higher than the batch adsorption, which could be since chemical or biological changes occurring in the adsorbent cannot be predicted by isotherms and columns do not operate under equilibrium condition due to less contact time. Also, the adsorption capacity of the columns with effluent water was 1 – 2 fold higher than ultrapure water demonstrating that adsorption could be promising in the removal of free DNA from wastewater effluent.
- From sewage-based biochar, an average log reduction of 1.19 ± 0.07 and 1.53 ± 0.10 for intracellular and extracellular genes was shown, respectively. On the other hand, iron-oxide-coated sands showed a log reduction of 0.79 ± 0.17 and 0.59 ± 0.09 when tested for

intracellular and extracellular genes. These results show that biochar as an adsorbent, could result in effective reduction of the *16S rRNA*, ARGs, and MGE.

- Adsorption with activated carbon is applied in most tertiary treatment systems for the removal of organic compounds. The results achieved in this research suggests the use of biochar as suitable adsorbent for the removal of eDNA along with a removal of 16S rRNA, ARGs, and MGE in a continuous column adsorption. By implementing the adsorption column in a lab scale along with further investigations by studying the performance of the bed under long run, process can be fully developed into an effective, low cost, tertiary treatment system.

Chapter

7 RECOMMENDATIONS

The executed experiments highlight on obtaining more knowledge regarding the electrostatic interaction of DNA with biochar and iron coated sands; their adsorption capacity for DNA removal in effluent wastewater in a continuous fixed bed adsorption. To obtain more understanding of other DNA adsorption mechanisms more research needs to be done.

From the initial experiments with possible porous materials, it was observed that DNA was well adsorbed onto materials with high surface area or low pore size (powdered activated carbon, biochar, and iron oxide coated sand). Pyrolysis operating conditions for biochar preparation such as temperature, residence time at this temperature, heating rate effects the surface properties. Thus, the correlation of DNA adsorption with surface area, pore size can be investigated by different preparing different types of biochar with pyrolysis conditions.

Studies to see DNA desorption by Tris-HCl, NaCl, phosphate to study the ligand exchange along with Fourier transform infrared (FTIR) analysis can be done to see the conformational change of DNA to better understand the mechanisms involved.

The presence of humic acids has shown a reduction of DNA adsorption on biochar which could be due to competition or electrostatic repulsion. Further confirmation of the presence of humic acids can be done by measuring the organic content in the water samples.

A faster uptake rate of DNA adsorption was observed in the column study after the interruption of the column for around 14 h. This could be due to the change in concentration gradient at the surface layer of adsorbent suggestion a phenomenon of intraparticle diffusion. Further study can be done with various interruption tests to provide evidence of this phenomenon.

In this study, DNA adsorption was studied based on the mass balance before and after treatment. Further research can be done to detect the adsorption on solid substrate by microscopic

test such as atomic force microscopic (AFM), quartz crystal microbalance, ellipsometry and X-ray photoelectron spectroscopy (XPS) (Kan et al., 2015).

For the development of a full scale plant, further investigations regarding the performance of a lab scale column reactor can be monitored for a long run. The removal of other wastewater parameters such as suspended solids, phosphorus, nitrogen etc., must be well-studied.

Finally, a full life cycle assessment can be made for further understanding the effectiveness of sewage-based biochar as a potential adsorbent for removing free DNA in the adsorption process with respect to other technologies such as disinfection, membrane filtration as an option for the tertiary treatment system.

REFERENCES

- Agrafioti, E., Bouras, G., Kalderis, D., & Diamadopoulos, E. (2013). Biochar production by sewage sludge pyrolysis. *Journal of Analytical and Applied Pyrolysis*, *101*, 72-78.
- Ahmed, M. B., Zhou, J. L., Ngo, H. H., & Guo, W. (2015). Adsorptive removal of antibiotics from water and wastewater: progress and challenges. *Science of The Total Environment*, *532*, 112-126.
- Al-Jassim, N., Ansari, M. I., Harb, M., & Hong, P.-Y. (2015). Removal of bacterial contaminants and antibiotic resistance genes by conventional wastewater treatment processes in Saudi Arabia: is the treated wastewater safe to reuse for agricultural irrigation? *Water research*, *73*, 277-290.
- Ali, I., Asim, M., & Khan, T. A. (2012). Low cost adsorbents for the removal of organic pollutants from wastewater. *Journal of environmental management*, *113*, 170-183.
- Anjum, M. F., Zankari, E., & Hasman, H. (2017). Molecular methods for detection of antimicrobial resistance. *Microbiology spectrum*, *5*(6).
- Arvanitoyannis, I. S., Kassaveti, A., & Ladas, D. (2008). Food waste treatment methodologies. *Waste Management for the Food Industries*, *345*.
- Arya, M., Shergill, I. S., Williamson, M., Gommersall, L., Arya, N., & Patel, H. R. (2005). Basic principles of real-time quantitative PCR. *Expert review of molecular diagnostics*, *5*(2), 209-219.
- Asano, T., & Levine, A. D. (1996). Wastewater reclamation, recycling and reuse: past, present, and future. *Water Science and Technology*, *33*(10-11), 1-14.
- Barancheshme, F., & Munir, M. (2018). Strategies to Combat Antibiotic Resistance in the Wastewater Treatment Plants. *Frontiers in Microbiology*, *8*(2603). doi:10.3389/fmicb.2017.02603
- Barancheshme, F., & Munir, M. (2019). Development of Antibiotic Resistance in Wastewater Treatment Plants. In *Antimicrobial Resistance-A Global Threat*: IntechOpen.
- Biology dictionary. (2019). Bacterial Conjugation Retrieved from <https://biologydictionary.net/bacterial-conjugation/>
- Biswas, S., & Mishra, U. (2015). Continuous fixed-bed column study and adsorption modeling: removal of lead ion from aqueous solution by charcoal originated from chemical carbonization of rubber wood sawdust. *Journal of Chemistry*, *2015*.
- Bonilla-Petriciolet, A., Mendoza-Castillo, D. I., & Reynel-Ávila, H. E. (2017). *Adsorption processes for water treatment and purification*: Springer.
- Borthong, J., Omori, R., Sugimoto, C., Suthienkul, O., Nakao, R., & Ito, K. (2018). Comparison of database search methods for the detection of Legionella pneumophila in water samples using metagenomic analysis. *Frontiers in microbiology*, *9*, 1272.
- Bouki, C., Venieri, D., & Diamadopoulos, E. (2013). Detection and fate of antibiotic resistant bacteria in wastewater treatment plants: a review. *Ecotoxicology and environmental safety*, *91*, 1-9.
- Bravo, A. G., Wildj, W., & Poté, J. (2010). Kinetics of plant material mass loss and DNA release in freshwater column. *Ecotoxicology and environmental safety*, *73*(7), 1548-1552.
- Cai, P., Huang, Q.-Y., & Zhang, X.-W. (2006). Interactions of DNA with clay minerals and soil colloidal particles and protection against degradation by DNase. *Environmental science & technology*, *40*(9), 2971-2976.
- Cai, P., Zhu, J., Huang, Q., Fang, L., Liang, W., & Chen, W. (2009). Role of bacteria in the adsorption and binding of DNA on soil colloids and minerals. *Colloids and Surfaces B: Biointerfaces*, *69*(1), 26-30.
- Callegari, A., & Capodaglio, A. G. (2018). Properties and beneficial uses of (bio) chars, with special attention to products from sewage sludge pyrolysis. *Resources*, *7*(1), 20.
- Capodaglio, A. G., & Callegari, A. (2018). Feedstock and process influence on biodiesel produced from waste sewage sludge. *Journal of environmental management*, *216*, 176-182.

- Carattoli, A. (2001). Importance of integrons in the diffusion of resistance. *Veterinary research*, 32(3-4), 243-259.
- Charola, S., Yadav, R., Das, P., & Maiti, S. (2018). Fixed-bed adsorption of Reactive Orange 84 dye onto activated carbon prepared from empty cotton flower agro-waste. *Sustainable Environment Research*, 28(6), 298-308.
- Chatterjee, S., Mondal, S., & De, S. (2018). Design and scaling up of fixed bed adsorption columns for lead removal by treated laterite. *Journal of cleaner production*, 177, 760-774.
- Chen, H., Rangasamy, M., Tan, S. Y., Wang, H., & Siegfried, B. D. (2010). Evaluation of five methods for total DNA extraction from western corn rootworm beetles. *PloS one*, 5(8), e11963.
- Chen, H., & Zhang, M. (2013). Effects of advanced treatment systems on the removal of antibiotic resistance genes in wastewater treatment plants from Hangzhou, China. *Environmental science & technology*, 47(15), 8157-8163.
- Chen, I., & Dubnau, D. (2004). DNA uptake during bacterial transformation. *Nature Reviews Microbiology*, 2(3), 241.
- Chen, J., Wei, X.-D., Liu, Y.-S., Ying, G.-G., Liu, S.-S., He, L.-Y., . . . Yang, Y.-Q. (2016). Removal of antibiotics and antibiotic resistance genes from domestic sewage by constructed wetlands: Optimization of wetland substrates and hydraulic loading. *Science of the Total Environment*, 565, 240-248.
- Chen, S., Yue, Q., Gao, B., Li, Q., Xu, X., & Fu, K. (2012). Adsorption of hexavalent chromium from aqueous solution by modified corn stalk: a fixed-bed column study. *Bioresource Technology*, 113, 114-120.
- Choi, K.-J., Kim, S.-G., & Kim, S.-H. (2008). Removal of antibiotics by coagulation and granular activated carbon filtration. *Journal of hazardous materials*, 151(1), 38-43.
- Chroma, M., & Kolar, M. (2010). Genetic methods for detection of antibiotic resistance: focus on extended-spectrum β -lactamases. *Biomed Pap Med Fac Univ Palacky Olomouc Czech Repub*, 154(4), 289-296.
- D'Costa, V. M., King, C. E., Kalan, L., Morar, M., Sung, W. W., Schwarz, C., . . . Debruyne, R. (2011). Antibiotic resistance is ancient. *Nature*, 477(7365), 457.
- Dada, A., Olalekan, A., Olatunya, A., & Dada, O. (2012). Langmuir, Freundlich, Temkin and Dubinin–Radushkevich isotherms studies of equilibrium sorption of Zn²⁺ onto phosphoric acid modified rice husk. *IOSR Journal of Applied Chemistry*, 3(1), 38-45.
- David P. Clark, & Nanette J. Pazdernik. (2013). *Chapter e20 - Plasmids* ("Second Edition" ed.).
- Davies, J., & Davies, D. (2010). Origins and evolution of antibiotic resistance. *Microbiol. Mol. Biol. Rev.*, 74(3), 417-433.
- De Rijck, G., & Schrevels, E. (1998). Distribution of nutrients and water in rockwool slabs. *Scientia Horticulturae*, 72(3-4), 277-285.
- DeMarco, M. J., SenGupta, A. K., & Greenleaf, J. E. (2003). Arsenic removal using a polymeric/inorganic hybrid sorbent. *Water research*, 37(1), 164-176.
- Desta, M. B. (2013). Batch sorption experiments: Langmuir and Freundlich isotherm studies for the adsorption of textile metal ions onto teff straw (*Eragrostis tef*) agricultural waste. *Journal of thermodynamics*, 2013.
- Destiani, R., & Templeton, M. (2019). Chlorination and ultraviolet disinfection of antibiotic-resistant bacteria and antibiotic resistance genes in drinking water.
- Ding, C., Shang, C., & Chang, Y. (2008). Aqueous natural organic matter removal by quaternary-ammonium-compound-modified iron-oxide-coated sand. *Water Science and Technology: Water Supply*, 8(5), 565-571.
- Ding, C., Yang, X., Liu, W., Chang, Y., & Shang, C. (2010). Removal of natural organic matter using surfactant-modified iron oxide-coated sand. *Journal of hazardous materials*, 174(1-3), 567-572.

- Ding, L., Mariñas, B. J., Schideman, L. C., Snoeyink, V. L., & Li, Q. (2006). Competitive effects of natural organic matter: parametrization and verification of the three-component adsorption model COMPSORB. *Environmental science & technology*, 40(1), 350-356.
- Dong, P., Wang, H., Fang, T., Wang, Y., & Ye, Q. (2019). Assessment of extracellular antibiotic resistance genes (eARGs) in typical environmental samples and the transforming ability of eARG. *Environment international*, 125, 90-96.
- Drainblock. (2017). Retrieved from <https://drainblock.nl/en>
- Fathi Dokht, H., Movahedi Naeini, S. A., Dordipour, E., Wollsene De Jong, L., & Hezarjaribi, E. (2017). Effects of sewage sludge and its biochar on soybean yield in fine-textured loess soil. *Environmental Health Engineering and Management Journal*, 4(2), 81-91.
- Fayad, A. A., Herrmann, J., & Müller, R. (2018). Octapeptins: Lipopeptide Antibiotics against Multidrug-Resistant Superbugs. *Cell chemical biology*, 25(4), 351-353.
- Foster, S., Lawrence, A., & Morris, B. (1998). *Groundwater in urban development: assessing management needs and formulating policy strategies*: The World Bank.
- Francino, M. P. (2012). *Horizontal gene transfer in microorganisms*: Caister Academic Press.
- Frost, L. S., Leplae, R., Summers, A. O., & Toussaint, A. (2005). Mobile genetic elements: the agents of open source evolution. *Nature Reviews Microbiology*, 3(9), 722.
- Fujiwara, M., Yamamoto, F., Okamoto, K., Shiokawa, K., & Nomura, R. (2005). Adsorption of duplex DNA on mesoporous silicas: possibility of inclusion of DNA into their mesopores. *Analytical chemistry*, 77(24), 8138-8145.
- Futalan, C. M., Kan, C.-C., Dalida, M. L., Pascua, C., & Wan, M.-W. (2011). Fixed-bed column studies on the removal of copper using chitosan immobilized on bentonite. *Carbohydrate polymers*, 83(2), 697-704.
- Gillings, M. R., Gaze, W. H., Pruden, A., Smalla, K., Tiedje, J. M., & Zhu, Y.-G. (2015). Using the class 1 integron-integrase gene as a proxy for anthropogenic pollution. *The ISME Journal*, 9(6), 1269-1279. doi:10.1038/ismej.2014.226
- Gorecki, A., Decewicz, P., Dziurzynski, M., Janeczko, A., Drewniak, L., & Dziewit, L. (2019). Literature-based, manually-curated database of PCR primers for the detection of antibiotic resistance genes in various environments. *Water research*.
- Greenbank, M., & Knepper, J. (2002). GAC/PAC: Use of Powdered Activated Carbon for Potable Water Treatment in Small Systems. *WATER CONDITIONING AND PURIFICATION INTERNATIONAL*, 44-51.
- Guppy, L., & Anderson, K. (2017). Water Crisis Report. United Nations University Institute for Water. *Environment and Health, Hamilton, Canada*.
- Hagemann, N., Spokas, K., Schmidt, H.-P., Kägi, R., Böhler, M., & Bucheli, T. (2018). Activated carbon, biochar and charcoal: linkages and synergies across pyrogenic carbon's ABCs. *Water*, 10(2), 182.
- Han, R., Wang, Y., Zhao, X., Wang, Y., Xie, F., Cheng, J., & Tang, M. (2009). Adsorption of methylene blue by phoenix tree leaf powder in a fixed-bed column: experiments and prediction of breakthrough curves. *Desalination*, 245(1-3), 284-297.
- Han, R., Zou, L., Zhao, X., Xu, Y., Xu, F., Li, Y., & Wang, Y. (2009). Characterization and properties of iron oxide-coated zeolite as adsorbent for removal of copper (II) from solution in fixed bed column. *Chemical Engineering Journal*, 149(1-3), 123-131.
- Hanan, N., & Abdelmottaleb, O. (2013). Modeling of the dynamics adsorption of phenol from an aqueous solution on activated carbon produced from olive stones. *Journal of Chemical Engineering & Process Technology*, 4(3).
- Hiller, C., Hübner, U., Fajnorova, S., Schwartz, T., & Drewes, J. (2019). Antibiotic microbial resistance (AMR) removal efficiencies by conventional and advanced wastewater treatment processes: A review. *Science of The Total Environment*.

- Hsu A, Esty D.C, de Sherbinin A, & Levy M.A, e. a. (2016). 2016 Environmental Performance Index : Global Metrics for the Environment. . *New Haven,CT:Yale Center for Environmental Law & Policy*. Retrieved from <https://epi2016.yale.edu/>
- Hwang, I., Ouchi, Y., & Matsuto, T. (2007). Characteristics of leachate from pyrolysis residue of sewage sludge. *Chemosphere*, 68(10), 1913-1919.
- Israel, D. A. (2001). Genetic exchange. In *Helicobacter pylori: Physiology and Genetics*: ASM Press.
- Jahangiri-Rad, M., Jamshidi, A., Rafiee, M., & Nabizadeh, R. (2014). Adsorption performance of packed bed column for nitrate removal using PAN-oxime-nano Fe₂O₃. *Journal of Environmental Health Science and Engineering*, 12(1), 90.
- Jansen, G., & Aktipis, C. A. (2014). Resistance is mobile: the accelerating evolution of mobile genetic elements encoding resistance. *J Evol Med*, 2, 1-3.
- Jindarom, C., Meeyoo, V., Kitiyanan, B., Rirkosomboon, T., & Rangsunvigit, P. (2007). Surface characterization and dye adsorptive capacities of char obtained from pyrolysis/gasification of sewage sludge. *Chemical Engineering Journal*, 133(1-3), 239-246.
- Jørgensen, E. (1975). "GRODAN" STONE WOOL AS MEDIUM FOR PROPAGATION AND CULTURE. Paper presented at the Symposium on Propagation in Arboriculture 54.
- Justo Llopis, A. (2015). Advanced technologies applied to wastewater treatment plant effluents.
- Kaiser, G. (2019, June 24). Plasmids and Transposons. Retrieved from [https://bio.libretexts.org/Bookshelves/Microbiology/Book%3AMicrobiology_\(Kaiser\)/Unit_1%3A_Introduction_to_Microbiology_and_Prokaryotic_Cell_Anatomy/2%3A_The_Prokaryotic_Cell_-_Bacteria/2.4%3A_Cellular_Components_within_the_Cytoplasm/2.4C%3A_Plasmids_and_Transposons](https://bio.libretexts.org/Bookshelves/Microbiology/Book%3AMicrobiology_(Kaiser)/Unit_1%3A_Introduction_to_Microbiology_and_Prokaryotic_Cell_Anatomy/2%3A_The_Prokaryotic_Cell_-_Bacteria/2.4%3A_Cellular_Components_within_the_Cytoplasm/2.4C%3A_Plasmids_and_Transposons)
- Kan, Y., Tan, Q., Wu, G., Si, W., & Chen, Y. (2015). Study of DNA adsorption on mica surfaces using a surface force apparatus. *Scientific reports*, 5, 8442.
- Karkman, A., Do, T. T., Walsh, F., & Virta, M. P. (2018). Antibiotic-resistance genes in waste water. *Trends in microbiology*, 26(3), 220-228.
- Khachatourians, G. G. (1998). Agricultural use of antibiotics and the evolution and transfer of antibiotic-resistant bacteria. *Cmaj*, 159(9), 1129-1136.
- Lehmann, J., & Joseph, S. (2015). *Biochar for environmental management: science, technology and implementation*: Routledge.
- Lerminiaux, N. A., & Cameron, A. D. (2018). Horizontal transfer of antibiotic resistance genes in clinical environments. *Canadian journal of microbiology*, 65(1), 34-44.
- Levy-Booth, D. J., Campbell, R. G., Gulden, R. H., Hart, M. M., Powell, J. R., Klironomos, J. N., . . . Dunfield, K. E. (2007). Cycling of extracellular DNA in the soil environment. *Soil Biology and Biochemistry*, 39(12), 2977-2991.
- Li, N., Sheng, G.-P., Lu, Y.-Z., Zeng, R. J., & Yu, H.-Q. (2017). Removal of antibiotic resistance genes from wastewater treatment plant effluent by coagulation. *Water research*, 111, 204-212.
- Li, P., & SenGupta, A. K. (2000). Intraparticle diffusion during selective ion exchange with a macroporous exchanger. *Reactive and Functional Polymers*, 44(3), 273-287.
- Li, W., Yue, Q., Tu, P., Ma, Z., Gao, B., Li, J., & Xu, X. (2011). Adsorption characteristics of dyes in columns of activated carbon prepared from paper mill sewage sludge. *Chemical Engineering Journal*, 178, 197-203.
- Lim, A. P., & Aris, A. Z. (2014). Continuous fixed-bed column study and adsorption modeling: Removal of cadmium (II) and lead (II) ions in aqueous solution by dead calcareous skeletons. *Biochemical Engineering Journal*, 87, 50-61.
- Lorenz, M. G., & Wackernagel, W. (1987). Adsorption of DNA to sand and variable degradation rates of adsorbed DNA. *Appl. Environ. Microbiol.*, 53(12), 2948-2952.

- Luby, E., Ibekwe, A. M., Zilles, J., & Pruden, A. (2016). Molecular methods for assessment of antibiotic resistance in agricultural ecosystems: prospects and challenges. *Journal of environmental quality*, 45(2), 441-453.
- Łuczkiwicz, A., Jankowska, K., Fudala-Książek, S., & Olańczuk-Neyman, K. (2010). Antimicrobial resistance of fecal indicators in municipal wastewater treatment plant. *Water research*, 44(17), 5089-5097.
- Ma, J., Sun, Y., & Yu, F. (2017). Efficient removal of tetracycline with KOH-activated graphene from aqueous solution. *Royal Society open science*, 4(11), 170731.
- MacGowan, A., & Macnaughton, E. (2017). Antibiotic resistance. *Medicine*, 45(10), 622-628.
- Maiti, A., DasGupta, S., Basu, J. K., & De, S. (2008). Batch and column study: adsorption of arsenate using untreated laterite as adsorbent. *Industrial & Engineering Chemistry Research*, 47(5), 1620-1629.
- Manaia, C. M. (2014). Antibiotic resistance in wastewater: origins, fate, and risks. *Prävention und Gesundheitsförderung*, 9(3), 180-184.
- Massé, D., Saady, N., & Gilbert, Y. (2014). Potential of biological processes to eliminate antibiotics in livestock manure: an overview. *Animals*, 4(2), 146-163.
- McKay, G., & Bino, M. (1990). Fixed bed adsorption for the removal of pollutants from water. *Environmental Pollution*, 66(1), 33-53.
- Morris, A., Kellner, J. D., & Low, D. E. (1998). The superbugs: evolution, dissemination and fitness. *Current opinion in microbiology*, 1(5), 524-529.
- Munita, J. M., & Arias, C. A. (2016). Mechanisms of antibiotic resistance. *Microbiology spectrum*, 4(2).
- Nagler, M., Insam, H., Pietramellara, G., & Ascher-Jenull, J. (2018). Extracellular DNA in natural environments: features, relevance and applications. *Applied microbiology and biotechnology*, 102(15), 6343-6356.
- Newcombe, G., & Drikas, M. (1997). Adsorption of NOM onto activated carbon: electrostatic and non-electrostatic effects. *Carbon*, 35(9), 1239-1250.
- Nielsen, K. M., Johnsen, P. J., Bensasson, D., & Daffonchio, D. (2007). Release and persistence of extracellular DNA in the environment. *Environmental biosafety research*, 6(1-2), 37-53.
- Otero, M., Rozada, F., Calvo, L., Garcia, A., & Moran, A. (2003). Elimination of organic water pollutants using adsorbents obtained from sewage sludge. *Dyes and Pigments*, 57(1), 55-65.
- Paget, E., Monrozier, L. J., & Simonet, P. (1992). Adsorption of DNA on clay minerals: protection against DNaseI and influence on gene transfer. *FEMS Microbiology Letters*, 97(1-2), 31-39.
- Pallares-Vega, R., Blaak, H., van der Plaats, R., de Roda Husman, A. M., Leal, L. H., van Loosdrecht, M. C., . . . Schmitt, H. (2019). Determinants of presence and removal of antibiotic resistance genes during WWTP treatment: A cross-sectional study. *Water research*.
- Pei, R., Kim, S.-C., Carlson, K. H., & Pruden, A. (2006). Effect of river landscape on the sediment concentrations of antibiotics and corresponding antibiotic resistance genes (ARG). *Water research*, 40(12), 2427-2435.
- Pietramellara, G., Franchi, M., Gallori, E., & Nannipieri, P. (2001). Effect of molecular characteristics of DNA on its adsorption and binding on homoionic montmorillonite and kaolinite. *Biology and fertility of soils*, 33(5), 402-409.
- Reed, B. E., & Matsumoto, M. R. (1993). Modeling cadmium adsorption by activated carbon using the Langmuir and Freundlich isotherm expressions. *Separation science and technology*, 28(13-14), 2179-2195.
- Rizzo, L., Manaia, C., Merlin, C., Schwartz, T., Dagot, C., Ploy, M., . . . Fatta-Kassinos, D. (2013). Urban wastewater treatment plants as hotspots for antibiotic resistant bacteria and genes spread into the environment: a review. *Science of The Total Environment*, 447, 345-360.
- Rogers, A. H. (2008). *Molecular oral microbiology*: Horizon Scientific Press.

- Rouf, S., & Nagapadma, M. (2015). Modeling of fixed-bed column studies for adsorption of azo dye on chitosan impregnated with a cationic surfactant. *International Journal of Scientific and Engineering Research*, 6(2), 124-132.
- Rozada, F., Otero, M., Morán, A., & García, A. (2008). Adsorption of heavy metals onto sewage sludge-derived materials. *Bioresource technology*, 99(14), 6332-6338.
- Sabri, N., Schmitt, H., Van der Zaan, B., Gerritsen, H., Zuidema, T., Rijnaarts, H., & Langenhoff, A. (2018). Prevalence of antibiotics and antibiotic resistance genes in a wastewater effluent-receiving river in the Netherlands. *Journal of Environmental Chemical Engineering*.
- Saeki, K., Ihyo, Y., Sakai, M., & Kunito, T. (2011). Strong adsorption of DNA molecules on humic acids. *Environmental Chemistry Letters*, 9(4), 505-509.
- Saeki, K., Kunito, T., & Sakai, M. (2010). Effects of pH, ionic strength, and solutes on DNA adsorption by andosols. *Biology and fertility of soils*, 46(5), 531-535.
- Science Learning Hub. (2019). Bacterial DNA - the role of Plasmids Retrieved from <https://www.sciencelearn.org.nz/resources/1900-bacterial-dna-the-role-of-plasmids>
- Shannon, M. A., Bohn, P. W., Elimelech, M., Georgiadis, J. G., Marinas, B. J., & Mayes, A. M. (2010). Science and technology for water purification in the coming decades. In *Nanoscience and technology: a collection of reviews from nature Journals* (pp. 337-346): World Scientific.
- Sheng, X., Qin, C., Yang, B., Hu, X., Liu, C., Waigi, M. G., . . . Ling, W. (2019). Metal cation saturation on montmorillonites facilitates the adsorption of DNA via cation bridging. *Chemosphere*.
- Singh, T. S., & Pant, K. (2006). Experimental and modelling studies on fixed bed adsorption of As (III) ions from aqueous solution. *Separation and Purification Technology*, 48(3), 288-296.
- Slipko, K., Reif, D., Wögerbauer, M., Hufnagl, P., Krampe, J., & Kreuzinger, N. (2019). Removal of extracellular free DNA and antibiotic resistance genes from water and wastewater by membranes ranging from microfiltration to reverse osmosis. *Water research*, 164, 114916.
- Solberg, S. M., & Landry, C. C. (2006). Adsorption of DNA into mesoporous silica. *The Journal of Physical Chemistry B*, 110(31), 15261-15268.
- Summers, R. S., Haist, B., Koehler, J., Ritz, J., Zimmer, G., & Sontheimer, H. (1989). The influence of background organic matter on GAC adsorption. *Journal-American Water Works Association*, 81(5), 66-74.
- Torti, A., Lever, M. A., & Jørgensen, B. B. (2015). Origin, dynamics, and implications of extracellular DNA pools in marine sediments. *Marine genomics*, 24, 185-196.
- Trikannad, S. (2018). Performance of Photobioreactor, constructed wetland and anaerobic membrane bioreactor in treating Antibiotic resistant bacteria in Barapullah drain, New Delhi. Retrieved from <http://resolver.tudelft.nl/uuid:7ae41c97-7e68-459d-b200-974af2c62f1f>.
<http://resolver.tudelft.nl/uuid:7ae41c97-7e68-459d-b200-974af2c62f1f>
- Tsybina, A., & Wuensch, C. (2018). ANALYSIS OF SEWAGE SLUDGE THERMAL TREATMENT METHODS IN THE CONTEXT OF CIRCULAR ECONOMY. *Detritus*(2), 3.
- UNESCO. (2019). Emerging Pollutants in Water and Wastewater Retrieved from <https://en.unesco.org/emergingpollutants>
- Uzuegbu, N. (2018). *Spread of Antibiotic Resistant Genes in Wastewater*. University of Stavanger, Norway,
- Van Hoek, A. H., Mevius, D., Guerra, B., Mullany, P., Roberts, A. P., & Aarts, H. J. (2011). Acquired antibiotic resistance genes: an overview. *Frontiers in microbiology*, 2, 203.
- von Wintersdorff, C. J., Penders, J., van Niekerk, J. M., Mills, N. D., Majumder, S., van Alphen, L. B., . . . Wolfs, P. F. (2016). Dissemination of antimicrobial resistance in microbial ecosystems through horizontal gene transfer. *Frontiers in microbiology*, 7, 173.
- Voulvoulis, N. (2018). Water reuse from a circular economy perspective and potential risks from an unregulated approach. *Current Opinion in Environmental Science & Health*, 2, 32-45.

- Wang, C., Wang, T., Li, W., Yan, J., Li, Z., Ahmad, R., . . . Zhu, N. (2014). Adsorption of deoxyribonucleic acid (DNA) by willow wood biochars produced at different pyrolysis temperatures. *Biology and fertility of soils*, 50(1), 87-94.
- Wanko, A., Laurent, J., Bois, P., Mosé, R., Wagner-Kocher, C., Bahlouli, N., . . . Provo kluit, P.-W. (2016). Assessment of rock wool as support material for on-site sanitation: hydrodynamic and mechanical characterization. *Environmental technology*, 37(3), 369-380.
- Water, U. (2017). The United Nations World Water Development Report 2017: wastewater the untapped resource. In: Paris: UNESCO.
- Wendling Z.A, Emerson J.W, Esty D.C, Levy M.A, & de Sherbinin A, e. a. (2018). 2018 Environmental Performance Index *New Haven,CT:Yale Center for Environmental Law & Policy*. Retrieved from <https://epi.yale.edu/>
- World Health Organisation. (2018). Antibiotic Resistance Retrieved from <https://www.who.int/news-room/fact-sheets/detail/antibiotic-resistance>
- World Wildlife Fund. (2019). Water Scarcity Retrieved from <https://www.worldwildlife.org/threats/water-scarcity>
- Wozniak, R. A., & Waldor, M. K. (2010). Integrative and conjugative elements: mosaic mobile genetic elements enabling dynamic lateral gene flow. *Nature Reviews Microbiology*, 8(8), 552.
- Wu, M., & Xu, X. (2019). Inactivation of antibiotic-resistant bacteria by chlorine dioxide in soil and shifts in community composition. *RSC advances*, 9(12), 6526-6532.
- Xu, Q., Tang, S., Wang, J., & Ko, J. H. (2018). Pyrolysis kinetics of sewage sludge and its biochar characteristics. *Process Safety and Environmental Protection*, 115, 49-56.
- Yang, L., He, L., Xue, J., Wu, L., Ma, Y., Li, H., . . . Zhang, Z. (2019). Highly efficient nickel (II) removal by sewage sludge biochar supported α -Fe₂O₃ and α -FeOOH: Sorption characteristics and mechanisms. *PloS one*, 14(6), e0218114.
- Yang, Y., & Zhang, T. (2017). Metagenomic Approaches for Antibiotic Resistance Gene Detection in Wastewater Treatment Plants. *Antimicrobial Resistance in Wastewater Treatment Processes*, 95-108.
- Yu, W. H., Li, N., Tong, D. S., Zhou, C. H., Lin, C. X. C., & Xu, C. Y. (2013). Adsorption of proteins and nucleic acids on clay minerals and their interactions: A review. *Applied Clay Science*, 80, 443-452.
- Yuan, J.-H., Xu, R.-K., & Zhang, H. (2011). The forms of alkalis in the biochar produced from crop residues at different temperatures. *Bioresource technology*, 102(3), 3488-3497.
- Yuan, Q.-B., Guo, M.-T., & Yang, J. (2015). Fate of antibiotic resistant bacteria and genes during wastewater chlorination: implication for antibiotic resistance control. *PloS one*, 10(3), e0119403.
- Zhang, Li, A., Dai, T., Li, F., Xie, H., Chen, L., & Wen, D. (2017). Cell-free DNA: a neglected source for antibiotic resistance genes spreading from WWTPs. *Environmental science & technology*, 52(1), 248-257.
- Zhang, X.-X., Zhang, T., & Fang, H. H. (2009). Antibiotic resistance genes in water environment. *Applied microbiology and biotechnology*, 82(3), 397-414.
- Zhang, Y., Niu, Z., Zhang, Y., & Zhang, K. (2018). Occurrence of intracellular and extracellular antibiotic resistance genes in coastal areas of Bohai Bay (China) and the factors affecting them. *Environmental pollution*, 236, 126-136.
- ZJUT - China 2018. (2018). Project Description. Retrieved from <http://2018.igem.org/Team:ZJUT-China/Description>

APPENDIX

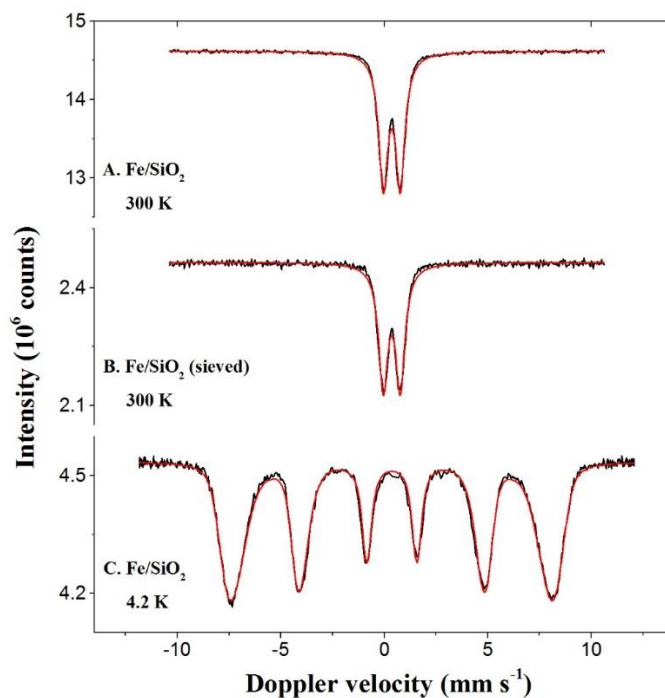
Mössbauer Spectroscopy study of iron oxide coated sand

Figure A1 Mössbauer spectra obtained at 300 and 4.2 K with the Fe/SiO₂ samples of unsieved and sieved (600 μm)

Table A1 Mössbauer fitted parameters of iron-oxide-coated sands un sieved and sieved (600 μm) at temperature obtained at 300 and 4.2 K. Experimental uncertainties: Isomer shift: I.S. ± 0.01 mm s⁻¹; Quadrupole splitting: Q.S. ± 0.01 mm s⁻¹; Line width: Γ ± 0.01 mm s⁻¹; Hyperfine field: ± 0.1 T; Spectral contribution: $\pm 3\%$; *Average magnetic field.

Sample	T (K)	IS (mm·s ⁻¹)	QS (mm·s ⁻¹)	Hyperfine field (T)	Γ (mm·s ⁻¹)	Phase	Spectral contribution (%)
IOCS (un sieved)	300	0.36	0.82	-	0.53	Fe ³⁺	100
IOCS (sieved)	300	0.36	0.82	-	0.53	Fe ³⁺	100
IOCS (un sieved)	4.2	0.35	-0.02	47.4*	0.48	Fe ³⁺	100

*Concentration of buffers used in the extraction of eDNA**Table A2 Concentration of the buffers used in the extraction of eDNA using diethylaminoethyl cellulose anion exchange column*

Buffer	Tris-HCL (mM)	EDTA (mM)	NaCl (M)
Equilibrium buffer	50	10	-
Elution buffer	50	10	1.5
Regeneration buffer	50	10	2
Cleaning solution	1 M NaOH		2
Storage solution	20 % ethanol		

Sequences of the standards for qPCR

Table A3 ARGs/ MGE gene sequences obtained from Resfinder of the standards used for the qPCR

Gene	Sequence
<i>qnrS</i>	GACGTGCTAACTTGCCTGATACGACATTCGTCAACTGCAAGTTCATTGAACAGG GTGATATCGAAGGCTGCCACTTTGATGTCGCAGATCTTCGTGATGCAAGTTTCCA ACAATGCCA
<i>16S rRNA</i>	ACTCCTACGGGAGGCAGCAGTGGGGAATATTGCACAATGGGCGCAAGCCTGATG CAGCCATGCCCGTGTATGAAGAAGGCCTTCGGGTTGTAAAGTACTTTCAGCGG GGAGGAAGGGAGTAAAGTTAATACCTTTGCTCATTGACGTTACCCGCAGAAGAA GCACCGGCTAACTCCGTGCCAGCAGCCGCGGTAAT
<i>intI1</i>	GCCTTGATGTTACCCGAGAGCTTGGCACCCAGCCTGCGCGAGCAGCTGTGCGGT GCACGGGCATGGTGGCTGAAGGACCAGGCCGAGGGCCGCAGCGGCGTTGCGCT TCCCGACGCCCTTGAGCGGAAGTATCCGCGCGCCGGGCATTCTGGCCGTGGTT CTGGGTTTTTGCAGCACACGCATTTCGACCGATC
<i>sul1</i>	CGCACCGGAAACATCGCTGCACGTGCTGTCGAACCTTCAAAGCTGAAGTCGGC GTTGGGGCTTCCGCTATTGGTCTCGGTGTGCGGAAATCCTTCTTGGGCGCCACC GTTGGCCTTCTGTAAAGGATCTGGGTCCAGCGAGCCTTGCGGCGGAACTTCA TGGAGGCCGGTATCTGGCGCCAGACGCAGCCATTGCGCAGGCGCGTAAGCTGAT
<i>sul2</i>	GGCCGAGGGGGCAGATGTGATCGACCTCGGTCCGGCATCCAGCAATCCCGACGC CGCGCCTGTTTCGTCCGACACAGAAATCGCGCGTATCGCGCCGGTGCTGGACGC GCTCAAGGCAGATGGCATTCCCG
<i>ermB</i>	AAAACCTACCCGCCATACCACAGATGTTCCAGATAAATATTGGAAGCTATATAC GTACTTTGTTTCAAATGGGTCAATCGAGAATATCGTCAACTGTTTACTAAAAAT CAGTTTCATCAAGCAATGAAACACGCCAAA
<i>bla_{CTXM}</i>	CTATGGCACCACCAACGATATCGCGGTGATCTGGCCAAAAGATCGTGCGCCGCT GATTCTGGTCACTTACTTCACCCAGCCTCAACCTAAGGCAGAAAGCCGT

Isotherm graphs

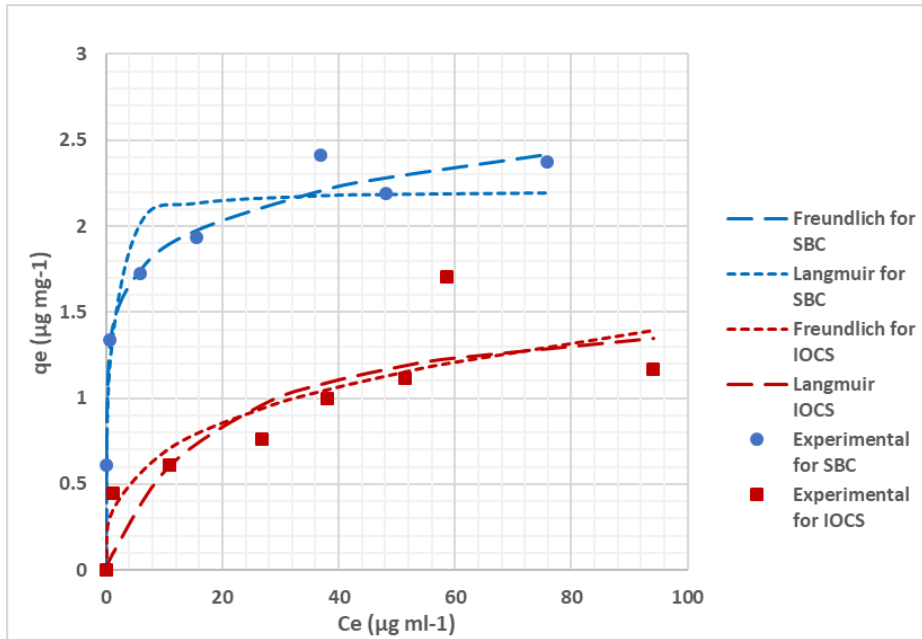


Figure A2 Freundlich and Langmuir isotherm graphs for sewage-based biochar and iron coated sand in ultrapure water

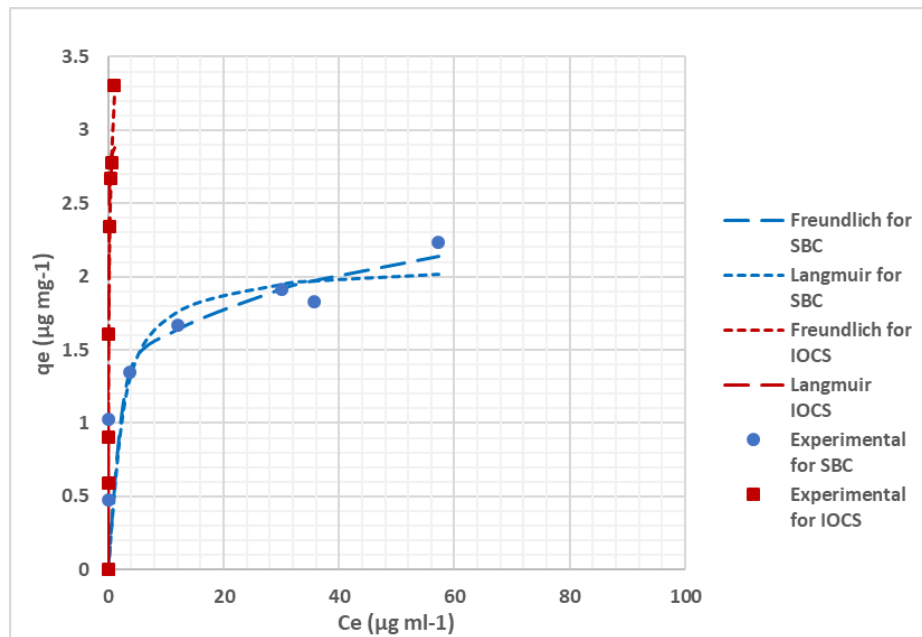


Figure A3 Freundlich and Langmuir isotherm graphs for sewage-based biochar and iron coated sand in tap water

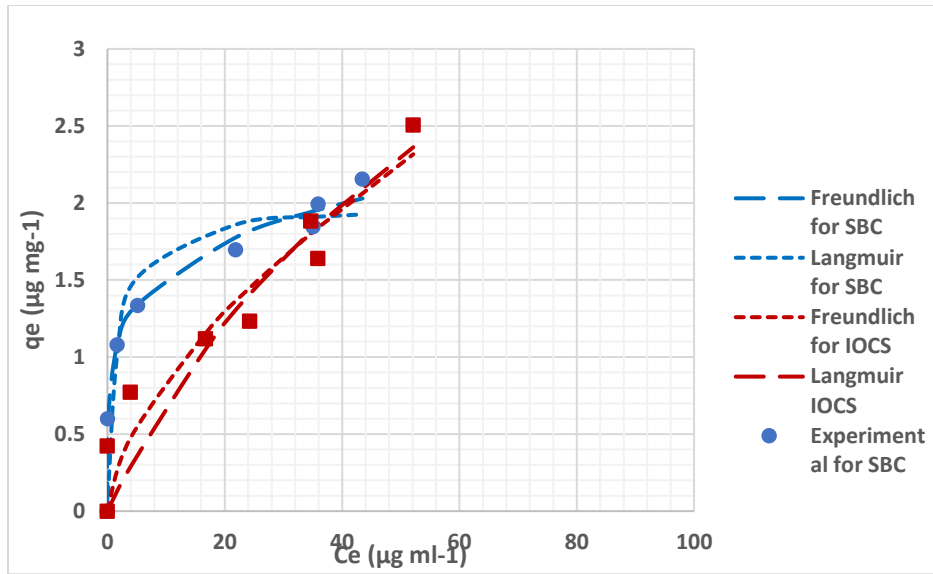


Figure A4 Freundlich and Langmuir isotherm graphs for sewage-based biochar and iron coated sand in effluent wastewater

*iDNA and eDNA concentration in the samples**Table A 4 Absolute concentration of intracellular DNA found in the unfiltered samples. SBC: sewage-based biochar, IOCS: iron oxide coated sands*

	Raw Influent (ng/μl)	SBC effluent (ng/μl)	IOCS effluent (ng/μl)
Sample 1	2.14	0.156	3.64
Sample 2	5.36	0.584	0.606

Table A 5 Absolute concentration of eDNA found in the filtered samples. SBC: sewage-based biochar, IOCS: iron oxide coated sands

	Raw Influent (ng/μl)	SBC effluent (ng/μl)	IOCS effluent (ng/μl)
Sample 1	2.14	0.156	3.64
Sample 2	5.36	0.584	0.606

*ARGs and MGE removal efficiencies**Table A6 Removal efficiency of intracellular ARGs and MGE in decadic logarithm value of the ration of raw influent and sewage-based biochar/iron coated sand treatment water*

Gene	SBC		IOCS	
	(log₁₀ removal)	% removal	(log₁₀ removal)	% removal
16S rRNA	1.31	95.10	0.40	95.10
<i>sul1</i>	1.04	90.83	0.12	90.83
<i>sul2</i>	0.32	52.00	0.71	52.00
<i>ermB</i>	2.11	99.22	2.11	99.22
<i>qnrS</i>	1.27	94.62	0.51	94.62
<i>bla_{CTXM}</i>	1.49	96.80	1.49	96.80
<i>int11</i>	0.82	84.74	0.22	84.74

Table A7 Removal efficiency of extracellular ARGs and MGE in decadic logarithm value of the ration of raw influent and sewage-based biochar/iron coated sand treatment water, Genes qnrS and blaCTXM were not detected in the raw influent of effluent wastewater

Gene	SBC		IOCS	
	(log₁₀ removal)	% removal	(log₁₀ removal)	% removal
<i>16S rRNA</i>	3.20	0.38	0.38	58.14
<i>sul1</i>	1.88	0.42	0.42	61.78
<i>sul2</i>	0.89	0.65	0.65	77.59
<i>ermB</i>	2.08	2.08	2.08	99.17
<i>qnrS</i>	-	-	-	-
<i>blaCTXM</i>	-	-	-	-
<i>intI1</i>	2.64	0.59	0.59	74.27

Wastewater quality parameters

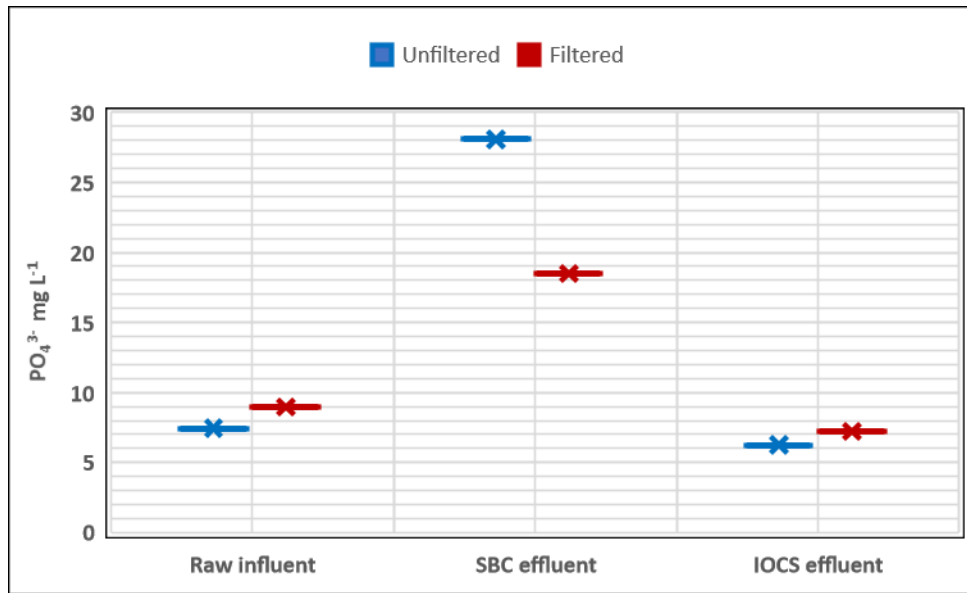


Figure A5 Phosphorus removal from filtered and unfiltered samples. Raw influent: effluent wastewater, SBC effluent: sewage-based biochar treated, IOCS effluent: iron-oxide-coated sands treated

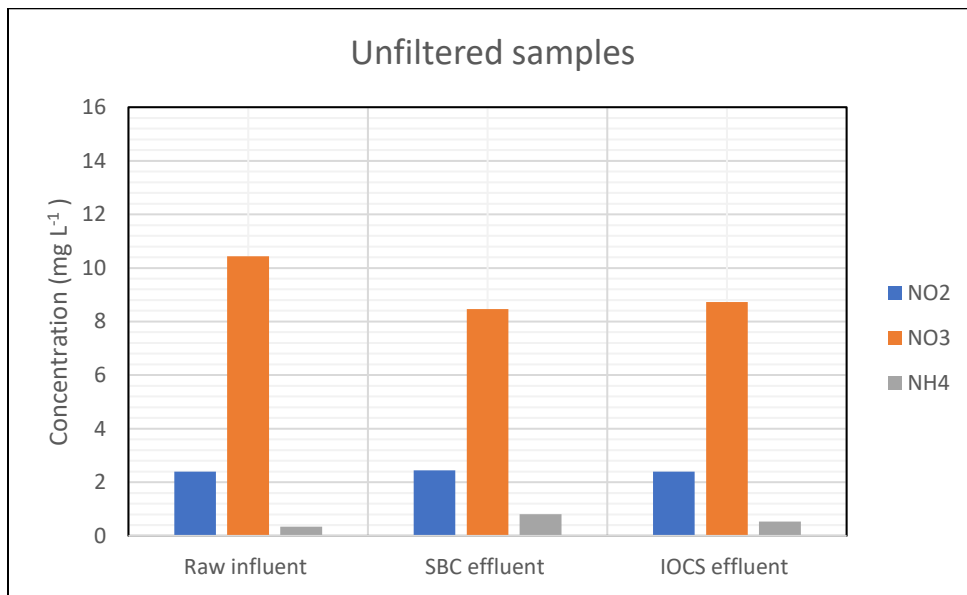


Figure A 6 Concentrations of NO₂⁻ (nitrite), NO₃⁻ (nitrate) and NH₄⁺ (ammonium) in the unfiltered samples. Raw influent: effluent wastewater, SBC effluent: sewage-based biochar treated, IOCS effluent: iron-oxide-coated sands treated

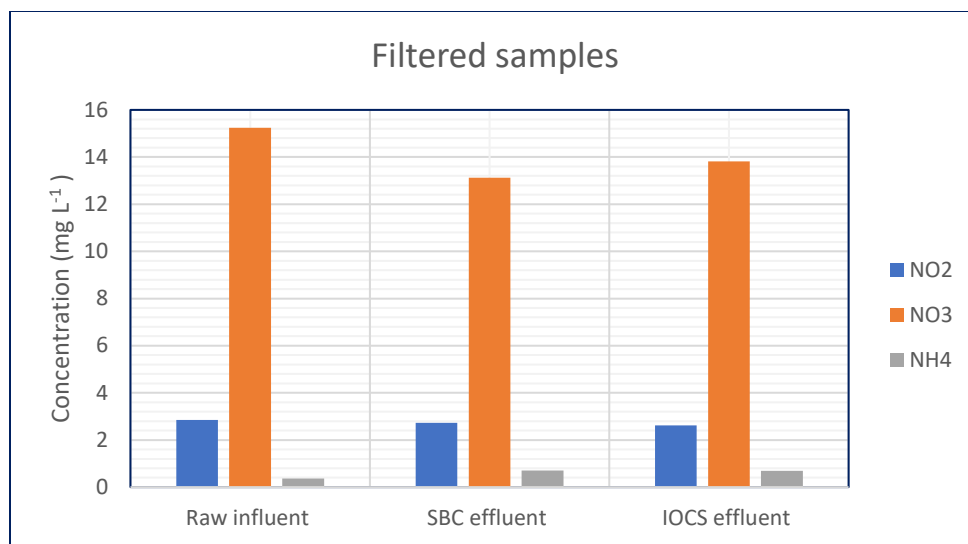
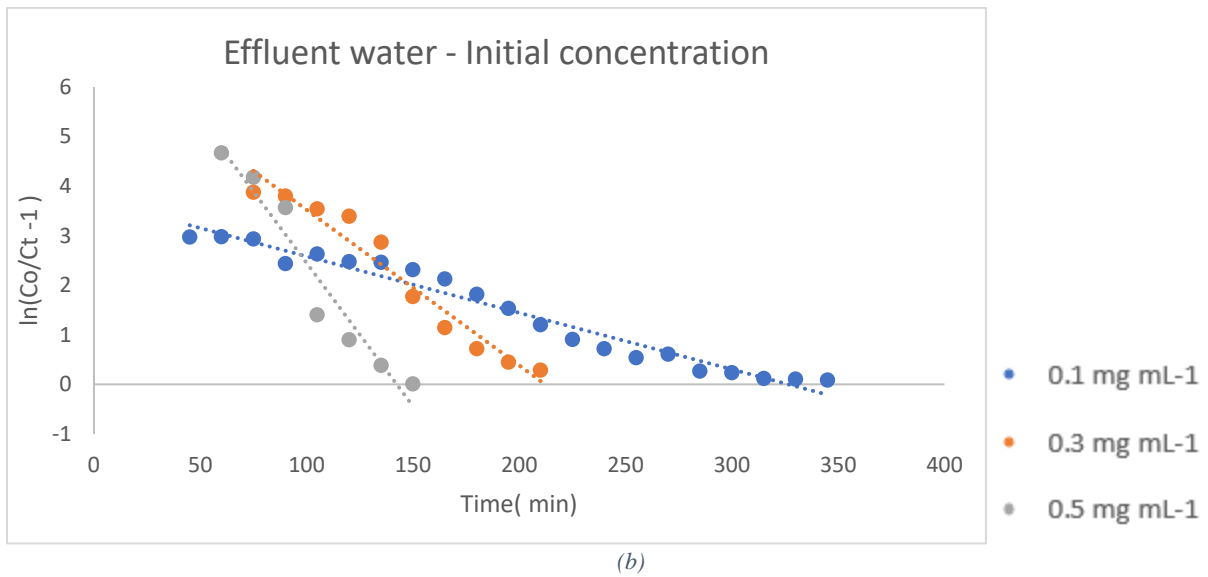
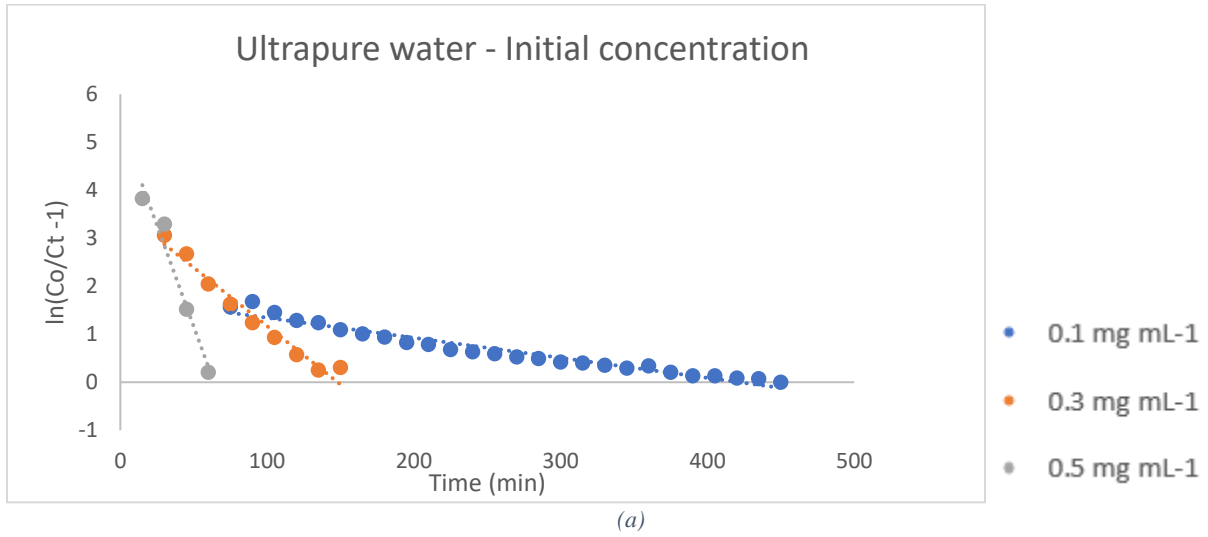
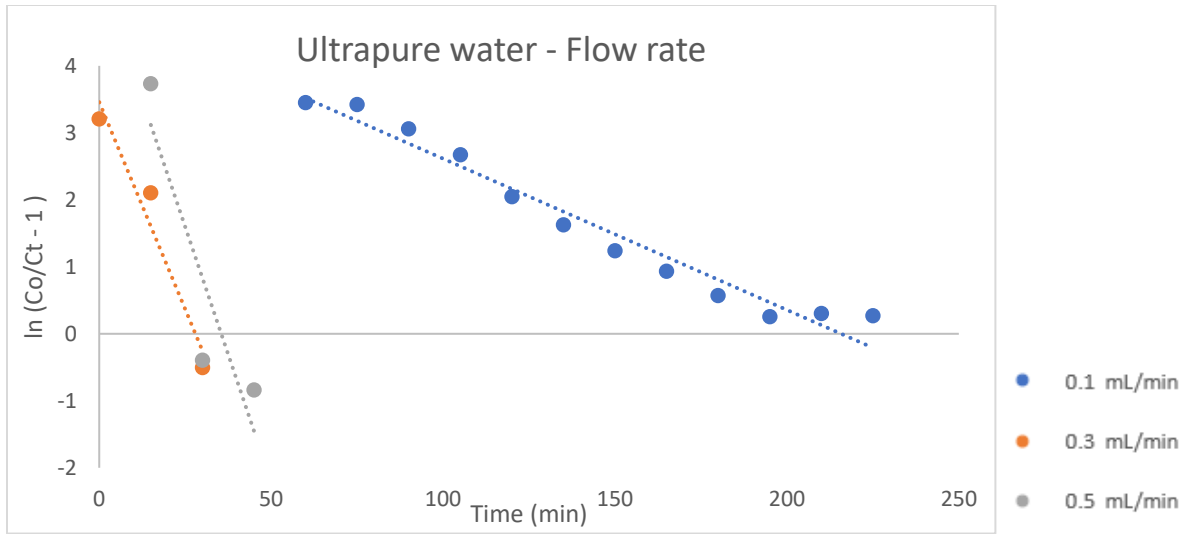


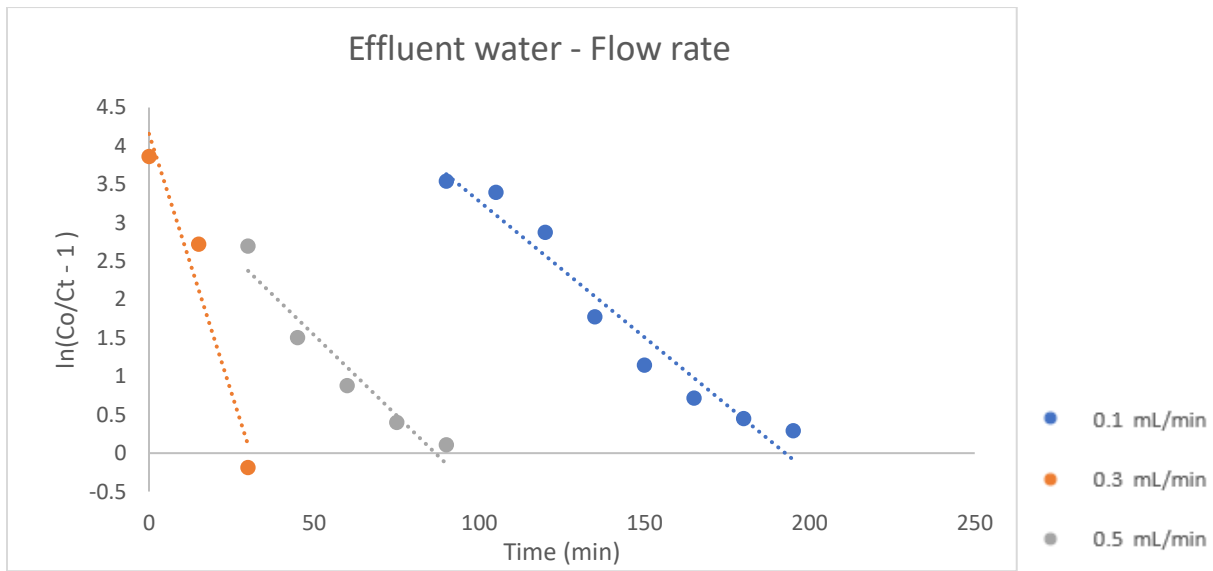
Figure A7 Concentrations of NO_2^- (nitrite), NO_3^- (nitrate) and NH_4^+ (ammonium) in the filtered samples. Raw influent: effluent wastewater, SBC effluent: sewage-based biochar treated, IOCS effluent: iron-oxide-coated sands treated

Thomas model plots – Iron-oxide-coated sands





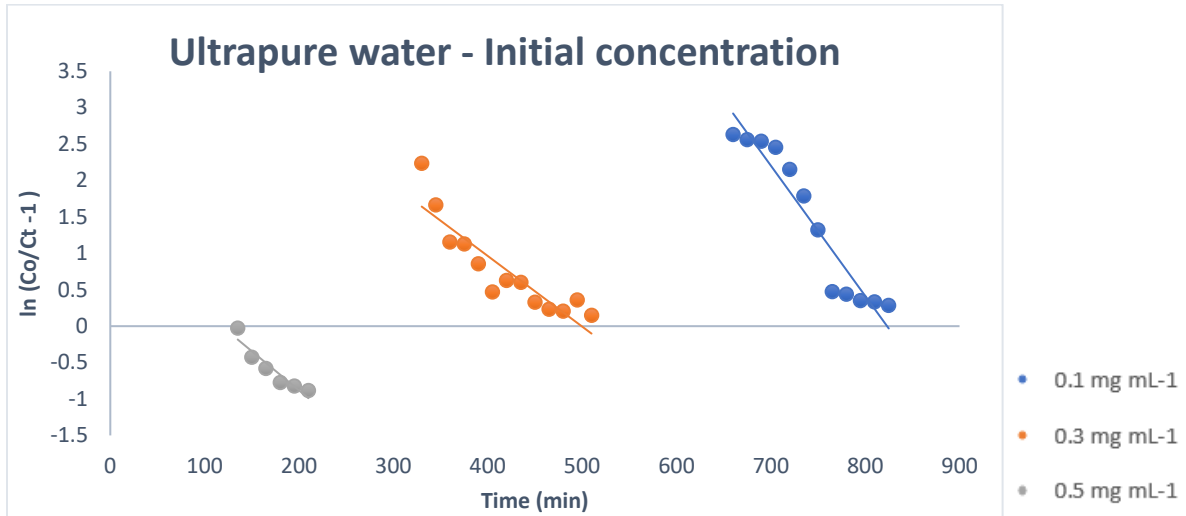
(c)



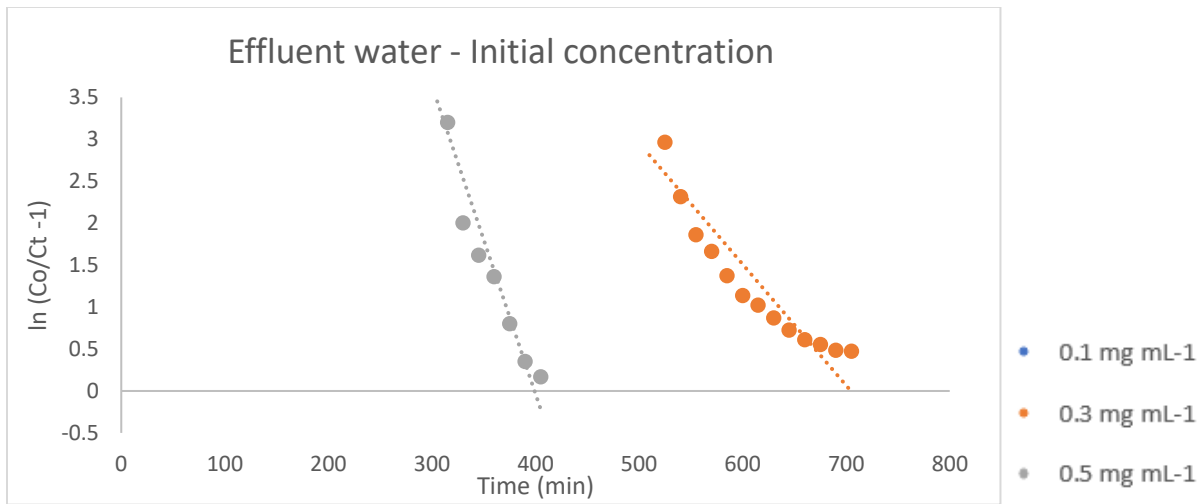
(d)

Figure A8 Linear plots of Thomas model plots of iron-oxide-coated sands (a) Ultrapure water with varying initial concentration (b) Effluent wastewater with varying initial concentration (c) Ultrapure water with varying flow rate (d) Effluent wastewater with varying flow rate

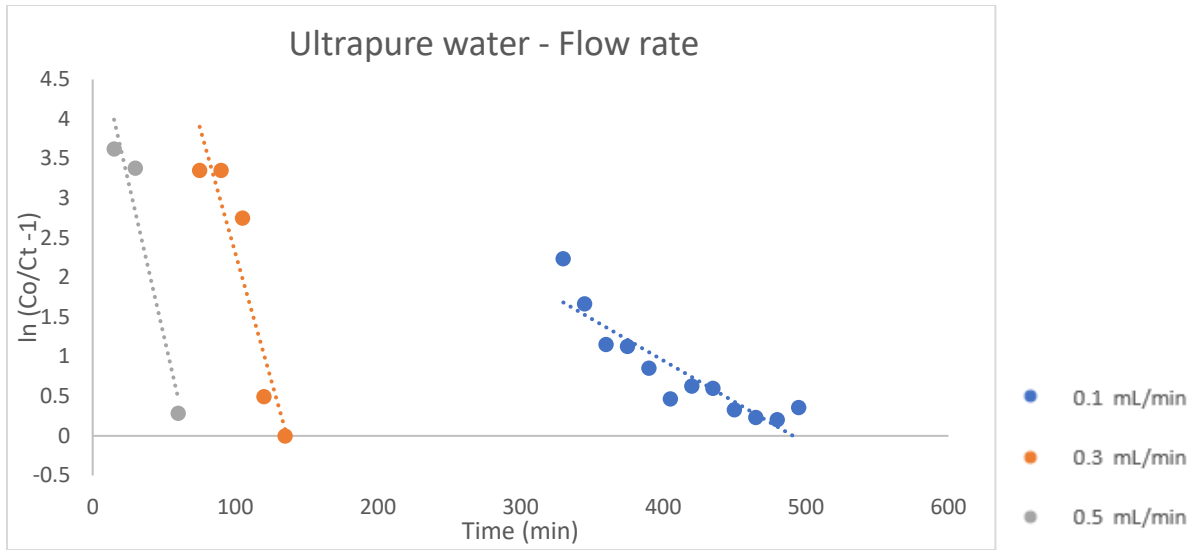
Thomas model plots – Sewage-based biochar



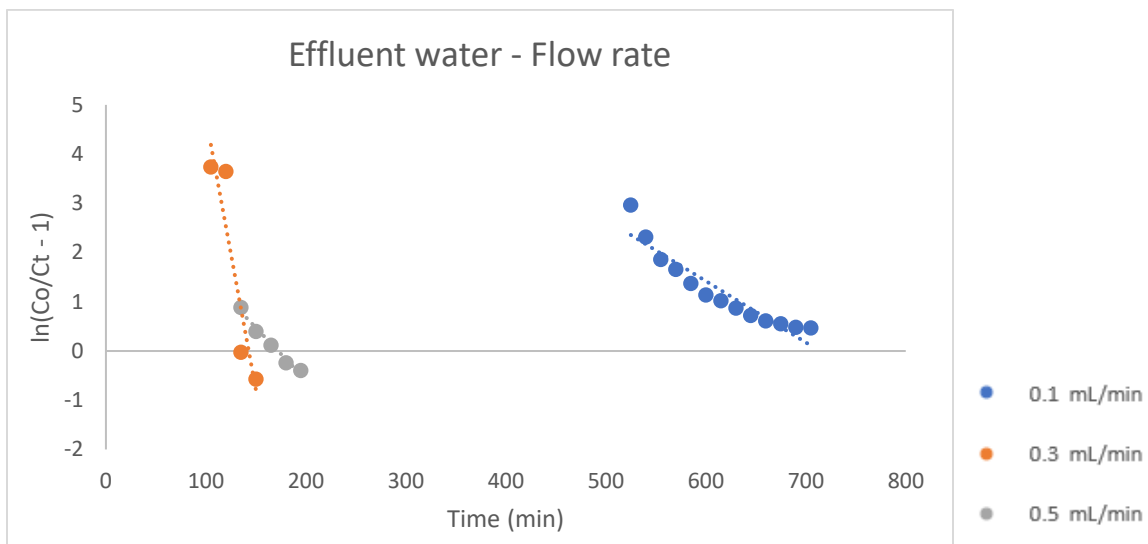
(a)



(b)



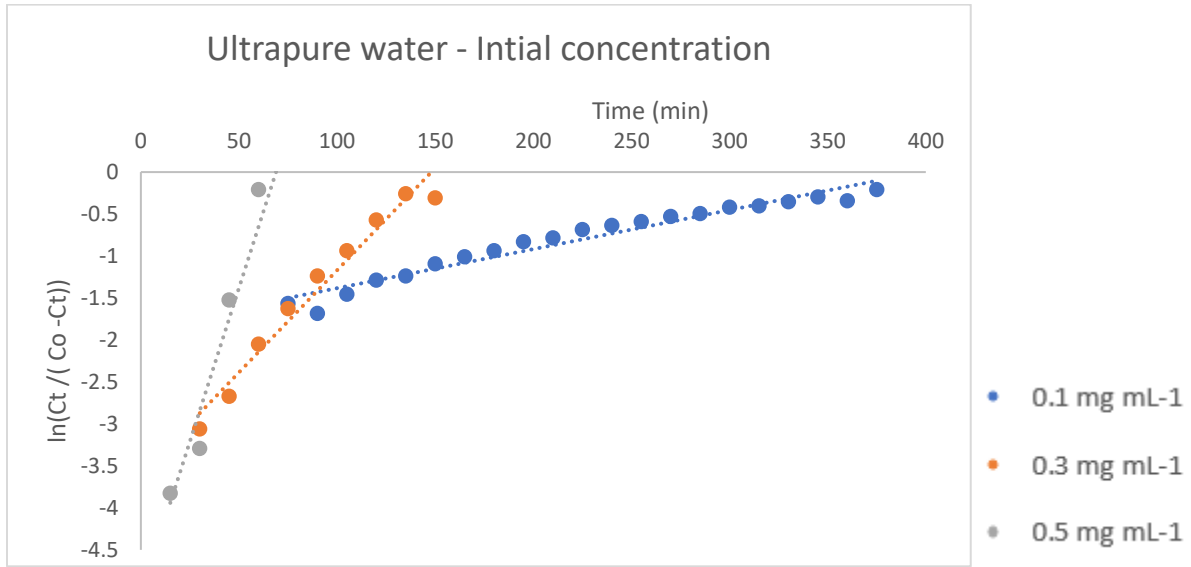
(c)



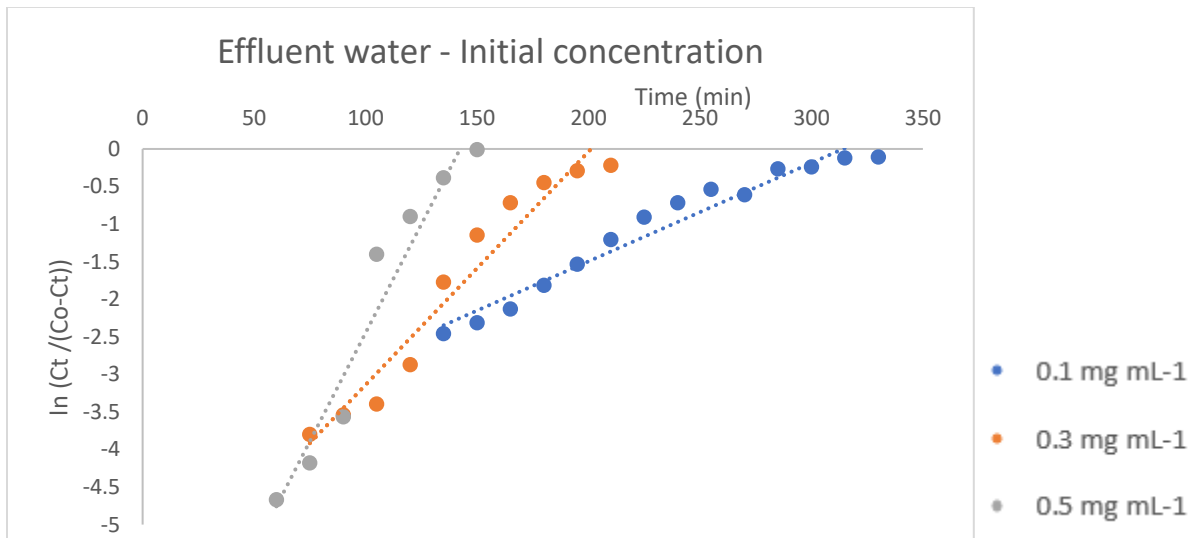
(d)

Figure A9 Linear plots of Thomas model plots of sewage-based biochar (a) Ultrapure water with varying initial concentration (b) Effluent wastewater with varying initial concentration (c) Ultrapure water with varying flow rate (d) Effluent wastewater with varying flow rates

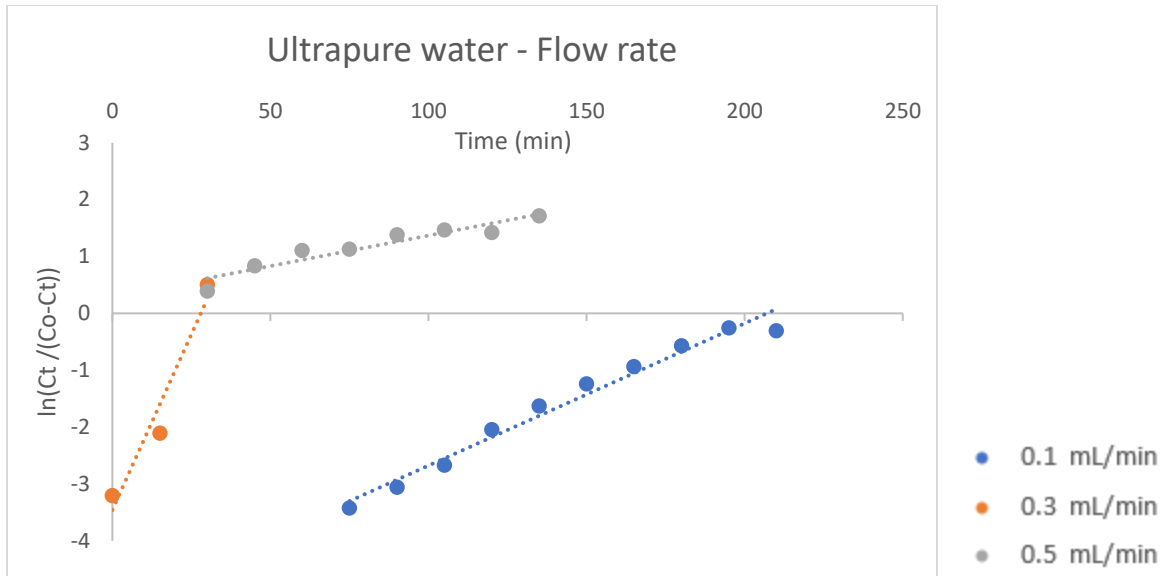
Yoon – Nelson plots – Iron-oxide-coated sands



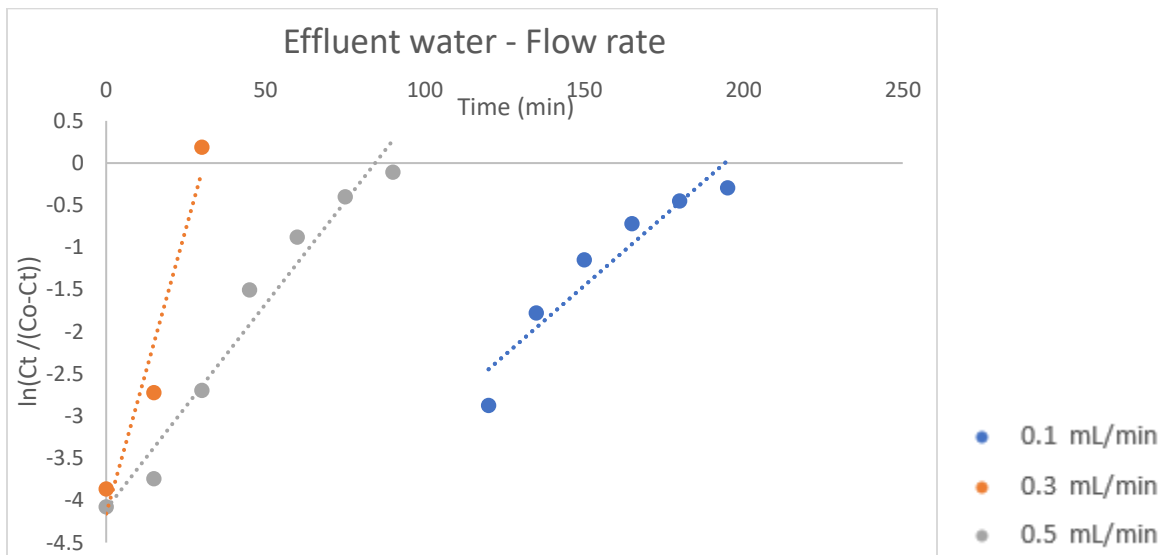
(a)



(b)



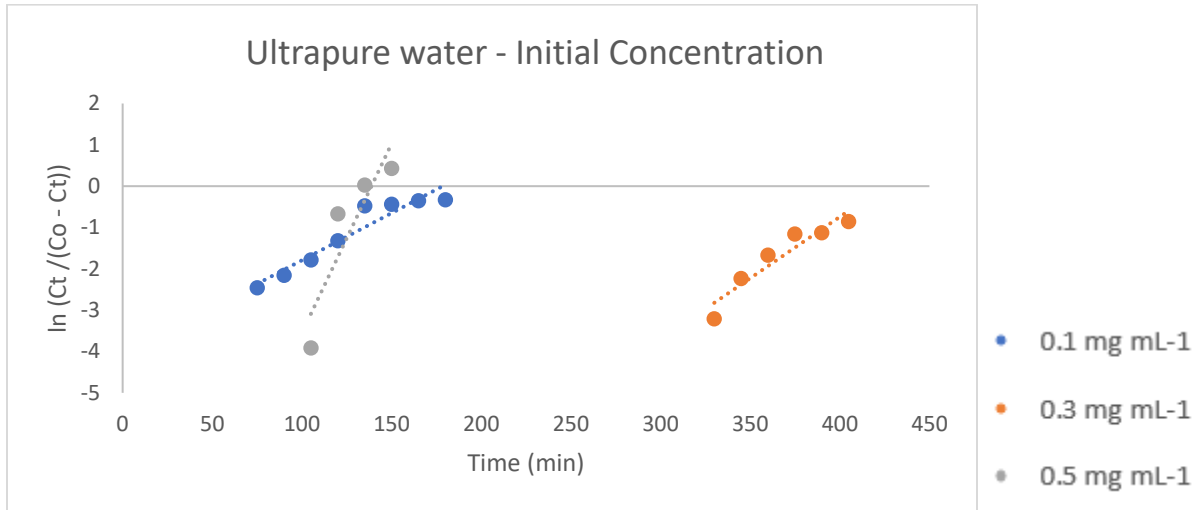
(c)



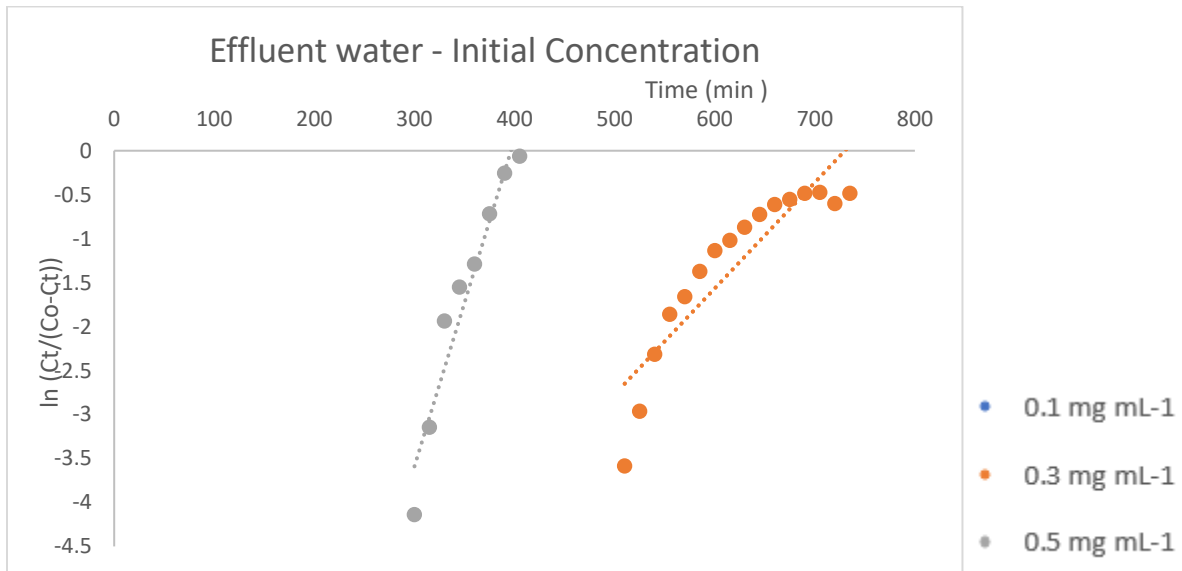
(d)

Figure A10 Linear plots of Yoon Nelson model plots of iron oxide coated sand (a) Ultrapure water with varying initial concentration (b) Effluent wastewater with varying initial concentration (c) Ultrapure water with varying flow rate (d) Effluent wastewater with varying flow rates

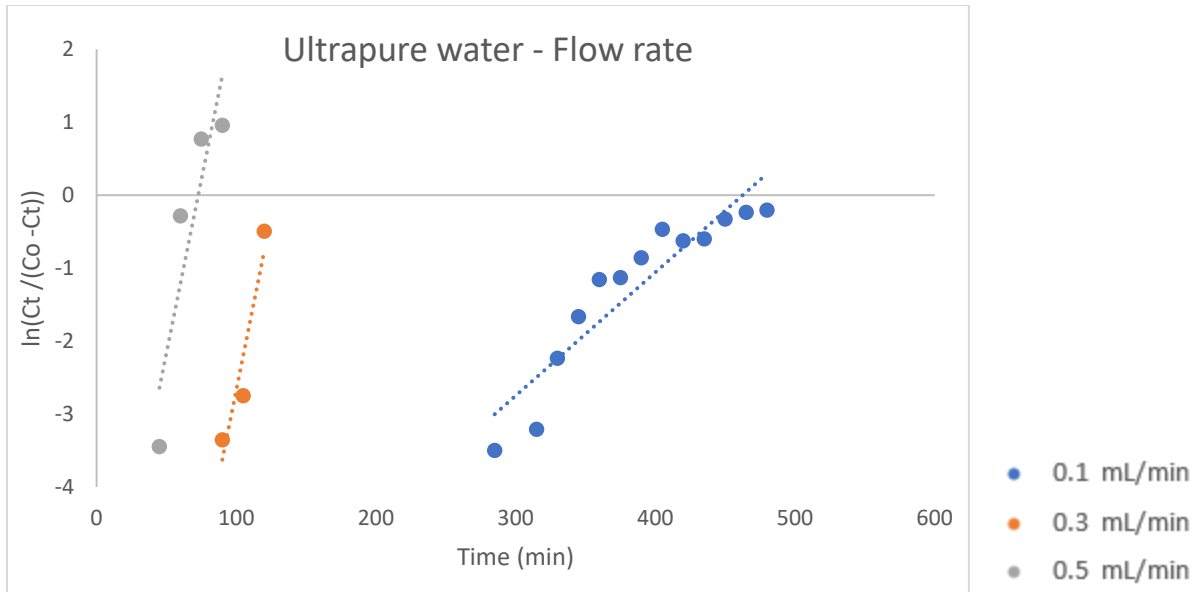
Yoon – Nelson plots – sewage-based biochar



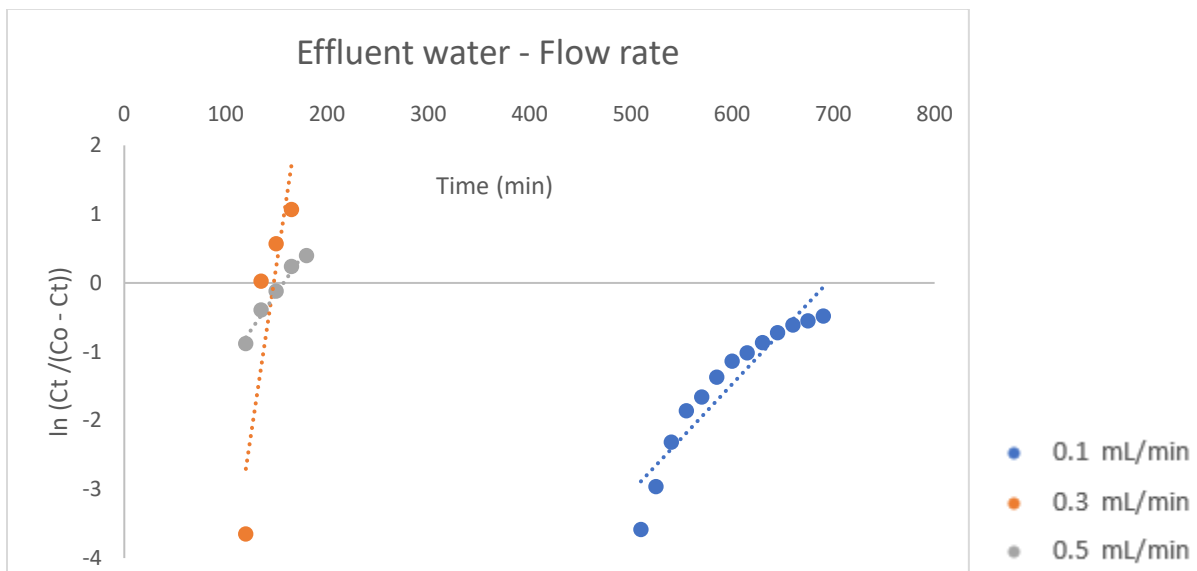
(a)



(b)



(c)



(d)

Figure A11 Linear plots of Yoon Nelson model plots of sewage-based biochar (a) Ultrapure water with varying initial concentration (b) Effluent wastewater with varying initial concentration (c) Ultrapure water with varying flow rate (d) Effluent wastewater with varying flow rates

Residence time of the column

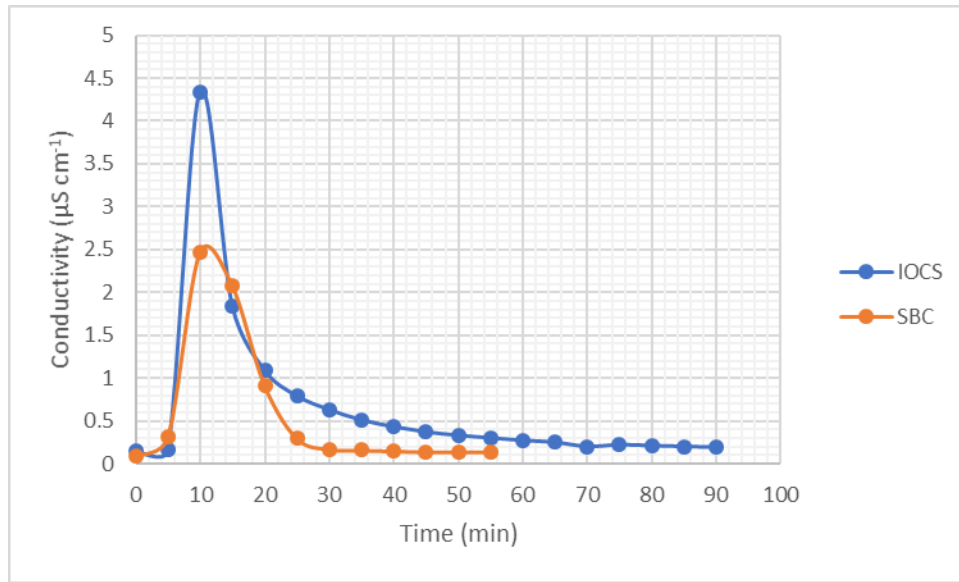


Figure A12 Residence time distribution of the column bed with iron-oxide-coated sands and sewage-based biochar

*ANOVA results for the effect of pH on adsorption**Table A8 One way ANOVA results for the effect of pH on DNA adsorption with an initial concentration of 20 µg mL⁻¹ by sewage-based biochar*

Anova: Single Factor						
SUMMARY						
Groups	Count	Sum	Average	Variance		
4	3	294.0625	98.02083	1.503499		
7	3	295.2381	98.4127	1.846542		
9	3	300	100	0		
ANOVA						
Source of Variation	SS	df	MS	F	P-value	F crit
Between Groups	6.590185	2	3.295093	2.950793	0.128127	5.143253
Within Groups	6.700083	6	1.11668			
Total	13.29027	8				

Table A9 One way ANOVA results for the effect of pH on DNA adsorption with an initial concentration of 20 µg mL⁻¹ by iron oxide coated sand

Anova: Single Factor						
SUMMARY						
Groups	Count	Sum	Average	Variance		
4	3	289.0625	96.35417	5.50588		
7	3	276.1905	92.06349	46.39781		
9	3	297.561	99.18699	2.620322		
ANOVA						
Source of Variation	SS	df	MS	F	P-value	F crit
Between Groups	77.17904	2	38.58952	2.123258	0.200782	34.79763
Within Groups	109.048	6	18.17467			
Total	186.2271	8				

Table A10 One way ANOVA results for the effect of pH on DNA adsorption with an initial concentration of 100 $\mu\text{g mL}^{-1}$ by sewage-based biochar

Anova: Single Factor						
SUMMARY						
Groups	Count	Sum	Average	Variance		
4	3	293.75	97.91667	0.403341		
7	3	295.9307	98.64358	0.420407		
9	3	296.7596	98.91986	0.047348		
ANOVA						
Source of Variation	SS	df	MS	F	P-value	F crit
Between Groups	1.611131	2	0.805565	2.774319	0.140237	5.143253
Within Groups	1.742191	6	0.290365			
Total	3.353322	8				

Table A11 One way ANOVA results for the effect of pH on DNA adsorption with an initial concentration of 100 $\mu\text{g mL}^{-1}$ by iron oxide coated sand

Anova: Single Factor						
SUMMARY						
Groups	Count	Sum	Average	Variance		
pH 4	3	296.7969	98.93229	0.070699		
pH 7	3	297.4026	99.1342	0.294222		
pH 9	3	298.0139	99.33798	0.744212		
ANOVA						
Source of Variation	SS	df	MS	F	P-value	F crit
Between Groups	0.246875	2	0.123438	0.333876	0.728644	5.143253
Within Groups	2.218267	6	0.369711			
Total	2.465142	8				

*One way ANOVA and Post hoc test results for the effect of ions on adsorption – SBC**Table A12 Statistical results for the effect of Na⁺ ions on DNA adsorption with an initial concentration of 100 µg mL⁻¹ by sewage-based biochar (a) ANOVA results (b) Post hoc results**(a) ANOVA results*

Anova: Single Factor						
SUMMARY						
Groups	Count	Sum	Average	Variance		
0 mM	3	5.769481	1.92316	0.013733		
1 mM	3	6.996753	2.332251	0.011421		
10 mM	3	6.348485	2.116162	0.024767		
30 mM	3	6.070346	2.023449	0.107244		
60 mM	3	6.585498	2.195166	0.022149		
ANOVA						
Source of Variation	SS	df	MS	F	P-value	F crit
Between Groups	0.296292	4	0.074073	2.065454	0.160609	3.47805
Within Groups	0.358628	10	0.035863			
Total	0.65492	14				

(b) Post hoc results

Post hoc test						
	1 mM vs 10 mM		1 mM vs 30 mM		1 mM vs 60 mM	
	1 mM	10 mM	1 mM	30 mM	1 mM	60 mM
Mean	2.332251	2.116162	2.332251	2.023449	2.332251	2.195166
Variance	0.011421	0.024767	0.011421	0.107244	0.011421	0.022149
Observations	3	3	3	3	3	3
Pooled Variance	0.018094		0.059333		0.016785	
Hypothesized Mean Difference	0		0		0	
df	4		4		4	
t Stat	1.967491		1.552672		1.29591	
P(T<=t) one-tail	0.060258		0.097729		0.132363	
t Critical one-tail	2.131847		2.131847		2.131847	
P(T<=t) two-tail	0.120515		0.195457		0.264726	
t Critical two-tail	2.776445		2.776445		2.776445	

Table A13 Statistical results for the effect of Ca^{2+} ions on DNA adsorption with an initial concentration of $100 \mu\text{g mL}^{-1}$ by sewage-based biochar (a) ANOVA results (b) Post hoc results

(a) ANOVA results

Anova: Single Factor						
SUMMARY						
Groups	Count	Sum	Average	Variance		
0 mM	3	5.769481	1.92316	0.013733		
1 mM	3	6.67316	2.224387	0.082359		
10 mM	3	7.091991	2.363997	0.023138		
30 mM	3	7.166667	2.388889	0.082137		
60 mM	3	7.044372	2.348124	0.072179		
ANOVA						
Source of Variation	SS	df	MS	F	P-value	F crit
Between Groups	0.448181	4	0.112045	2.048021	0.163184	3.47805
Within Groups	0.54709	10	0.054709			
Total	0.995272	14				

(b) Post hoc results

Post hoc test						
	1 mM vs 10 mM		1 mM vs 30 mM		1 mM vs 60 mM	
	1 mM	10 mM	1 mM	30 mM	1 mM	60 mM
Mean	2.224387	2.363997	2.224387	2.388889	2.224387	2.348124
Variance	0.082359	0.023138	0.082359	0.082137	0.082359	0.072179
Observations	3	3	3	3	3	3
Pooled Variance	0.052748		0.082248		0.077269	
Hypothesized Mean Difference	0		0		0	
df	4		4		4	
t Stat	-0.74449		-0.70251		-0.54519	
P(T<=t) one-tail	0.24897		0.260545		0.3073	
t Critical one-tail	2.131847		2.131847		2.131847	
P(T<=t) two-tail	0.49794		0.521089		0.614601	
t Critical two-tail	2.776445		2.776445		2.776445	

Table A14 ANOVA results for the effect of Mg^{2+} ions on DNA adsorption with an initial concentration of $100 \mu\text{g mL}^{-1}$ by sewage-based biochar

Anova: Single Factor						
SUMMARY						
<i>Groups</i>	<i>Count</i>	<i>Sum</i>	<i>Average</i>	<i>Variance</i>		
0 mM	3	5.769481	1.92316	0.013733		
1 mM	3	6.742424	2.247475	0.013728		
10 mM	3	8.332251	2.777417	0.029099		
30 mM	3	6.867965	2.289322	0.058416		
60 mM	3	8.25974	2.753247	0.301235		
ANOVA						
<i>Source of Variation</i>	<i>SS</i>	<i>df</i>	<i>MS</i>	<i>F</i>	<i>P-value</i>	<i>F crit</i>
Between Groups	1.590297	4	0.397574	4.776115	0.020505	3.47805
Within Groups	0.832422	10	0.083242			
Total	2.422719	14				

*One way ANOVA and Post hoc test results for the effect of ions on adsorption – IOCS**Table A15 Statistical results for the effect of Na⁺ ions on DNA adsorption with an initial concentration of 100 µg mL⁻¹ by iron oxide coated sand (a) ANOVA results (b) Post hoc results**(a) ANOVA results*

Anova: Single Factor						
SUMMARY						
Groups	Count	Sum	Average	Variance		
0 mM	3	4.202381	1.400794	0.011109		
1 mM	3	4.566017	1.522006	0.016459		
10 mM	3	5.343074	1.781025	0.141851		
30 mM	3	4.957792	1.652597	0.02375		
60 mM	3	5.024892	1.674964	0.011714		
ANOVA						
Source of Variation	SS	df	MS	F	P-value	F crit
Between Groups	0.260176	4	0.065044	1.587342	0.251829	3.47805
Within Groups	0.409766	10	0.040977			
Total	0.669942	14				

(a) Post hoc results

Post hoc test						
	1 mM vs 10 mM		1 mM vs 30 mM		1 mM vs 60 mM	
	1 mM	10 mM	1 mM	30 mM	1 mM	60 mM
Mean	1.522006	1.781025	1.522006	1.652597	1.522006	1.674964
Variance	0.016459	0.141851	0.016459	0.02375	0.016459	0.011714
Observations	3	3	3	3	3	3
Pooled Variance	0.079155		0.020104		0.014087	
Hypothesized Mean Difference	0		0		0	
df	4		4		4	
t Stat	-1.12755		-1.12802		-1.57839	
P(T<=t) one-tail	0.161282		0.161195		0.094808	
t Critical one-tail	2.131847		2.131847		2.131847	
P(T<=t) two-tail	0.322565		0.322391		0.189617	
t Critical two-tail	2.776445		2.776445		2.776445	

Table A16 Statistical results for the effect of Ca^{2+} ions on DNA adsorption with an initial concentration of $100 \mu\text{g mL}^{-1}$ by iron oxide coated sand (a) ANOVA results (b) Post hoc results

(a) ANOVA results

Anova: Single Factor						
SUMMARY						
Groups	Count	Sum	Average	Variance		
0 mM	3	4.202381	1.400794	0.011109		
1 mM	3	4.91342	1.637807	0.029833		
10 mM	3	5.180736	1.726912	0.030601		
30 mM	3	5.734848	1.911616	0.014749		
60 m M	3	5.90368	1.967893	0.266283		
ANOVA						
Source of Variation	SS	df	MS	F	P-value	F crit
Between Groups	0.619376	4	0.154844	2.195904	0.142759	3.47805
Within Groups	0.705149	10	0.070515			
Total	1.324525	14				

(b) Post hoc results

Post hoc test						
	1 mM vs 10 mM		1 mM vs 30 mM		1 mM vs 60 mM	
	1 mM	10 mM	1 mM	30 mM	1 mM	60 mM
Mean	1.637807	1.726912	1.637807	1.911616	1.637807	1.967893
Variance	0.029833	0.030601	0.029833	0.014749	0.029833	0.266283
Observations	3	3	3	3	3	3
Pooled Variance	0.030217		0.022291		0.148058	
Hypothesized Mean Difference	0		0		0	
df	4		4		4	
t Stat	-0.62781		-2.24611		-1.05065	
P(T<=t) one-tail	0.282095		0.044012		0.176351	
t Critical one-tail	2.131847		2.131847		2.131847	
P(T<=t) two-tail	0.56419		0.088023		0.352703	
t Critical two-tail	2.776445		2.776445		2.776445	

Table A17 Statistical results for the effect of Mg^{2+} ions on DNA adsorption with an initial concentration of 100 $\mu\text{g mL}^{-1}$ by iron oxide coated sand (a) ANOVA results (b) Post hoc results

(a) ANOVA results (b) Post hoc results

Anova: Single Factor						
SUMMARY						
Groups	Count	Sum	Average	Variance		
0 mM	3	4.202381	1.400794	0.011109		
1 mM	3	3.953463	1.317821	0.025516		
10 mM	3	5.812771	1.93759	0.191517		
30 mM	3	6.254329	2.084776	0.135996		
60 mM	3	5.769481	1.92316	0.243943		
ANOVA						
Source of Variation	SS	df	MS	F	P-value	F crit
Between Groups	1.453497	4	0.363374	2.987875	0.073027	3.47805
Within Groups	1.216163	10	0.121616			
Total	2.66966	14				

(b) Post hoc results

Post hoc test						
	1 mM vs 10 mM		1 mM vs 30 mM		1 mM vs 60 mM	
	1 mM	10 mM	1 mM	30 mM	1 mM	60 mM
Mean	1.317821	1.93759	1.317821	2.084776	1.317821	1.92316
Variance	0.025516	0.191517	0.025516	0.135996	0.025516	0.243943
Observations	3	3	3	3	3	3
Pooled Variance	0.108517		0.080756		0.13473	
Hypothesized Mean Difference	0		0		0	
df	4		4		4	
t Stat	-2.30424		-3.30543		-2.01982	
P(T<=t) one-tail	0.041277		0.014891		0.056761	
t Critical one-tail	2.131847		2.131847		2.131847	
P(T<=t) two-tail	0.082553		0.029782		0.113521	
t Critical two-tail	2.776445		2.776445		2.776445	

*Statistical results for 16S rRNA, ARGs, and MGE removal**Table A18 Statistical results of the significance differences after treatment with sewage-based biochar and iron oxide coated sand for unfiltered samples*

Adsorbent	<i>16S rRNA</i>	<i>sul1</i>	<i>sul2</i>	<i>ermB</i>	<i>qnrS</i>	<i>bla_{CTXM}</i>	<i>int11</i>
IOCS	0.027	ns	0.00000	0.004	0.02	0.009	ns
SBC	0.0027	0.004	ns	0.002	0.003	0.009	0.0025

Table A19 Statistical results of the significance differences after treatment with sewage-based biochar and iron oxide coated sand for filtered samples

Adsorbent	<i>16S rRNA</i>	<i>sul1</i>	<i>sul2</i>	<i>ermB</i>	<i>qnrS</i>	<i>bla_{CTXM}</i>	<i>int11</i>
IOCS	ns	ns	0.014	0.0000	0.009	-	ns
SBC	0.0001	0.005	0.0001	0.0000	0.009	-	0.0001